UNIVERSITY OF OKLAHOMA

GRADUATE COLLEGE

MOLECULAR EVOLUTION OF A NA, K-ATPASE IN WEAKLY ELECTRIC FISH

A THESIS

SUBMITTED TO THE GRADUATE FACULTY

in partial fulfillment of the requirements for the

Degree of

MASTER OF SCIENCE

By

HILIARY L. RIEDMANN
Norman, Oklahoma
2016

MOLECULAR EVOLUTION OF A NA, K-ATPASE IN WEAKLY ELECTRIC FISH

A THESIS APPROVED FOR THE
DEPARTMENT OF BIOLOGY

BY

_____
Dr. Michael Markham, Chair

_____
Dr. Richard Broughton

_____
Dr. John Masly

Table of Contents

List of Tables

Chapter 3

List of Figures

Chapter 1

Chapter 2

Chapter 3

Abstract

African mormyrids and South American gymnotiforms are two independently evolved lineages of weakly electric fish that produce electric organ discharges (EODs) as sensory and communication signals. EOD frequency varies across species, ranging from less than 10 Hz to more than 2000 Hz. EODs are the summed action potentials generated by electrocytes, specialized electrically excitable cells of the electric organ. The Na^+ currents that depolarize the electrocyte during the action potential can exceed 10 microamperes, several orders of magnitude larger than Na^+ currents in other excitable cells such as neurons and myocytes. The Na, K-ATPases expressed by electrocytes must re-establish the necessary ionic gradients in the interval between action potentials by the active transport of K^+ and Na^+. This interval decreases as EOD frequency increases, becoming less than one millisecond at EOD frequencies above 500Hz and creating significant demands for rapid transport on the Na, K-ATPase. Because the voltage-gated Na^+ channels responsible for producing the EOD have undergone molecular evolution driven by positive selection in both the mormyrids and gymnotiforms, I examined the Na, K-ATPase α2 subunit for evidence of a similar pattern of positive selection. I further hypothesized that increased positive selection occurred within lineages that emit higher frequency EODs. I found evidence for positive selection acting on the Na, K-ATPase α2 subunit of gymnotiforms with both low and high frequencies, while purifying selection occurred within the mormyrid lineage. Eighteen amino acid sites within functionally important regions of the Na, K-ATPase protein were identified as possibly under positive selection and therefore of

interest in future studies aimed at determining the functional consequences of molecular evolution in the Na, K-ATPase.

Chapter 1: Evolution of Animal Communication Systems – The Role of Energetics

Monkeys bare their teeth, passerine birds emit alarm calls in the presence of predatory hawks, and ants leave pheromone trails all with the same goal: to prompt a specific response from a target receiver. Across these various modalities of animal communication, signals have evolved because they confer adaptive advantages. These advantages range from getting the attention of potential mates, to the prevention or resolution of conflicts. Communication with conspecifics may also provide an organism with important information about their environment, for example, when one sounds an alarm call about nearby predators or signals that there is a nearby food source. Different communication modalities have their own advantages. For example, the visual system relies on external energy for an organism to be able to see signals from others and therefore may not be as energetically costly as other systems. However, when this external energy is not available and the visual system is therefore not as effective, auditory systems where the organism produces its own vocalizations allow for continuing communication. These advantages and signaling effectiveness are important in the development of stable communication systems.

Signaling systems have also been shaped by their associated costs which include opportunity costs, predation risks, and metabolic costs of signaling (Bradbury and Vehrencamp, 2011). This results in signaling systems that reflect the balance of a signal's costs and benefits to the organism. The primary costs associated with communication signals are risk of exposure to predators and energetic expenditure (Bradbury and Vehrencamp, 2011). For example, sexual advertisement signals can be subject to 'eavesdropping' resulting in mating calls that also attract predators. Risks of

eavesdropping by predators can be mitigated in many cases. For example, a singing bird may stop singing in the presence of predators while other animals, like the Tungara frog, may instead vocalize at night when fewer predators are active.

Animal signaling systems also require varying degrees of energetic investment (reviewed by Markham et al., 2016; Stoddard and Salazar, 2011). Some signals, like bright feathers or pigmentation, only require an initial energy investment during development. Other signals, like birdsong and prairie dog vocalizations incur energetic costs for every call, with increasing signal frequency incurring corresponding increases in metabolic cost. In most cases, an organism can simply stop signaling to reduce energetic costs, but this comes at a loss of the signal's function. For example, a silent bird might be conserving energy, but it is also attracting fewer possible mates or potentially losing territory to a rival. In other cases, if it is important to continue signaling even during times of low energy availability, this energetic expenditure comes at the cost of other important activities such as reproduction, foraging, or maintaining immune function.

The evolution of stable communication systems relies on signal honesty, where the signal provides accurate information about the associated attributes of the signaler or the environment. Two leading hypotheses attempt to explain how the balance of costs and benefits results in an honest signal. The handicap principle suggests that honesty in a signaling system occurs because animals of a lower quality cannot incur the cost of signaling and therefore prevents them from bluffing over their willingness to escalate fights or desirability as a mate (Zahavi, 1975). Another hypothesis suggests a signal is an 'index' that is honest because it is impossible to bluff (Smith and Harper, 1995).

Some signals may also develop out of pre-existing sensory biases. For example, a female could have preference for a trait that does not actually give information about the quality of a male, like having a preference for male coloration similar to colors of typical food items. The male's coloration may be associated with food, with the result of commonly being selected as a mate by females. This trait and preference then becomes more likely to show up in following generations, ultimately resulting in a stable system (Bradbury and Vehrencamp, 2011).

Communication Signals and Active Sensory Systems

The cost-benefit tradeoffs of signaling are different in cases where animal communication systems are coupled to an active sensory modality. The most important difference is that signal reduction or cessation will reduce signal costs at the expense of sensory performance necessary for navigation and foraging. For bats that rely on echolocation, signal cessation causes the loss of valuable sensory input from the environment. This is also the case for the South American gymnotiforms and African mormyrids, two orders of weakly electric fish that generate electric fields for the purpose of communication and electrolocation.

Active sensory systems have several advantages including the ability to control the characteristics of the signal or ability to signal when required external energy might not be available (Nelson and MacIver, 2006). For the signals of weakly electric fish, generating their own sensory signals allow them to navigate their environment and communicate with conspecifics even at night and in murky waters, when their visual system is less effective. While this is a similar benefit to that of echolocation in bats, the ability to generate electric fields has additional limitations and advantages. Specifically,

while the range of signaling is limited for these fish, there are no echoes or environmental filtering of the signal, which means the signal received is accurate to the signal generated (Hopkins, 1999).

In the case of weakly electric fish, signaling has developed under pressures to balance effective sensory performance, communication, mate attraction, and the associated predation and energetic costs of the signals. In many species of these fish, competition amongst males can often result in more conspicuous and energetically demanding signals, while overall energetic demand and risk of predation drives both sexes' signals to become more energetically efficient and less detectable by electroreceptive predators (Salazar and Stoddard, 2008; Stoddard, 1999; Stoddard and Markham, 2008). In what seems to be an effort to conserve energy, many species display circadian rhythms in regards to signal amplitude, duration, and frequency, with these parameters decreasing during daytime when nocturnal electric fish are inactive and increasing during nighttime periods of activity (Markham et al., 2009; Stoddard et al., 2007). Often the magnitude of circadian variation is larger in males than in females, suggesting that the additional energetic demand of signaling for males results from sexual selection for particular signal traits (Salazar and Stoddard, 2008).

The Electric Communication and Sensory Systems of Weakly Electric Fish

Weakly electric fish generate electric organ discharges (EODs) as communication and short range sensory signals using specialized electric organs (EOs). Electrogenesis has evolved independently multiple times in bony fish, including two orders of freshwater fish, the South American gymnotiforms and the African mormyrids (Moller, 1995). Although the two freshwater lineages evolved independently, there are

several similarities in their EOs and EODs consistent with convergent evolution of these traits. The estimated time for evolution from a non-electric ancestor is similar in both orders, occurring (~100 MYA) right around the final separation of the continents (Lavoué et al., 2012). Both lineages also had similar evolutionary delays between initial development of passive electroreception and the myogenic electric organ needed for active electrosensation (Lavoué et al., 2012). These similarities make these lineages strong candidates for comparative analyses of pathways leading to new systems and the role of these systems in speciation (Lavoué et al., 2012).

Both orders of freshwater electric fish are diverse and broadly distributed (Albert and Crampton, 2005). Gymnotiforms are found throughout South America, including the Amazon basin, a location of remarkable diversity in other organisms. The diverse gymnotiform families can be differentiated by head and snout shape and the presence or absence of dorsal organs, caudal fins, and teeth. Differences in jaws, mouth, snout, and head are also some criteria in differentiating between the different genera (Albert and Crampton, 2006). Snout and head morphologies can also be sexually dimorphic, with the genus *Apteronotus* demonstrating the largest range, possibly due to their aggressive nature and tendency to engage in more conflict (Albert and Crampton, 2006). More recent phylogenies based on both morphological characteristics and molecular markers have provided the highest resolution of species within the gymnotiform clade (Tagliacollo et al., 2016). Mormyrids also show a lot of diversity and represent a large part of the biomass of African fish. Mormyrids are found throughout the Nile river and in most of the freshwater habitats south of the Sahara desert, especially in rivers and streams (Hopkins, 1986). Many have long snouts

specialized for feeding and sensation (Hopkins, 1986). Many species can only be differentiated based on the species specific EOD phases and duration.

Within the broad diversity of freshwater electric fish, there are only two species capable of generating strong electric fields to stun prey or repel attackers, the South American electric eel (*Electrophorus electricus*) and African electric catfish (*Malapterurus electricus*). While given the misnomer of 'eel,' the electric eel is in fact the only representative of the gymnotiform genus *Electrophorus*. The electric eel uses a high voltage attack to induce full body tetanus in prey, therefore temporarily preventing voluntary movement (Catania, 2014). The eel is also unique in having no post-coelomic tail, having the largest gymnotiform body that continues to grow throughout its long lifespan (2+ meters, up to 20 years in captivity), and having 3 distinct electric organs (Hunter's Organ, Sachs Organ, and Main Organ).

Electric Organs, EOD Production, and EOD Characteristics

All gymnotiforms have larval myogenic EOs that are replaced in most cases by adult electric organs also derived from skeletal muscle, extending along ~80-90% of the fish's length. An exception to the adult myogenic electric organ is the gymnotiform genus *Apteronotus*, whose electrocytes are actually the elongated spinal motoneurons that once innervated the myogenic larval EO. The electric organ of all mormyrids is also derived from skeletal muscle, but compacted into the fish's caudal peduncle (Hopkins, 1986). Electrocyte innervation in mormyrids is via a stalk system often resulting in complex multi-phasic waveforms that are species specific in EOD phases and duration. The exception to this body plan and innervation is also the only wave-type

mormyrid representative, *Gymnarchus niloticus*, with both being similar to that of the gymnotiforms (Hopkins, 1986).

Electrocytes are large, non-contractile, and highly insulated electrically excitable cells. Both gymnotiforms and mormyrids have several similarities in regulation of genes for development of these characteristics. Two collagen genes for cell insulation are upregulated in the electric organs of both gymnotiforms and mormyrids, as are several IGF genes which could contribute to cell size (Gallant et al., 2014). Several genes involved in excitation contraction coupling and muscle contraction are downregulated in both gymnotiforms and mormyrids, with gymnotiforms lacking the machinery for contraction completely, while the machinery of mormyrids is just unorganized (Gallant et al., 2014). It was previously identified that for some of these skeletal muscle specific proteins, like sarcomeric proteins, mormyrids express several paralogs that gymnotiforms post-transcriptionally repress (Gallant et al., 2012). In differences between electrocytes and myocytes in electrical excitability, genes for a voltage-gated Na^+ channel and regulator (*scn4aa* and *fgf13a*), as well as the Na, K-ATPases and their regulators (*atp1a2a*, *atp1a3a*, and *znrf2a*) are all upregulated in the EOD of mormyrids and gymnotiforms (Gallant et al., 2014). This similar expression of common genes and regulators suggests utilization of many of the same pathways and transcription factors in the formation of electric organs.

Electrocytes generate the EOD by producing action potentials (Figure 1). The electrocyte membrane depolarizes when there is an influx of Na^+ through voltage-gated Na^+ channels, and repolarizes due to an efflux of K^+ through voltage-gated K^+ channels. The movements of these ions are driven by the concentration gradients of the ions

across the membrane of the cell, which are restored after each action potential by the Na, K-ATPase (Bean, 2007). The EOD is the result of all the electrocytes' simultaneous or near-simultaneous action potentials summing together, both in series and parallel (Aguilera and Caputi, 2003; Aguilera et al., 2001; Caputi, 1999). The rate of EOD generation is controlled by a pacemaker nucleus located in the midline medulla. This pacemaker nucleus consists of approximately 50-100 pacemaker neurons that are coupled by chemical and electrical synapses to the other pacemaker neurons allowing them to fire in synchrony. Pacemaker neurons connect to relay cells that project to specialized electromotoneurons which then innervate the electrocytes within the EO at a cholinergic synapse that resembles the neuromuscular junction (Bennett, 1961; Markham, 2013a)

Weakly electric fish are divided into two categories, wave-type fish and pulse-type fish. Wave-type fish generate EODs at fixed rates, with the interval between EODs roughly the same as the EOD duration. Pulse type fish generate EODs at irregular rates, with long intervals between individual EODs. Wave-type fish produce EODs over a very wide range of frequencies with the lowest known frequency being that of *Sternopygus branco* at approximately 30 Hz, while *Apteronotus sp.* fire at up to 2200 Hz (Albert and Crampton, 2005). The high-frequency Apteronotids have the largest medullary pacemaker nucleus (Albert and Crampton, 2005). While firing at these high frequencies is likely energetically costly, it allows faster sensory sampling of rapidly changing environments while also shifting the peak energy of the signal to higher frequencies that are less detectable by electroreceptive predators (Stoddard and Markham, 2008). Among the ~200 species of gymnotiforms there are dozens of wave-

type species and the wave-type clades are derived from pulse-type ancestors. In contrast, within the African mormyrids, there is just one known wave-type species (*G. niloticus*) which is basal to the remaining ~200 mormyrid pulse-type (Hopkins, 1986).

Electrosensory Mechanisms and Sensory Performance

Weakly electric fish obtain high-resolution (millimeter-scale) images of their environment because the electrosensory system can analyze object resistance and capacitance separately (von der Emde, 2006), an ability that has been said to be analogous to 'electric color' (Sawtell et al., 2005). However, this image is limited in area around the fish's body so that the fish must move in order to visualize more of the environment. The size of the imaged area is influenced by several factors including water conductivity and EOD amplitude. The electric field generated by most gymnotiforms is very weak and as it moves away from the body, amplitude decreases as an inverse square of distance. As a result, the effective signaling range is usually not more than a body length, and to double this distance, EOD amplitude must be increased eight-fold (Hopkins, 1999).

By sensing the alterations of their own EOD and modulations of conspecific EODs, weakly electric fish are capable of imaging their world and communicating within this electric modality. Objects sensed by the fish can be more conductive or more resistive than surrounding waters. More conductive objects cause electric field lines to converge while more resistive objects cause them to diverge. These alterations to EOD waveform are sensed by electroreceptors along the fishes' bodies. Information is also gathered from the spatial alteration of the EOD, with a prey object causing more localized and lower frequency distortions (less than 10 Hz) whereas conspecifics' EODs

create more global and higher frequency distortions (more than 50 Hz). As a communication signal, interactions with signaling conspecifics can convey valuable information such as aggression and mating opportunities (Bullock et al., 2005).

Hormonal Regulation of EOD Waveform

Like many other communication signals, EODs are under hormonal control for several purposes, including rapid signal modulations during social interactions, modulating the signal in response to long-term social conditions, and regulating signal amplitude to conserve energy. Rapid socially-induced changes to EOD waveform are mediated by the peptide adrenocorticotropic hormone (ACTH) and occur within a matter of minutes (Markham and Stoddard, 2005). In *Sternopygus macrurus* and *Eigenmannia virescens*, such rapid changes in EOD amplitude are caused by insertion of Na^+ channels into the membrane to increase Na^+ current by as much as 50% (Markham, 2013a; Markham et al., 2009). Serotonin also quickly and transiently enhances masculine EOD characteristics, providing some information on dominance (Stoddard et al., 2003).

Androgens masculinize EOD waveforms over a timescale of days to weeks in response to prevailing social conditions. While having no effects in mormyrid species without EOD sexual dimorphism, testosterone doubles EOD duration in females and immature males in a sexually dimorphic mormyrid species (Bass and Hopkins, 1983). In the gymnotiform *S. macrurus*, androgens also increase EOD duration through changes of the electrocyte membrane's electrical properties (Mills et al., 1992). These androgen-mediated changes to EOD duration result from reductions in the rate of Na^+ current inactivation (Ferrari et al., 1995; McAnelly and Zakon, 1996). In *S. macrurus*,

the sexual dimorphisms in EOD waveform appear to be in part due to estrogens and androgens having opposing effects, with estradiol treatment acting to increase inactivation rates in the same Na^+ current to shorten female EOD duration and increase frequency (Dunlap et al., 1997). Consistent with the hypothesis that EOD duration may be an honest indicator of testosterone levels and other characteristics, circulating testosterone levels correlate with EOD duration and other reproductive traits for both male and female *Brachyhypopomus gauderio* (Gavassa et al., 2011). As indicators of male physiological state, EOD waveforms also are under control of social isolation, social competition, and the specific order of these social conditions, an effect mediated by steroid hormones (Salazar and Stoddard, 2009).

Hormonal regulation of EOD amplitude is also a mechanism for moderating the energetic demand of signaling. When under acute metabolic stress, *E. virescens* EOD amplitude decreases (Reardon et al., 2011). During chronic metabolic stress caused by food deprivation, EOD amplitude also decreases, with amplitude levels recovering after feeding, a process mediated by leptin (Sinnett and Markham, 2015). Reduction of EOD amplitude during food deprivation is likely a proactive mechanism to conserve energy during metabolic stress, rather than an absolute shortfall of energy in the electric organ, as EOD amplitude transiently increases when faced with a social challenge or ACTH treatment (Sinnett and Markham, 2015).

Costs of Electric Sensory and Communication Signals

Predation Risk

As for most communication signals, electric signaling may expose weakly electric fish to predation. Some piscivorous predators are electroreceptive, allowing

them to track and locate weakly electric fish as prey items. These predators rely on passive electrosensory receptors that respond only to low frequencies (below 100 Hz). Thus, EODs with low-frequency power content are more readily detected by electroreceptive predators. The African Catfish, *Clarias gariepinus*, is a common predator of mormyrid weakly electric fish (Hanika and Kramer, 2000) while South American gymnotiforms were found to be some of the main prey for the catfish *Pseudoplatystoma tigrinum*. These catfish more readily detect EODs of longer duration (thereby exhibiting enhanced low-frequency power). A longer EOD is characteristic of males for many species, ultimately matching sizes of the fish in stomach contents of electroreceptive predators (Hanika and Kramer, 2000). The electric eel, a predator of other gymnotiforms, also is more sensitive to monophasic over biphasic waveforms, likely because of the enhanced low-frequency content of monophasic waveforms (Stoddard, 1999).

Unlike visual signals, 'camouflage' is not possible for electric signals because the fish cannot match the conductivity of their environment (Ruxton, 2009). Because the electric communication signals also serve as an active sensory system, going 'silent' to avoid detection by predators would compromise sensory input. A small number of gymnotiform species, such as *Gymnotus carapo*, have been known to use this strategy (Stoddard and Markham, 2008). Wave-type fish cannot cease or significantly reduce the frequency of signaling due to the physiology of the pacemaker in these species, and accordingly, signaling is continuous throughout the lifespan. For these reasons, electric signaling may be unique among animal communication signals as predation pressures have produced more complex signals, instead of the more common signal constraint.

The result is electric signals with peak power in higher frequency ranges (Stoddard, 1999).

For pulse fish, like *B. gauderio*, their biphasic waveform with an initial head positive phase followed by a negative phase shifts the peak power of the signal to higher frequencies. In wave-type species, such as *E. virescens*, the sinusoidal EOD waveform is centered on a slightly negative voltage rather than 0 volts through physiological mechanisms that still are not understood (Bennett, 1961; Markham, 2013a). In both cases the net result is to reduce the signal's detectability by electroreceptive predators by masking or eliminating low-frequency components of the signal (Stoddard and Markham, 2008)

Energetic costs of EOD Production

Estimates for the cost of EOD production have varied widely over the past 40 years and are assumed to vary for the different waveforms and frequencies. Early predictions estimated the cost of EOD activity to be approximately one percent of basal metabolic rate (Hopkins, 1999). These estimates were apparently supported by measurement of oxygen consumption in several species of electric fish which indicated that respiration was not strongly associated with EOD waveform but varied across species and was dependent on body mass. Oxygen consumption was furthermore independent of a fish being wave or pulse-type. Overall, metabolic rates for electric fish were no higher than what would be predicted for nonelectric teleost fish at neotropical temperatures (Julian et al., 2003), a finding that could be interpreted to mean that electrogenesis adds little to overall metabolic rates or that electric fish have a lower metabolism overall.

More recently, both theoretical analyses and direct experimental results suggest that EOD production is, in fact, metabolically costly. Two independent theoretical approaches to predicting the metabolic costs of EOD production placed the relative energetic investment at 10-30% of the animal's daily energy budget (Markham et al., 2013; Salazar et al., 2013). These estimates were supported by direct experimental evidence showing that EOD production can require up to 22% of the daily energy budget in pulse fish (Salazar and Stoddard, 2008) and 30% or more of the daily energy budget in wave-type fish (Lewis et al., 2014). These findings place the communication signals of weakly electric fish among the most metabolically expensive animal communication signals (Markham et al., 2016). Additional evidence for the metabolic costs of EOD signaling comes from the effects of metabolic stress on EOD signal amplitude. In the wave-type fish *E. virescens*, EOD amplitude is reduced under acute metabolic stress from hypoxia (Reardon et al., 2011). During more prolonged and mild metabolic stress from food restriction, *E. virescens* also reduces EOD amplitude over longer timescales (Sinnett and Markham, 2015).

Ultimately, the metabolic cost of EOD generation derives primarily from the metabolic costs of the electrocyte action potentials (Salazar et al., 2013), which result from the energy required by the Na, K-ATPase to restore ionic gradients after each action potential (Carter and Bean, 2009). The metabolic cost of action potentials ultimately depends on the amount of Na^+ that enters the cell during the action potential because the Na, K-ATPase must hydrolyze one ATP for each three Na^+ ions returned to the extracellular space (Attwell and Laughlin, 2001; Howarth et al., 2012; Niven and Laughlin, 2008).

Most action potentials are energetically wasteful to some degree because Na^+ and K^+ channels are open concurrently during at least part of the action potential. As a result, Na^+ is entering the cell without altering membrane potential, although ATP is still necessary to remove it. In high frequency neurons this overlap is often necessary resulting in decreased metabolic efficiency (Carter and Bean, 2009). Signaling can be made more efficient by rapidly inactivating Na^+ channels, and K^+ channels that activate only during the latter phases of the action potential. Na^+-activated K^+ channels (K_{Na} channels) have been found to minimize this overlap of Na^+ influx and K^+ efflux. *E. virescens* are currently the only known weakly electric fish where K_{Na} channels terminate the action potential, rather than voltage-gated K^+ channels, and numerical simulations suggest that electrocyte K_{Na} channels are necessary for maintenance of high frequencies, while also reducing energetic cost by 30% (Markham et al., 2013).

Despite the energetic savings conferred by K_{Na} channels in *E. virescens*, direct measurements of Na^+ influx during the action potential in *E. virescens* showed that 6.6 $x10^{10}$ Na^+ ions enter the cell with each action potential, requiring $2.2x10^{10}$ ATP molecules per action potential to restore ionic gradients, a value two orders of magnitude more than that of central neurons (Lewis et al., 2014). In the low-frequency pulse-type fish *Steatogenys elegans* computational models constrained by physiological data predict an influx of 9.76×10^9 Na^+ ions per electrocyte action potential and a predicted energy expenditure of 3.25×10^9 ATP per action potential, a value approximately an order of magnitude lower than the energetic cost per EOD measured in *E. virescens*.

Beyond the sometimes extreme metabolic demands created by the Na, K-ATPases following each action potential, a related issue that focuses our attention on this molecule is that the time available to restore ionic gradients can be very short, depending on EOD frequency. For example, in *E. virescens* with an EOD frequency of 500 Hz, the Na, K-ATPases have less than one millisecond to remove ~6 x 10^{10} Na^+ ions before the next action potential. This task is further complicated by the large disparity between the flux of Na^+ through ion channels (10^7 ions per second) and the rate of active transport by the Na, K-ATPase (10^3 ions per second) (Holmgren et al., 2000; Morais-Cabral et al., 2001). Because wave-type fish emit EODs round-the-clock, the electrocyte Na, K-ATPases are functioning under these demands 24 hours a day.

The purpose of this research is to examine how electrocyte Na, K-ATPases contend with the challenges of extremely large ionic fluxes and thereby give rise to the primary energetic cost of EOD production. One obvious hypothesis is that electrocytes express a very large number of pumps within the electrocyte membrane. A second hypothesis, which is the focus of this work, is that molecular evolution of the Na, K-ATPases has modified them to produce increased efficiency or speed. The most likely explanation is a combination of these two adaptations.

For the high frequency *E. virescens*, electrocytes do express Na, K-ATPases at very high densities and these are located on both the anterior and posterior faces of the electrocyte (Ban et al., 2015; Schwartz et al., 1975). Little is known about the functional properties of electrocyte Na, K-ATPases for weakly electric fish. However, preliminary data found in both *E. virescens* and *E. electricus* a genomic single amino acid substitution (isoleucine to valine) that increased pump turnover by 40% in giant squid

where this substitution arises from RNA editing (Colina et al., 2010). This suggests the tantalizing possibility that additional amino acid substitutions in electric fish might further enhance pump turnover rate. Such a scenario would be consistent with the rapid molecular evolution of voltage-gated Na^+ channels, another key molecular component necessary for the biophysical generation of these signals (Arnegard et al., 2010).

The evolution of such a costly high-frequency and high-current signaling system raises many questions regarding the role of the Na, K-ATPase in determining the energetic demands of this signal as well as making high-frequency signaling possible from a biophysical standpoint. The goal of this research was to examine if positive selection acted on the Na, K-ATPases of weakly electric fish and if so, if there was additional positive selection acting on those clades that generate wave-type EODs at higher frequencies.

Figures

Figure 1: Gymnotiform and Mormyrid electrocyte and EOD diversity. Electrocytes are represented by line drawings. Synaptic innervation is represented by triangles (active synapses are black, quiet synapses are gray). Excitable membranes are bold dashed lines, with arrows representing current direction. Below each electrocyte is the EOD waveform resulting from synaptic innervation. **Left Top Panel:** Monophasic EODs are produced by electrocytes with only an electrically excitable posterior face. After innervation, one action potential results in current flowing towards the head with the resulting EOD waveform composed of a single phase in the head-positive direction. **Left Bottom Panel:** Biphasic EODs are produced by electrocytes with electrically excitable posterior and anterior faces. Phase 1 (P1) of the EOD is produced after synaptic innervation of the posterior face. The resulting action potential produces current flowing towards the head and the EOD phase is head-positive. The second phase (P2) is the result of an action potential from the non-innervated anterior face, with the resulting current flowing towards the tail and a second head-negative phase. **Right Panel:** There are several ways to get a multiphasic EOD waveform. Gymnotiform *Gymnotus carapo* produces a multiphasic EOD via innervation of three regions of the electric organ (red, blue, and green) composed of three types of electrocytes. One type is only innervated on the posterior face, while the other two types have synaptic innervation on both the anterior and posterior faces (Macadar et al., 1989). The electrocytes with only posterior innervation produce an action potential on the posterior face followed by one on the anterior face (red). One type of the electrocytes with double innervation produces an action potential on both faces (blue), while the others activate the anterior producing a postsynaptic potential, followed by posterior innervation producing an action potential (green). The resulting waveform after the non-simultaneous innervation of the 3 electric organ regions has two head-negative (a and b), followed by a head-positive (c), and finally another head-negative component (d). *Gymnotus carapo* illustrations modified from (Caputi, 1999). *Brienomyrus niger* is a mormyrid representative with a multiphasic EOD resulting from stalk innervation of a single electrocyte population. The stalk innervation begins at the anterior face of the electrocyte, which it then enters before meeting the posterior face. When innervated, the action potential within the stalk propagates through the entrance into the electrocyte, resulting in a head-negative first phase (a). An action potential then occurs on the posterior face resulting in the second phase being head-positive, with the final action potential on the anterior face producing a final head-negative phase (c). Mormyrid illustrations adapted from (Hopkins, 1999). Electrocyte discharge diagrams modified from (Bennett and Grundfest, 1961).

Figure 1

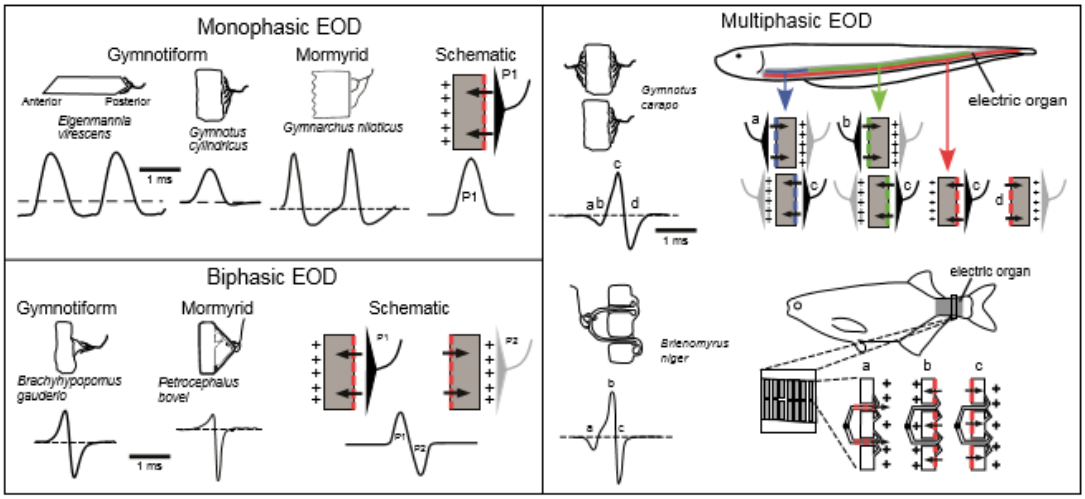
Monophasic EOD
Gymnotiform
Mormyrid
Schematic
Anterior
Posterior
Eigenmannia virescens
Gymnotus cylindricus
Gymnarchus niloticus
P1
1 ms
Biphasic EOD
Gymnotiform
Mormyrid
Schematic
Brachyhypopomus gauderio
Petrocephalus bovei
P1
P2
1 ms
Multiphasic EOD
Gymnotus carapo
electric organ
a
b
c
d
1 ms
Brienomyrus niger
electric organ

Chapter 2: The Na, K-ATPase

The Na, K-ATPase was originally identified as a molecule for ion regulation and transport in 1957 by Dr. Jens S Skou, a finding for which he received the Nobel Prize in 1997 (Skou, 1957). The Na, K-ATPase, also known as the 'pump' throughout this thesis, is a member of the P-type ATPase family. The designation of being a 'P-type' ion transporter refers to a conserved phosphorylation step of the pump during the catalytic cycle. The P-type pumps are separated into 5 subfamilies based on conserved regions and further divided into subclasses according to their ion specificity. The PII ATPase subfamily consists of several pumps including the Na, K-ATPase, Sarcoendoplasmic Reticulum Ca-ATPase (SERCA), gastric H, K-ATPase, and H-ATPase. Of these, only the Na,K-ATPase and gastric H, K-ATPase exchanger are antiporters (Vedovato and Gadsby, 2014). The similarity of the Na, K-ATPase to other P-type pumps (like SERCA) allows for predictions about enzyme structure and function (Jorgensen et al., 2003; Kaplan, 2002).

In the case of the Na, K-ATPase, its role in establishing electrochemical gradients is also linked to many other cellular processes such as Na^+ coupled transport and maintenance of osmotic balance. Another important function of the pump is maintenance of transmembrane ionic gradients, a necessary condition for bioelectric signaling in excitable cells such as neurons and myocytes. A functional Na, K-ATPase requires two subunits, one α subunit and one β subunit. A third γ subunit is an accessory component not necessary for function, but has been implicated in modulation of pump function and regulation (Crambert and Geering, 2003). The α and β subunits insert into the membrane of the endoplasmic reticulum independently and there the two necessary

subunits are coupled together through the actions of other proteins prior to vesicular transport of the pump complex to the plasma membrane (Ackermann and Geering, 1992; Beggah et al., 1996).

Several known isoforms of the Na, K-ATPase subunits are found in organisms ranging from platyhelminths to teleost fish to mammals, suggesting that these pumps diverged fairly early in evolution. Multiple genes encode several isoforms of each Na, K-ATPase subunit, which can be alternatively spliced in some cases producing even more variation (Kaplan, 2002). Different isoforms of the subunits have diverse patterns of tissue and cell-compartment specific expression, which are under the control of various hormonal and developmental regulators. In rats, a canonical mammalian model, the most common isoform combination is the α1 and β1 complex, which is found in all tissues (Blanco and Mercer, 1998). However tissue-specific expression patterns differ for the remaining subunit isoforms. Since α1 is considered ubiquitous, it is known as the "housekeeping" isoform. The α2 subunit is primarily found in muscles, nerves, and the adult heart, while α3 is expressed predominantly in nervous tissue, brain, and fetal heart. α4 is only found in the testes and is involved in sperm motility (Jimenez et al., 2011; Segall et al., 2001). The β subunit isoforms are similar in that β1 is considered ubiquitous, β2 is typically found in muscle and nervous tissue, and β3 in liver, lung, and testis. While most research is done on the complexes of a single α1 and β1, more complex associations between multiple α subunits have been identified. These associations are dependent on cytoplasmic region Glycine 554-Proline 785 (Koster et al., 1995). The various combinations of the four α isoforms and three β isoforms leads to pumps with a wide range of unique functional properties (Blanco and Mercer, 1998).

The α subunit is the main functional subunit of the Na,K-ATPase, consisting of ~1000 amino acids with numerous binding sites for regulatory ligands (Morth et al., 2011; Morth et al., 2007; Morth et al., 2009; Ogawa et al., 2009). There are also several sites that undergo phosphorylation from various kinases, a mechanism for regulating the pump's role in signal transduction (Kanai et al., 2013; Laursen et al., 2013; Nyblom et al., 2013). The α subunit has 10 transmembrane segments, connected by several extracellular and intracellular loops (Figure 1). At least two of the extracellular loops, M7-M8 and M9-M10, interact with the β subunit. Large portions of the intracellular α subunit region make up 3 functionally important domains: the actuator 'A' domain, the nucleotide binding 'N' domain, and phosphorylation 'P' domain (Figure 2).

The β subunit is composed of ~300 amino acids with only one transmembrane segment. The β subunit also has a role in localization of the α subunit to the plasma membrane. The β subunit is a small glycoprotein whose initial function is essentially acting as a chaperone protein, which is required for proper insertion of the α subunit into the cell membrane (Geering, 2001). The β subunit interacts with the α transmembrane segment M7 and M10 and, while it assists with regulation of ion transport, it does not actually catalyze the reaction (Kanai et al., 2013; Morth et al., 2011; Morth et al., 2007; Morth et al., 2009). The large extracellular region of the β subunit is involved in occluding ions during pump conformational changes.

The γ subunit is a member of the FXYD protein family and is ~ 60 amino acids long. It is often involved in regulation of the α subunit by modification of its affinities for various ligands (Cheung et al., 2013). Members of the FXYD family are widely distributed, and often found in electrically excitable tissues or tissues that are usually

transporting fluids and solutes. Four of seven FXYD proteins have been identified as tissue specific regulators of Na,K-ATPase function, with the remaining three proteins not yet well characterized (Crambert and Geering, 2003). Each isoform has distinct effects on overall pump function. Thermal denaturation experiments suggest α and γ associate at α M8-M10, while a cavity formed by M2, M6, and M9 have been suggested by density maps produced from electron crystallography (Crambert and Geering, 2003). The γ subunit modulates pump function in many ways including decreasing pump affinity to Na^+, changing pump affinity to potassium, or increasing sensitivity to ATP (Crambert and Geering, 2003). However, because the α subunit is the main functional subunit of the Na,K-ATPase, this research will focus on the α subunit.

The α Subunit

The binding site for ATP is within the N domain, with the ATP eventually phosphorylating a highly conserved aspartic acid (369D of the DKTGTL motif) within the P domain (375 in full alignment appendix figure). The A domain pairs this reaction with the necessary changes in the transmembrane segments to open either the Na^+ or K^+ binding sites. The pump cycle is often greatly simplified but actually consists of more than two dozen kinetic steps, changes to any of which can modify pump function. The catalytic cycle is often represented by the Post-Albers cycle, which demonstrates the steps involved in ion transport (Figure 3) (Albers, 1967; Post et al., 1972).

Whether Na^+ or K^+ ions bind within the pump depends on pump conformation. A pump in the E1 conformation has a binding pocket with open sites for three intracellular Na^+, binding of each being an individual kinetic step. Within the cation binding pocket and transmembrane segment 4, there is a vital glutamic acid residue,

which in the E1 state interacts with cytoplasmic ions and helps with occlusion by capping the cavity. When ATP phosphorylates the pump, ADP is released and the pump changes to the E2 conformation, releasing the Na^+ ions to the extracellular environment and opening two binding sites for potassium. When the pump is dephosphorylated, the conformation of the pump returns to E1. ATP binds once again, releasing K^+ ions to the cytoplasm and allowing the cycle to begin again. For correct transitioning between the conformations, all three domains are moving throughout this cycle, with the P domain rotation leading N domain movement and A domain rotation to lock onto the P domain. With the pump working to create the vital ionic gradients, its function relies on the membrane potential. The Na, K-ATPase catalytic cycle happens at the highest rate at more positive membrane potentials and becomes inhibited at more negative potentials. This voltage dependence is the result of both the negative membrane potentials and high extracellular Na^+ concentration retaining bound Na^+ ions in the pump binding sites instead of being released.

The different α subunit isoforms exhibit different functional properties. Compared to α1, both α2 and α3 have higher affinities for ATP. While ion affinities between α1 and α2 are similar, α3 is considered to have a lower affinity for Na^+ but a higher affinity for K^+(Jewell and Lingrel, 1991). With respect to catalytic rate, both α2 and α3 isoforms are slower than α1 with rates approximately 40 and 50 percent that of α1, respectively (Segall et al., 2001). These differences for α2 appear to be due to the shifting of the conformational equilibrium to the E1 conformation. However, the conformational equilibrium of α3 is similar to that of α1, and therefore the differences likely result from more complex factors (Segall et al., 2001). While the higher K^+

affinity is considered secondary to the differences in reaction rates before and after K^+ activated dephosphorylation of the pump, the lower Na^+ affinity appears to be an intrinsic difference of binding cations. Some properties, like an increased affinity for a certain ion, can be due to the actual isoform of one subunit, or due to association with other subunits with distinct characteristics. For example, ATP affinity of α1 could increase to be similar to that of α3 through association with specific γ subunits (Segall et al., 2001). The different isoform characteristics and subunit combinations of the functional pump complex likely aid in tuning pump function to the demands of various tissues. Some identified examples include the lower affinity for Na^+ of α3 possibly being beneficial in high frequency firing neural tissue, so the pump only becomes active when intracellular Na^+ is high, while the decreased inhibition of α2 in lower pH conditions could be useful in skeletal muscle (Segall et al., 2001; Segall et al., 2003).

More details on pump structure and therefore function are currently under examination through examination of crystal structures of Na, K-ATPases from various organisms crystalized in different pump states. Several known crystal structures have been solved by x-ray crystallography, including the whole α1-β1-γ complex. A shark pump structure has provided information on a low affinity binding location for cardiotonic steroids, located between α M1, M2, and M4-6 (Håkansson, 2003; Kanai et al., 2013; Laursen et al., 2013; Morth et al., 2007; Nyblom et al., 2013; Ogawa et al., 2009; Shinoda et al., 2009; Toyoshima et al., 2011). Information gained via crystal structures is expected to contribute to our understanding of disease states associated with defects in the ion channels and pumps (Ashcroft, 2006).

Na, K-ATPase Regulation

With all the roles the Na, K-ATPase plays in the cell, along with all of the components and steps vital to proper pump function, any changes that modify pump function have the potential to produce disease states. For this reason, this molecule is under several different forms of regulation by hormones, transcriptional regulators, and compounds known as cardiac glycosides (Lopina, 2000). This means the pump can be a target of treatment for these diseases and disorders, as first described by William Witherling in 1785 in the use of foxglove (digitalis) in treatment of congestive heart failure (Silverman, 1989). Cardiac glycosides are steroid molecules that inhibit the Na, K-ATPase. An ether bond connects carbon 3 to a sugar group, while a lactone ring is joined at carbon 17 of the steroid ring. There are two groups of cardiac glycosides: Cardenolides with a 5-ring lactone and bufadienolides with a 6-ring lactone. Ouabain, oleandrin, and digoxin are examples of Cardenolides, and bufalin and hellebrin are bufadienolides.

When a cardiac glycoside, like digoxin, binds a Na,K-ATPase, it stabilizes the E2-P state, resulting in pump inhibition. Due to this inhibition, there is less removal of Na^+ from the inside of the cell. This increase in intracellular Na^+ means the $Na^+/Ca2^+$ exchanger (NCX), which moves 3 Na^+ into the cell to 1 $Ca2^+$ out, is also inhibited and results in an increase in intracellular calcium. SERCA2 is then able to increase calcium reuptake into the sarcoplasmic reticulum leading to the release of more calcium when stimulated, resulting in cardiac myocytes with faster, stronger contractions. Heart rate also slows because of the lengthening of the atrioventricular node refractory period. Due to these effects on the heart, the various cardiac glycosides must be used carefully due to possibility of cardiac toxicity (Gheorghiade et al., 2004).

Cardiotonic steroids can regulate the Na, K-ATPase via alterations of several pathways or cell components. Binding of the cardiotonic steroids may lead to downregulation of pump through tyrosine kinases, with this downregulation interacting with various pathways including ERK1/2, PKC, ROS production, PI3K, Akt, mTOR, and various cellular processes like autophagy and apoptosis. These pathways and processes altered by Na, K-ATPase function have been implicated in development of many kinds of cancers, and therefore have become targets of treatments, especially in those resistant to traditional chemotherapies (Chen et al., 2014). Even inhibition of the pump has been found to downregulate cancer cell proteins involved in this resistance (Mijatovic and Kiss, 2013). This may be through conformational changes due to interactions between the pump and the cardiotonic steroid, with the cardiotonic steroid possibly then able to move to the nucleus to affect transcription of proteins like tumor necrosis factor-α(TNF-α) (Durlacher et al., 2015). Surprisingly, patients treated with cardiac glycosides are at lower risk for development of various cancers. For this reason, the role of the pump in the development of cancer, as well as using cardiac glycosides for treatment of cancer, has been a growing field (Alevizopoulos et al., 2014; Babula et al., 2013; Dimas et al., 2014; Durlacher et al., 2015; Mijatovic and Kiss, 2013; Prassas and Diamandis, 2008).

Changes to pump expression have been implicated in causing several types of cancer. For example, malignant gliomas have been found to have cells with increased levels of α1, and ultimately increased resistance to apoptosis and ability to migrate. These abilities decrease when the pump is inhibited by a cardenolide (Lefranc and Kiss, 2008). In a cell line for human neuroblastoma, expression of both α1 and α3 are

necessary for cell survival, but silencing of only α3 prevents ouabain induced ERK1/2 signaling (Karpova et al., 2010). Levels of β2 mRNA were found to be less in human carcinomas and neuroblastomas, with β1 mRNA also decreased in some, but not all cancer types (Akopyanz et al., 1991). Therefore the role of the β subunit in cancer development and metastasis is of interest as well. The β subunit was also found to have a role in tumorigenesis via a role in the epithelial-to- mesenchymal transition. Dimerization of β subunits creates a bridge with roles in cell adhesion. Snail, or zinc finger protein SNAI1, a suppressor of E-cadherin, was also found to suppress β1 in cancer cells (Espineda et al., 2004). When β 1 is silenced through methylation via epigenetic regulation, the downregulation of β1 and e-cadherin can result in various cancers including renal cell and colorectal carcinomas (de Souza et al., 2014; Selvakumar et al., 2014).

The p38 MAPK signaling pathway, which promotes ERK1/2 signaling is involved in cell proliferation and apoptosis. P38 MAPK signaling is activated when the Na,K-ATPase is inhibited by ouabain binding which can ultimately result in apoptosis via several pathways including through Src kinase (Liu et al., 2007). Src kinase is a non-receptor tyrosine kinase that promotes cancer cell invasion, which is able to be suppressed through an α subunit tyrosine residue, so inhibition of the pump can result in upregulation and cell proliferation (Wang et al., 2009; Weigand et al., 2012; Ye et al., 2013).

The PI3K/mTOR pathway interaction with Na, K-ATPase is also involved in the proliferation or apoptosis/autophagy of cancer cells. The α subunit of the pump can regulate PI3K, upregulated when a regulatory p85 subunit is bound to the pump. These

interactions are dependent on PKC (Barwe et al., 2005). Upregulation of α subunit expression and PI3k are associated with more phosphorylation of phosphatidylinositol 4,5 biphosphate, which leads to Akt phosphorylation, stimulation of mTOR, and ability of cancer cells to proliferate while avoiding autophagy (Dai et al., 2013; Wu et al., 2013). Bufalin treatment has been found to lead to apoptosis in lung cancer via PI3K/Akt pathway, affecting expression of several proteins (Bcl-2, p53, caspase-3) and decreasing phosphorylation of Akt, MAPK ERK1/2, and p38 MAPK (Jiang et al., 2010; Zhu et al., 2012).

Alterations to Na, K-ATPase function are also implicated in many disorders besides cancer. Mutations of the different pump isoforms have been implicated in some instances of bipolar disorder, diabetes mellitus, Alzheimer's, Parkinsonism, and familial hemiplegic migraine type II (FHM) (Morth et al., 2009; Rose and Valdes, 1994; Yan and Shapiro, 2016). Changes to specific isoforms are likely responsible for different disorders. Certain mutations to α2 can lead to FHM type II as well as some other issues identified in mice like deficiencies in learning and anxiety (Gritz and Radcliffe, 2013). Mutations of α3 have been identified as leading to two different neurological diseases: alternating hemiplegia of childhood and rapid-onset dystonia Parkinsonism. Of the identified mutations leading to disease, all except one are specific to one of these diseases and while some functional changes of the mutations have been elucidated, mechanisms for most have not (Heinzen et al., 2014). The α3 subunit is also the target of amylospheroids, that bind within the 4^{th} extracellular loop (containing Asparagine 879 and Tryptophan 880), ultimately leading to neurodegeneration in Alzheimer's patients (Ohnishi et al., 2015). The central role of the Na, K-ATPase in so many disease

states indicates the central importance of this molecule for normal physiological function, and the potentially catastrophic consequences of mutations or dysregulation of this molecule. The opposite also can be true, where mutations and regulation of pump function can have adaptive consequences.

Regulation of pathways and expression of isoforms are not the only forms of pump regulation. RNA editing was recently identified as a novel mechanism of pump regulation in squid. Three codons underwent RNA editing leading to changes of typically highly conserved amino acid residues, with one being more uncommon and specific to certain tissues (Colina et al., 2010). This editing of a highly conserved isoleucine to a valine at location 877 is located in the seventh transmembrane segment and results in the loss of a single methyl group. While the other codons were found to be frequently edited, this I877V substitution was very rarely found in the periphery but almost 50% of the time in parts of the CNS. While this did not appear to significantly affect pump function at positive membrane potentials, at more inhibitory negative potentials, I877V edited pumps had an approximately 40% increase in pump turnover rate. This change in function was due to the shifting of pump voltage dependence, correlating with the release of Na^+ ions to the extracellular space (Colina et al., 2010). These authors surveyed cDNA sequences encoding the Na,K-ATPase of many other organisms, and found that, among published gene sequences, the I877V substitution was present only in the Na,K ATPase expressed in electric organ cells of electric eel (*Electrophorus electricus)* where the substitution is genomic (Colina et al., 2010).

The Na, K-ATPases of Weakly Electric Fish

In electrocytes from the main EO of *E. electricus*, western blot and IHC analysis identified distinct distribution of the Na,K-ATPase α1 isoform on the innervated face and α2 on the noninnervated face (Lowe et al., 2004). This distribution matched the different ouabain sensitivities of the faces, with the non-innervated face being 2.6 times more sensitive than the innervated (Lowe et al., 2004). More recent research has suggested that the three electric organs of *E. electricus* differ in levels of pump expression (with higher expression in the electric organs compared to skeletal muscle) and kinetic properties (Ching et al., 2015). In looking at expression levels of various skeletal muscle proteins in the mormyrid *Brienomyrus brachyistius*, western blot revealed expression levels of the Na,K-ATPase were similar in skeletal muscle and electric organ (Gallant et al., 2012). However, skeletal muscle had two isoforms of the pump compared to a single form in the electric organ (Gallant et al., 2012). RT-PCR and suppressive subtractive hybridization (SSH) revealed upregulation of certain copies while overall levels remained similar, ultimately leading to the hypothesis that the EO pumps may have kinetic enhancements to make up for the high demand on the pump in these cells (Gallant et al., 2012).

Molecular Evolution in Electric Organs of Weakly Electric Fish

The molecular evolution of voltage-gated Na^+ channels has been implicated in several examples of adaptive evolution, including development of TTX resistance in pufferfish, newts, and garter snakes, insensitivity to the sting of carbonic acid in naked mole rats, and insecticide resistance (Jost et al., 2008; Zakon, 2012). For weakly electric fish, it appears that molecular evolution of voltage-gated Na^+ channels gave rise to the

large diversity of EOD waveforms and the capacity for high frequency EOD signaling (Jost et al., 2008; Zakon, 2012; Zakon et al., 2009).

The whole genome duplication in the teleost lineage produced duplicate copies of voltage-gated Na^+ channel genes. Skeletal myocytes of non-electric teleosts express both copies of the voltage gated Na^+ channel, Nav1.4a and Nav1.4b, encoded by *scn4aa* and *scn4ab*. However, in gymnotiform and mormyrid electric organ, electrocytes express both copies while skeletal muscle lost expression of Nav1.4a (Zakon et al., 2006). After loss of expression in skeletal muscle, Nav1.4a in electric organs of many electric fish accumulated amino acid substitutions. These amino acid substitutions occurred in what are usually highly conserved locations and are involved in channel phosphorylation, toxin binding, and sites known to lead to channelopathies (Arnegard et al., 2010). These changes could be the result of relaxed constraint and/or positive selection acting on the channel, which can be measured by dN/dS (the ratio of rates of nonsynonymous to synonymous substitutions). For the *scn4aa* gene, expressed only in electric organ, the dN/dS averaged over the whole gene significantly increased for both gymnotiforms and mormyrids, while the ratio for *scn4ab* did not change (Arnegard et al., 2010). When comparing dN/dS ratios, the Nav1.4a orthologs of weakly electric fish had more amino acid substitutions than nonelectric fish, with many of them occurring in functionally important regions of the channel (Zakon et al., 2006). It also appears the Nav channel inactivation step is targeted in both mormyrids and gymnotiforms but in different manners. The gymnotiform Na^+ channels were modified at the receptor site for the channel's cytoplasmic loop responsible for inactivation, while the mormyrid channels were modified within the inactivation loop itself (Zakon et al., 2006).

Given this dramatic molecular evolution observed in the voltage-gated Na^+ channels expressed in electrocytes of weakly electric fish, I reasoned that similar patterns of molecular evolution would likely occur in the electrocyte Na,K-ATPase because this molecule is necessary for restoring Na^+ and K^+ gradients after the large ionic currents produced by the electrocyte action potential. This work will focus on the α2 subunit which is expressed in skeletal muscle and therefore most likely to be centrally important for the myogenic electrocytes of all electric fish clades except for the neurogenic EOs of the Apteronotids (Bennett, 1961; Bennett, 1971). In the research reported here, I gathered the *atp1a2a* coding sequences for multiple representatives of the gymnotiform and mormyrid clades and analyzed these for evidence of molecular evolution. I tested two specific hypotheses 1) high rates of molecular evolution occurred at the emergence of electric fish and 2) increased rates of molecular evolution occurred at the emergence of high-frequency wave-type fish.

Figures

Figure 1: Illustration of the 2D structure of the Na, K-ATPase alpha subunit from Kaplan, 2002. The intracellular loops and regions are much larger than the extracellular loops and contain the three important cytoplasmic domains (A, N, and P domains). The cytoplasmic N-terminus and loop between transmembrane segments 2 and 3 (containing the TGES motif involved in pump dephosphorylation) are part of the A domain. The intracellular loop between transmembrane segments 4 and 5 contains the N domain within the P domain (DKTG motif for phosphorylation).

Figure 2: Figure adapted from Morth, 2011. The subunits and domains of a functioning Na, K-ATPase. The alpha subunit core of P-type ATPases is composed of 6 transmembrane segments and 3 cytoplasmic domains (A, P, and N). The beta subunit is necessary for function, while an accessory gamma subunit is not. The Na, K-ATPase also has transmembrane regions 7-10 before the important C-terminal region.

Figure 3: Figure adapted from Morth, 2011 representing the Post-Albers cycle of the Na, K-ATPase. (Clockwise starting at top left): Three sodium ions bind the E1-ATP pump. This leads to pump autophosphorylation and the occlusion of the Na^+ ions. A conformational change to the E2P state results in decreased affinity for Na^+, releasing the three ions to the extracellular space. Two K^+ ions (and a cytoplasmic proton) bind the pump before occlusion, leading to pump dephosphorylation ([K2]E2). ATP binds once again resulting in a conformational change to E1, E1 conformations have lower K^+ affinity resulting in the release of the ions to inside the cell, allowing the cycle to start again.

Figure 1

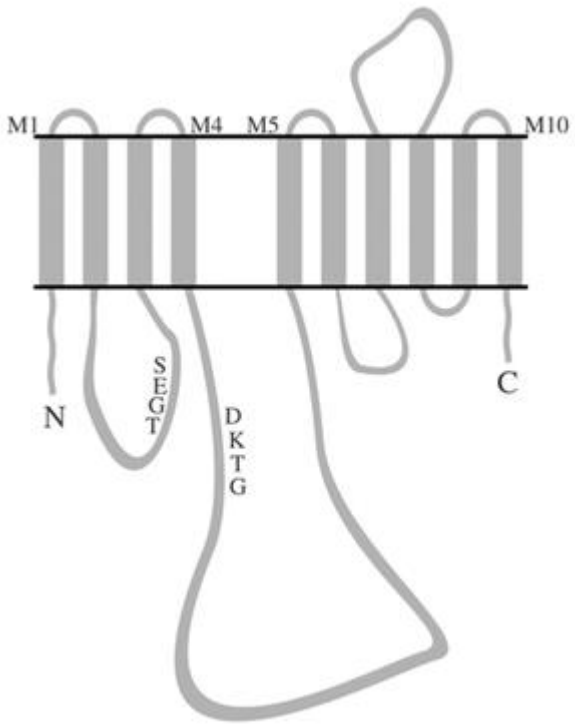

Figure 2

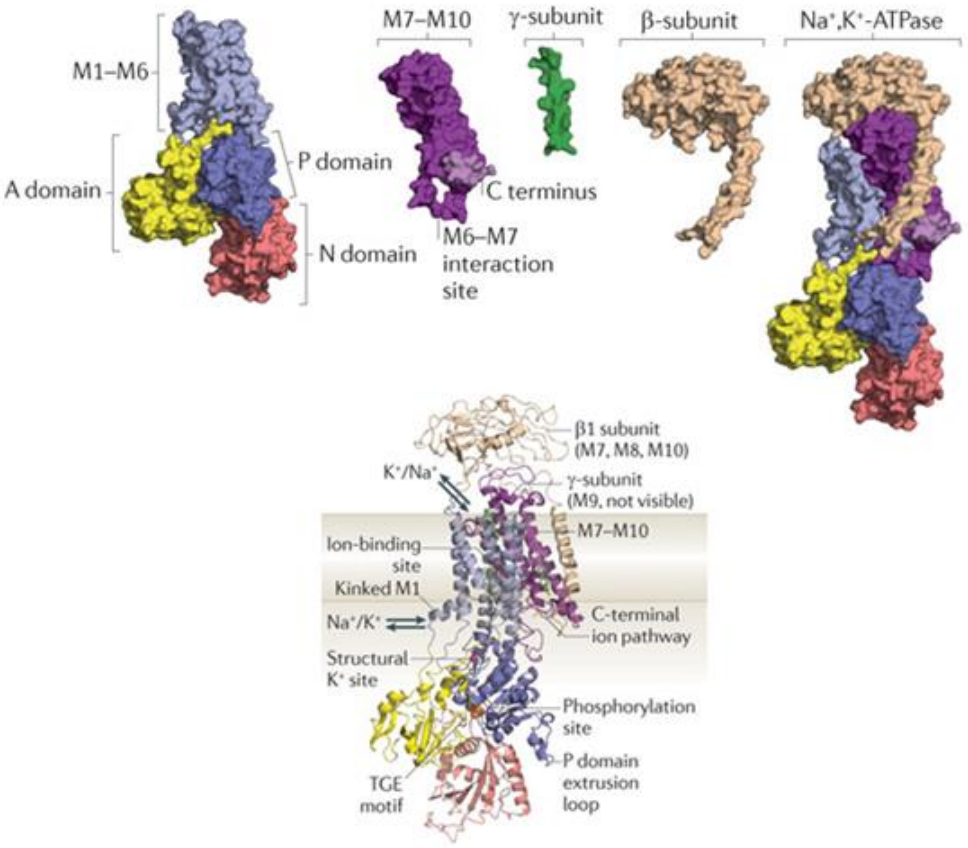
M1–M6
A domain
P domain
N domain
M7–M10
γ-subunit
β-subunit
Na⁺,K⁺-ATPase
C terminus
M6–M7
interaction
site
β1 subunit
(M7, M8, M10)
K⁺/Na⁺
γ-subunit
(M9, not visible)
M7–M10
Ion-binding
site
Kinked M1
Na⁺/K⁺
C-terminal
ion pathway
Structural
K⁺ site
Phosphorylation
site
P domain
extrusion
loop
TGE
motif

Figure 3

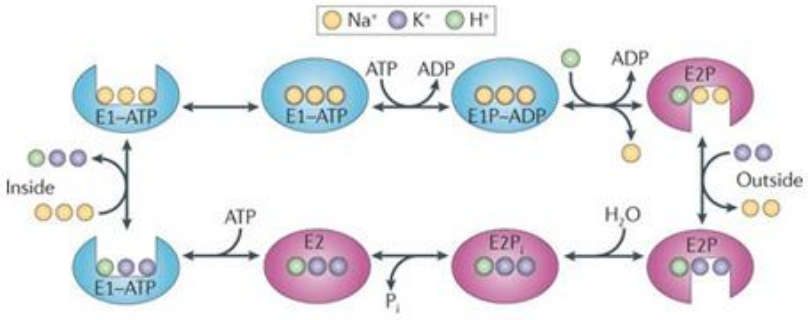
Na+ K+ H+
E1–ATP
E1–ATP
ATP
ADP
E1P–ADP
ADP
E2P
Inside
Outside
E1–ATP
ATP
E2
E2P$_i$
H_2O
E2P
P_i

Chapter 3: Molecular Evolution of the Na, K-ATPase α2 of Weakly Electric Fish

Introduction

All stable animal communication systems evolved under pressures to balance the benefits of signaling against its associated costs. The primary costs of signaling include predation risk, energetic cost, and opportunity costs (Bradbury and Vehrencamp, 2011). The energetic cost of communication signals vary depending on the type of signal and organism. Some communication signals require only an initial energy investment, such as pigmentation for bright feathers, whereas emitted signals such as birdsong require ongoing energetic input for signal production. The most energetically demanding animal communication systems include a variety of auditory and mechanical signals like the songs of Carolina wrens, the trilling of katydids, and the drumming of wolf spiders (reviewed by Markham et al., 2016; Stoddard and Salazar, 2011).

For some species, communication signals are coupled to active sensory systems, which alter the cost-benefit balance of communication. These systems include echolocation in bats and dolphins, and electric signaling in weakly electric fish. In these cases, the emission of auditory or electric signals is necessary for the animal to both image their environments and communicate with conspecifics. Two independently evolved lineages of weakly electric fish, the South American gymnotiforms and African mormyrids, produce energetically demanding electric organ discharges (EODs) as both communication and sensory signals.

These fish generate electric signals with specialized electric organs (EOs) composed of cells known as electrocytes. The electrocytes produce simultaneous or

near-simultaneous action potentials, synchronized by a medullary pacemaker nucleus (Figure 1). Similar to all other types of excitable cells, electrocyte action potentials are initiated by inward Na^+ current and terminated by outward K^+ current (Markham, 2013). Compared to other excitable cells such as neurons or myocytes, the ionic currents driving electrocyte action potentials are several orders of magnitude larger, with single-cell currents in electrocytes exceeding 10 microAmperes compared to neuronal currents that are typically on the order of picoAmperes (Ferrari and Zakon, 1993; Lewis et al., 2014; Markham et al., 2013; Markham et al., 2009). The summed action potentials of hundreds to thousands of electrocytes produce the EOD.

Most electric organs are derived from skeletal muscle and therefore myogenic in nature (Hopkins, 1986). One exception is the gymnotiform genus, *Apteronotus*, whose adult neurogenic EO is composed of the elongated spinal motorneurons that had previously innervated a larval myogenic EO. Two types of weakly electric fish, wave-type and pulse-type, produce EODs over a wide range of frequencies. Wave-type fish produce EODs at fixed intervals, while pulse-type fish can change rate and timing of signaling. Frequency varies widely with some pulse-type fish producing EODs at ~10 Hz and some wave-type fish producing EODs anywhere from 500-2000 Hz, depending on species, sex, and individual (Albert and Crampton, 2005; Hopkins, 1986). Gymnotiforms have many examples of both types of fish, with the wave-type fish being derived from a pulse-type ancestor. However, mormyrids have a single wave-type representative, which is actually basal to the many pulse-type representatives.

In a pulse-type fish (*Brachyhypopomus pinnicaudatus*) energetic cost of EOD production can be as high as 22% of the daily energy budget (Salazar and Stoddard,

2008). Theoretical estimates suggest wave-type fish incur a higher cost, with EOD production using ~30% of the daily energy budget (Salazar et al., 2013), and these theoretical estimates were later confirmed experimentally (Lewis et al., 2014). While pulse-type fish can briefly slow or stop signaling to reduce energetic cost, this would result in at least temporary loss of vital information from their surroundings. Wave-type fish are unable to use this strategy because EOD frequencies are steady and continuous 24 hours per day. Moreover, the energetic cost of EOD production increases exponentially as EOD frequency increases (Lewis et al., 2014).

The energetic demands of EOD production arise because of the extremely large ionic currents that produce the electrocyte action potential. After each action potential, the Na,K-ATPases hydrolyze one ATP for every three Na^+ ions removed to the extracellular space. In the best-studied case, the gymnotiform *Eigenmannia virescens*, $6.6x10^{10}$ Na^+ ions enter each electrocyte with each action potential, requiring hydrolysis of $2.2x10^{10}$ ATP molecules (Lewis et al., 2014). Because ion pumps such as the Na, K-ATPase transport ions much slower (10^3 ions per second)(Holmgren et al., 2000) than ions move through voltage-gated ion channels (10^7 ions/second)(Morais-Cabral et al., 2001), the large Na^+ influxes during electrocyte action potentials create significant demands on the Na, K-ATPases that must remove so much Na^+. The demands on these pumps are magnified as EOD frequency increases. In extreme cases, such as wave-type fish where EOD frequency can exceed 500 Hz, the Na, K-ATPases must remove all Na^+ within a matter of milliseconds. A key unanswered question is how the Na, K-ATPases function within this system to transport extremely large ionic loads under demands for extreme speed, especially for wave-type fish with high EOD frequencies.

The Na, K-ATPase is part of the P-type pump family, so called due to the brief but conserved phosphorylation step in the pump cycle. During each pump cycle the Na, K-ATPase hydrolyzes one ATP and moves three Na^+ ions out of the cell and two K^+ ions into the cell against their concentration gradients. One α subunit and one β subunit are necessary for a functional pump, with an accessory subunit (γ) sometimes present as part of the pump complex. The α subunit is the main functional unit with 10 transmembrane segments and 3 large cytoplasmic domains containing important ion and ligand binding sites, and phosphorylation sites (reviewed in Jorgensen et al., 2003; Kaplan, 2002). There are four α and three β isoforms. Differences among isoforms include changes in ion or ligand affinity that produce pumps with different functional characteristics (reviewed in Blanco and Mercer, 1998). These differences can be useful in expression of a pump with qualities best fit for a certain cell or tissue type and can also be subject to various developmental or hormonal regulators.

There are two conformations of the Na, K-ATPase in each pump cycle: E1 and E2. When the E1 conformation pump is open to the cytoplasm, three binding sites are open to allow for sequential binding of cytoplasmic Na^+ ions. The pump also binds ATP within the cytoplasmic 'N' domain, which then phosphorylates the pump within the cytoplasmic 'P' domain. After phosphorylation, there is a release of ADP and a conformational change of the pump to the E2 conformation. The 3 Na^+ ions are released, which then allows the binding of 2 K^+ ions. Dephosphorylation of the pump and a conformational change returns the pump back to the E1 conformation and releases two K^+ ions to the cytoplasm.

Two likely mechanisms for increasing the whole-cell rate of ion transport are to dramatically increase the number of functional pumps in the cell membrane, or the evolutionary modification of these pumps to enhance their efficiency. Some experimental work suggests that pumps are indeed densely expressed on the active membrane regions of both gymnotiform and mormyrid electrocytes (Ban et al., 2015; Gallant et al., 2012). It is also possible that molecular evolution of the Na, K-ATPases within electric fish lineages has increased pump efficiency. This possibility seems likely given that other molecules central to the electrogenic properties of electrocytes (the voltage-gated Na^+ channels) have undergone pronounced molecular evolution in both gymnotiform and mormyrid electric fish (Arnegard et al., 2010; Zakon et al., 2006).

Both gymnotiforms and mormyrids show a unique expression pattern of two voltage-gated Na^+ channel paralogs between skeletal muscle and electric organ. Nav1.4 channels are typically expressed in skeletal muscle. Because of the whole-genome duplication that preceded the teleost lineage (Hurley et al., 2007), teleosts have two copies of this Nav1.4 channel, Nav1.4a and Nav1.4b. In both weakly electric lineages, only Nav1.4b is expressed in skeletal muscle, while electrocytes express both Nav1.4a and Nav1.4b, such that Nav1.4a is only expressed in EO (Zakon et al., 2006). The Nav1.4a channels in EO accumulated numerous amino acid substitutions in what are typically highly conserved and functionally important regions of the channel, especially regions associated with increases in the kinetic rates of channel activation, inactivation, and recovery from inactivation (Arnegard et al., 2010). These substitutions led to increased ratios of nonsynonymous to synonymous substitutions (dN/dS) averaged over

the whole gene, evidence for positive selection acting on the Nav1.4a channels expressed only in the EO (Arnegard et al., 2010). These findings suggest that molecular evolution of the Nav1.4a gene served to significantly speed up Na^+ channel kinetics, thereby allowing the evolutionary emergence of high-frequency EODs.

Given that molecular evolution of electrocyte Na^+ channels clustered in regions that accelerate channel kinetics, I hypothesized that a parallel pattern of molecular evolution occurred in the electrocyte Na, K-ATPase, potentially speeding up pump kinetics to match the demands created by large ionic currents that can occur at high frequencies in electrocytes. I tested this hypothesis by determining the nucleotide and predicted amino acid sequences of the Na, K-ATPase α subunit expressed in EO of weakly electric fish (*atp1a2a*) for representative species of all gymnotiform and mormyrid families with myogenic EOs. We focused on fish with myogenic EOs because there are no neurogenic mormyrid representatives. These sequences were analyzed using site and branch models, under the hypothesis positive selection occurred on branches leading to weakly electric fish, with enhanced positive selection on branches leading to high-frequency wave-type fish. I further hypothesized positively selected sites would be in functionally significant regions of the protein.

Methods

Animals and tissue harvesting

Fish used in the study were wild caught in either South America (gymnotiforms) or Africa (mormyrids) and obtained from tropical fish importers. Fish were kept in 10 or 40 liter tanks of a recirculating aquarium system at 28+/-1°C and water conductivity was kept from 200-500 µS/cm.

For all gymnotiform species in the present study, EO tissue was obtained by clipping a small (1-2 cm) piece of the caudal tail filament. This procedure is done without anesthesia because induction and recovery from anesthesia is more harmful for the fish than the tail clip itself. Tissue was either immediately processed or stored in RNAlater RNA Stabilization Reagent (QIAGEN) at -20°C. All procedures were approved by the Institutional Animal Care and Use Committee of the University of Oklahoma.

Nucleotide sequence acquisition

Previously published sequences for the *atp1a2a* gene of several non-electric species included in this analysis were obtained from NCBI GenBank (Table 1). All mormyrid sequences were from published or unpublished transcriptome data from collaborators (Gallant et al., 2014; Gallant, unpublished) (Table 2). For the remaining gymnotiform representatives (*B. gauderio, G. carapo, R. rostratus, S. elegans, E. trilineata, E. virescens*), total RNA was extracted using Quick-RNA™ MiniPrep Plus (Zymo Research) or RNeasy Plus kits (QIAGEN). mRNA enrichment, ethanol precipitations, or TRIzol®-chloroform (Ambion) extractions were performed as needed. Total RNA was then used to create cDNA using SuperScript® III Reverse Transcriptase (Invitrogen), PrimeScript™ Reverse Transcriptase (Clontech), or SMARTer PCR cDNA synthesis kit (Clontech).

PCR amplification using species-specific primers was used to obtain the full coding sequence of *E. virescens* and *B. gauderio* (Tables 3 and 4, respectively). Various degenerate primers (Table 5) were used to obtain partial nucleotide sequence of the *atp1a2a* gene from the remaining gymnotiform representatives EO (*G. carapo, R.*

rostratus, S. elegans, E. trilineata). PCR was performed using either SapphireAmp® (TaKaRa), EmeraldAmp® (TaKaRa), Platinum®Taq DNA Polymerase High Fidelity (Invitrogen), or Phusion® High-Fidelity DNA polymerase (New England Biolabs Inc.). PCR protocols were determined according to recommended conditions and optimized as needed. TOPO® TA cloning® (Invitrogen) or FX cloning (Geertsma and Dutzler, 2011) were performed as needed to clone PCR products for sequencing. Frozen stocks were created from analyzed colonies by adding 1 milliliter of liquid culture to 1 ml of 50% glycerol and storage at -80*C. Plasmid extractions were performed using either Zyppy™ Plasmid Miniprep (Zymo Research) or QIAprep Spin Miniprep (QIAGEN) kits. Samples were sequenced by the Biology Core Molecular Lab at the University of Oklahoma via forward and reverse sequencing using Big-Dye® technology.

Analysis for positive selection

A transcription alignment of all *atp1a2a* nucleotide sequences (Appendix figure), including 18 full or partial atp1a2a sequences of 14 electrogenic species and 4 non-electrogenic fish was produced using Geneious version 7 (http://www.geneious.com,(Kearse et al., 2012)) by the CLUSTALW algorithm (Larkin et al., 2007). This alignment was then used to generate a single-gene neighbor-joining tree under the Jukes-Cantor distance model (Jukes and Cantor, 1969) within Geneious Tree Builder (Figure 2). To examine the *atp1a2a* of weakly electric fish for positive selection, I first used the PAML (Phylogenetic Analysis by Maximum Likelihood) software suite to run codon site models (Codeml Version 4.8a) (Yang, 2007), followed by likelihood ratio tests (LRTs) comparing specific model pairs. The LRT compares the doubled difference between the likelihood values of the more complex model and a

more null model to Chi Square critical values. Comparison of model M0 and M3 test that ω (the ratio of non-synonymous to synonymous substitution rates) varies within the tree, while comparisons of M1-M2 and M7-M8 test for positive selection within the tree (PAML). I also ran branch models using Codeml within PAML to test whether selected foreground branches were likely under greater positive selection than background branches. LRTs compared a more complex model (allowing a foreground branch to have different ω values than the rest) to a model allowing for one ω value for the entire tree. We ran these models sequentially testing each branch of the *atp1a2*a gene tree as a foreground branch to determine which, if any, lineages of are under positive selection. False discovery rate adjustments (of 0.022) were made to significance values (Benjamini, 2010).

Results

Alignment and gene tree of atp1a2a

The total number of nucleotides and amino acids as well as the protein coverage for the *atp1a2a* of the species obtained by PCR, cloning, and sequencing are shown in Table 6. The full translation alignment of these sequences, as well as those obtained from GenBank and published and unpublished transcriptome data (Tables 1 and 2, respectively), is shown in the figure in the appendix.

The single-gene tree derived from this alignment (Figure 2) corresponds closely with currently accepted phylogenies of teleost fishes (Betancur et al., 2013), and is consistent with recently published phylogenies for both the gymnotiform and mormyrid lineages (Tagliacollo et al., 2016). Some discrepancies between the *atp1a2a* tree and recently published phylogenies are likely due to the *atp1a2a* tree including some partial

sequences, having fewer representatives of all clades, and being created from a single gene rather than from more molecular and morphological data.

Site models of positive selection

PAML random site models detect whether positive selection is acting somewhere within the phylogenetic tree and identify individual sites that may be under positive selection. Likelihood values and parameters for the different site models are listed in Table 7. The difference of models M0 and M3, testing that ω varies across sites, was statistically significant. Site model LRTs between models M1 and M2, and models M7 and M8 test for positive selection. The M1-M2 comparison was not significant, while the comparison of the M7-M8 models was statistically significant, suggesting that positive selection acts somewhere within the tree. The comparison of M7 and M8 site models identified 18 amino acids that are likely under long-term positive selection or across multiple branches (Table 8). Two residues in particular, 881S and 882T, were highly significant at Bayesian likelihood probabilities of 0.998 and 0.982 respectively.

A visual examination of the amino acid alignment also identified several regions and residues where amino acid substitutions occurred primarily within the gymnotiform or mormyriform clades. Although these regions did not emerge statistically as being under positive selection, these sites nonetheless occur in functionally important regions of the pump where several specific single amino acid substitutions are known to have dramatic effects on pump function. Throughout the protein, there are at least three locations where this pattern is found within a span of four amino acids (207-209, 253-

254, and 395-398). There are six sites within three amino acids of a positively selected site with similar substitution patterns (sites 51,300, 409, 410, 558, and 561).

Branch models of positive selection

Branch model results are listed in Table 9. For the branch models the null background ω ratio was 0.0694, indicating strong purifying selection operating generally across the *atp1a2a* protein. The ω ratios for four foreground branches were significantly decreased from the background ω, suggesting even more intense purifying selection on these branches (Figure 2). The branches with potentially enhanced purifying selection were Branch 1 (non-electrogenic *O. niloticus* branching from the electrogenic African mormyrids), Branch 2 (the only wave-type mormyrid, *G. niloticus*, from all pulse-type mormyrid representatives), Branch 7 (*D. rerio* from *I. punctatus* and the gymnotiforms), and Branch 8 (non-electrogenic *I. punctatus* from the electrogenic South American gymnotiforms). Branch 9 (leading to separation of S. American wave-type and pulse-type fish) had a foreground ω of 0.15, which was statistically significant and higher than the background ω, which suggests perhaps a relaxation of the background purifying selection on this branch. Branches 10 (gymnotiform wave-type) and 11 (gymnotiform pulse-type) were the only two branches identified as lineages under positive selection with ω ratios of 4.06 and 3.56, respectively.

Discussion

The question addressed in the present project is whether the Na, K-ATPase expressed in electrocytes of weakly electric fish was the target of positive natural selection, like the voltage-gated Na^+ channels expressed in electrocytes. My specific hypothesis was that the Na, K-ATPase *atp1a2a* subunit expressed in electrocytes would

be under positive selection in weakly electric fish, with increased positive selection in those lineages with higher frequency EODs. The results did not support this specific hypothesis, but the present data do provide evidence for a more nuanced pattern of molecular evolution in the Na, K-ATPase α2 subunit. I found evidence for positive selection in two specific subsets of electric fish lineages, and 18 sites within the protein that may be under long –term positive selection or across multiple branches.

The Na, K-ATPase α2 protein is across vast reaches of evolutionary time, even when aligning the sequence of *A. anguilla* to the most derived of the weakly electric fish (*Eigenmannia spp*.). Within the alignment of 18 AA sequences (14 electrogenic and 4 non-electrogenic species) 679 of the 1024 sites (66.4%) were identical. Across the 18 sequences, the mean pairwise identity was 87.2%, and the mean pairwise BLSM62 similarity (threshold = 1) was 93.5%. The full alignment shows several long regions of high similarity bracketed by shorter areas of very low similarity (appendix figure). Although the initial N-terminal region (which is part of the A domain) shows low similarity, a 46 AA region (210-252) (within the cytoplasmic loop part of the A domain) is highly conserved (appendix figure). Within the N domain, a low conservation area (420-447), is immediately followed by a highly conserved region involved in ATP binding (448-462). This pattern is immediately repeated with regions of low conservation (463-478) and high conservation (479-494). A span of 90 residues (702-791) with close to 100% similarity includes part of the P domain and all of transmembrane segment five.

Despite these areas of strong conservation in this molecule, my data identified bursts of substitutions at the base of both wave-type and pulse-type gymnotiform fish.

No further branches to the higher frequency wave-type fish were found to be under selection. Surprisingly, the present data suggest an enhancement of purifying selection acting on *atp1a2a* in the mormyrid lineage. Because the African mormyrids show much less diversity in EOD frequencies, with only 1 example of a wave-type fish (*G. niloticus*) that produces EODs at lower frequencies (~200-300 Hz) (Moller et al., 1976) than some gymnotiforms that can reach frequencies exceeding 600 Hz (like *E. virescens*), the more intense purifying selection acting on the Na, K-ATPases of mormyrids could be the result of the pump performing well enough to meet these lower performance demands prior to emergence of electrogenesis. While the *atp1a2a* of mormyrids may not be under positive selection, the Na^+ load and energetic costs of EOD production might be managed through other mechanisms, including changes to expression pattern of *atp1a2a* or enhanced expression of the alternate α isoforms (Gallant et al., 2012; Gallant et al., 2014). These alternate isoforms may then themselves be under positive selection.

The modest degree of molecular evolution in electric organ Na, K-ATPase α2 observed in this study is surprising and stands in stark contrast to the pervasive pattern of convergent molecular evolution in the voltage-gated Na^+ channels of both mormyrids and gymnotiforms (Zakon, 2012). These voltage-gated Na^+ channels are vital for producing diverse and high frequency EODs, with the consequence being very large, fast Na^+ currents. Our results suggest that the ion pump responsible for dealing with these currents, and therefore necessary for electrical signaling, are not under similar patterns of selection in both clades.

Amino acids of interest

Six of the eighteen sites identified by the site models with probability (> 0.50) of being under positive selection were located in the ATPase N Domain (406S, 408T, 466S, 469D, 475V, 559F). Three of these sites (466, 469, and 475) are closely surrounded by sites in the N-Domain ATP binding pocket. The N domain is located within the P domain, all of which is located in the intracellular loop connecting transmembrane segments 4 and 5. During the catalytic cycle, ATP binds within this domain. This ATP must be in proper position in order to phosphorylate a highly conserved aspartic acid residue located within the P domain, a process assisted by magnesium for P-type pumps (reviewed in Bublitz et al., 2011; Sorensen et al., 2004). The autophosphorylation results in the pump being in a high energy state (E1P-ADP), with the separation of the N and P domains leading to A domain rotation. A change in conformation to a lower energy state results in the E2P pump. Ultimately, when ligands bind this region, protein regions near and far may be affected (Kubala et al., 2009).

The amino acids identified as under positive selection within the N domain, as well as those found in other pump regions, do not appear to have predictable or similar patterns of substitution. Site 406S has a serine or threonine for all species in the alignment. These two amino acids differ by a methyl group and have similar polarities and levels of hydrophobicity. Residue 466S also has all polar uncharged residues with gymnotiforms having a slightly more hydrophobic residue (cysteine) than mormyrids (serine). The same pattern is seen at site 408T with most gymnotiforms having a cysteine and mormyrids the more hydrophilic asparagine. 469D shows a similar pattern with slightly more variation. Mormyrids have a more hydrophilic residue (asparagine) while gymnotiforms have several different and more hydrophobic residues (alanine,

serine, or threonine). At site 475V, mormyrids have the polar uncharged proline, while all gymnotiforms have the polar, basic, and more hydrophilic histidine or arginine. Site 559F has the most differences with mormyrids having either the hydrophobic leucine or phenylalanine, while there is no pattern for gymnotiforms with some representatives having an asparagine (hydrophilic), alanine, isoleucine, or valine (hydrophobic). These amino acid substitutions, especially if there are large differences in structure, polarity, charge, and hydrophobicity, could ultimately lead to changes in the N domain interactions with the P domain which are important steps of the catalytic cycle. Substitutions such as these could also alter how ligands, like ATP, bind to the pump because many amino acids throughout the N domain are involved in this binding. These steps are critical for proper pump function and changes could impair or improve pump function.

Seven of 18 sites identified with a probability (>0.50) of being under positive selection are located in the N-terminal region of the protein, which is part of the A domain (sites 13, 16, 17, 46, 52, 59, and 68) (Figure 3). Another residue identified in the site models, 304S (0.611), is within transmembrane segment 3, which is moved by the A domain via linker regions while opening the ion pathway (Morth et al., 2011). The A domain is a cytoplasmic domain composed of the N-terminal region before transmembrane segment 1 and the intracellular loop connecting transmembrane segments 2 and 3. This domain is crucial for pairing the events of the catalytic cycle with ion transport. The A domain pairs ATP hydrolysis with ion transport via linker regions connected to transmembrane segments 1-3 (Toyoshima and Mizutani, 2004). After the gamma phosphate of ATP is transferred, the connection between the N and P

domains is broken, and the A domain is free to rotate ~120 degrees, pulling the linker regions, and causing TMs 1-3 to tilt away from M5-M10 to open the exit pathway (Olesen et al., 2007). When the linker regions are shortened or changed, pump function may be impaired (Bublitz et al., 2011; Daiho et al., 2007; Holdensen and Andersen, 2009; Lenoir et al., 2004).

While the N-terminal region (part of the A domain) is not as highly conserved as other regions, changes or mutations in this region of the alpha subunit are known to alter function. Removal of the first 32 amino acids of the α1 was found to shift the pump's conformational equilibrium towards the E1 state, the state the α2 isoform prefers, which could be further shifted by a mutation in the intracellular loop region of the A domain (Segall et al., 2001). These changes lead to α1 having characteristics more similar to the α2 isoform, exhibiting faster E2 to E1 conformational change, slower catalytic turnover, and high Na^+ and ATP affinity (Daly et al., 1994; Jewell and Lingrel, 1991; Kaplan, 2002; Segall et al., 2001). These changes are potentially due to modifications in how the N-terminus and regulatory loop region of this A domain interacts with the P domain in binding or release of ions and changing between the two conformations (Kaplan, 2002; Segall et al., 2001). While the removal of amino acids at the start of the protein affected these characteristics of pump function, it was also proposed that any changes to the primary and secondary structures of the protein in this region may alter pump function by changing how the N-terminal region interacts with the other cytoplasmic domains (Kaplan, 2002; Segall et al., 2001). Amino acid mutations in the N-terminal region have been proposed to have caused familial

hemiplegic migraine (FHM) through destabilizing these important interactions (Tonelli et al., 2007).

In this region, at sites 13A and 16S, most mormyrids do not have an amino acid residue, while the few gymnotiforms with this region covered mainly have polar, uncharged serine residues. Site 17 has more diversity with mormyrids having more hydrophilic residues (asparagine, glutamic acid, and glycine), while two gymnotiforms have the slightly more hydrophobic proline. At site 46T, most electrogenic species have a serine residue (except *G. carapo* with arginine and *B. gauderio* with a threonine). Serine and threonine are similar in polarity and hydrophobicity, while arginine is very hydrophilic. At site 52R most mormyrids have a histidine (positively charged side chain, hydrophilic) while most gymnotiforms have a serine (polar, uncharged, and less hydrophilic). At site 59T most mormyrids and gymnotiforms have polar uncharged residues that are slightly hydrophilic (threonine and serine, respectively), except *G. niloticus* which has a more hydrophobic methionine. At site 68A, most mormyrids have a lysine residue (positively charged and hydrophilic) except *G. niloticus* with an uncharged, polar glutamine. All gymnotiforms have a non-polar, more hydrophobic alanine (except *B. gauderio* having a nonpolar, slightly more hydrophilic serine residue). Within the third transmembrane segment at site 304S, all fish in the alignment have a serine or threonine except *E. electricus* which has an alanine. These are polar uncharged amino acids with serine and threonine being more hydrophobic than alanine. Considering the role of the A domain in the catalytic cycle, any of the amino acids under selection in this region could very well be involved in altering the interactions

with other regions of the protein (including other cytoplasmic domains and transmembrane segments) and therefore modifying pump function.

Site 1012 was identified with a probability (0.726) of being under positive selection. This site is near the end of transmembrane segment 10, and is the third position of what is usually a trio of arginine residues. The third arginine of this motif was identified as a positively selected site, and while many mormyrids retain an arginine at this location, no gymnotiform representatives do (two have a hydrophobic tyrosine substitution, two a polar uncharged asparagine, and one polar uncharged serine) (Figure 4).

These three arginines, plus three more arginines from a different locus collocate once the protein is folded, and form a positively charged region located at the membrane's edge. This region potentially acts as a voltage sensor, moving in response to depolarization of the membrane (Morth et al., 2007). In humans the nonsense mutation of the third arginine to a stop codon (and therefore expression of a truncated version of the protein) was identified in a case of sporadic hemiplegic migraine syndrome (Gallanti et al., 2011; Gallanti et al., 2008). The change of a positively charged arginine to a polar uncharged amino acid as observed in some of the gymnotiforms could alter the voltage sensing abilities of this region.

The PGG motif at 1013 (Figure 4), and the ~8 subsequent residues of the C-terminus form a small helix that acts as a plug to a buried channel between M5, 7, 8 and 10 (Morth et al., 2011). When five of these residues are removed (KETYY), Na^+ affinity is greatly reduced (26x) without affecting affinity for K^+ (Morth et al., 2007). It was proposed that direct contact of this region, α M5, and the loop between M8-9 is

involved in optimizing Na^+ binding at the third ion binding site (Morth et al., 2007). While not identified by site models as significant, the KETYY sequence (which acts as a cytoplasmic plug) is not conserved, even in the non-electrogenic species included in the alignment. Both mormyrids and gymnotiforms have representatives with a K-R substitution in this motif.

The only two loci under statistically significant (>0.95) positive selection by the site models were 881 and 882. These amino acids are located in the extracellular loop between transmembrane segments 7 and 8. This loop is vital for the interacting with the β subunit, without which the α subunit does not properly fold or insert into the plasma membrane. This loop also interacts with the second extracellular loop between transmembrane segments 3 and 4, with large movements of these loops occurring during the conformational changes of the pump, specifically the closing of an extracellular gate (Capendeguy et al., 2008). Several amino acids of this loop, along with these movements, are also involved in creating the ouabain binding site (Capendeguy et al., 2008). Sites 881 and 882 do not show a discernable pattern in amino acid properties (Figure 5). At site 881, non-electric species have polar uncharged, electrically positive, or hydrophobic amino acid residues. Mormyrids mostly have hydrophobic amino acids, with one electrically positive residue, while most gymnotiforms have mostly electrically positive with a few hydrophobic residues. At location 882 mormyrids have mostly electrically positive residues with gymnotiforms having a mixture of several types of amino acid residues. These different amino acid characteristics could affect one of the several important processes that this extracellular loop is involved in and may result in functional consequences.

There are several locations within the extracellular loop between transmembrane segments 7 and 8 that have been identified as causing FHM, one of which (W890) is 7 amino acids away from the positively selected sites 881 and 882 (Figure 5). While this residue is highly conserved in weakly electric fish, a mutation in humans led to the complete loss of pump function which demonstrates how important this region is for proper pump function (Koenderink et al., 2005). This was proposed as due to the tryptophan to arginine substitution (and therefore from a neutral to positive residue), could interfere with the α and β interactions during the catalytic cycle, changes to which could even cause issues with other areas of the pump such as ion binding sites.

Locus 872, which is eight amino acids in the opposite direction from the positively selected sites (881-882), was not identified as under positive selection by site models, but is known to have a significant impact on pump kinetics. An isoleucine to valine substitution (a difference of one methyl group) found at this locus in squid increased pump turnover by ~40% by targeting the voltage dependent release of Na^+ to the extracellular space (Colina et al., 2010). In their examination of 250 other α isoforms, this substitution was only found in the Na, K-ATPase of the electric eel, a gymnotiform (Colina et al., 2010). In the present study, this I-V substitution was found in all gymnotiform representatives, whereas the mormyrids and all non-electric fish retained the isoleucine residue. While this suggests that this substitution could be biologically significant for the gymnotiforms by increasing the pump turnover rate, it was not identified by the site models as an amino acid under positive selection. This suggests that, while the site models may indicate some amino acids to examine further

in mutagenesis and electrophysiology studies, they may not be the only residues or regions to focus on in future research.

An informal visual examination of the alignment suggests areas with substitution patterns that may also be of interest in further research. There are several loci where an amino acid substitution is found primarily in all representatives of either the mormyrids or gymnotiforms. In several of these instances, a nearby residue shows a different substitution that is primarily within the other electrogenic lineage. In the intracellular loop between transmembrane segments 3 and 4, which is also part of the A domain, there are three amino acids that make up such a cluster of interest. First, locations 204, 207, and 209 have all gymnotiforms or mormyrid representatives different from the other lineage (Figure 6). These amino acids are ~8 amino acids away from the conserved TGES region of the A domain on one side, which is involved in the dephosphorylation of the pump, and on the other side they are one amino acid away from a supposed FHM site. A similar substitution pattern is found from loci 494 to 501 (Figure 6) which are in the N domain relatively near the ATP binding pocket. Since these electric fish-specific substitution patterns occur within functional domains important for proper pump function, and individual amino acid changes throughout the pump have been identified in either improving or impairing pump function, these amino acids should not excluded from future research of which substitutions are biologically significant in the Na, K-ATPases of weakly electric fish.

The Na, K-ATPases of weakly electric fish are directly responsible for handling large Na^+ currents in very little time and at high metabolic cost. While we hypothesized that electric signaling would be putting these molecules under pressures that might

ultimately lead to extensive molecular evolution, we observed very limited positive selection in this molecule. In fact, positive selection only acted on the branches leading to both pulse-type and wave-type gymnotiforms, but not the African mormyrids as we expected. Amino acid residues identified as having high probability of being under positive selection were identified in several vital cellular regions and domains. These residues are a good starting point for future mutagenesis studies to examine how these pumps may function differently from the *atp1a2a* of other organisms, research that could yield important insights on the structure-function relationships of Na, K-ATPases. Given the central importance of the Na, K-ATPase for both normal and pathological function in excitable tissues such as nerve, muscle, and heart, better understanding of structure-function modifications that could improve pump kinetics might also have important implications for treatment of disease states.

Tables

Table 1: Accession numbers of previously published sequences used in this analysis.

Species	Accession number
A. anguilla	X76108
D. rerio	NM_131683
E. electricus	KM282055
I. punctatus	XM_017461876
O. niloticus	XM_003447457

Table 2: Final lengths of the full coding region of the *atp1a2a* from electric organ obtained from transcriptome data (Gallant, 2014). *S. macrurus* is a gymnotiform, while all others are African mormyrids.

Species	# Nucleotides	# Amino acids
B. brachyistius	3042	1013
C. compressirostrus	3042	1013
G. niloticus	3054	1017
M. nigricans	3042	1013
P. kingsleyae	3042	1013
P. soudenesis	3042	1013
S. macrurus	3030	1009

Table 3: PCR primers designed and used to obtain *atp1a2a* from *Eigenmannia virescens*.

Primer name	Primer sequence (5'-3')
NaK_Alpha_For_1	GGAGACCTGGTGGAGATTAA
NaK_Alpha_Reverse_one	TCGATGCAGAGGATGGT
NaK_Alpha_For_2	GAGCCTACATGGAGCTGGG
NaK_Alpha-Reverse_Two	GCCTGGATCATACCGATCTGT
Eig_NaK_for_1	CGGGTACTACTCTTGTCCTT
Eig_NaK_rev_1	AGAGCAGATGTAACTCCTGAC
Eig_NaK_for_2	TCCTCATGACCTCAGCTATG
Eig_NaK_rev_2	TCATAGCTGAGGTCATGAGG
Eig_NaK1_gap_seq_for	CTGGTGAAGAACCTGGAGGC
Eig_NaK1_gap_seq_rev	ACCTTTATCCCAGCGGAGCG
NaK_A_RACE_For	GGGTGTTGGCATCATCTCCGAGGGCAA
NaK_A_RACE_rev	CCACCTTGCACCCGCTGCAGGAGA
3'Eig_End_For	CAGAGACAGGGTGCTATTG
3'Eig_End_rev	TATATTGGAGATTAATAGTAGGTCTCTC

Table 4: PCR primers designed and used to obtain *atp1a2a* from *Brachyhypopomus gauderio*.

Primer name	Primer sequence (5'-3')
Brac_NaK_A_For1	CACTTCATCCACATCATCACGG
Brac_NaK_A_Rev1	GTTTCGGGGCTGACGCTT
Brac_NaK_A_For2	CCTCCCTCTCAGTTCCCACG
Brac_NaK_A_Rev2	TTGCCCTCAGAGATGATGCC
Brac_A_5'end_for	GAGAGAACACACACATCC
Brac_A_5'end_rev	GAGGGAGAGGAAGAAGAAG
Brac_NaK_A_Mid_Seq_for	CATGAGATGGAGGACACACC
Brac_NaK_A_mid_seq_rev	CGATCATGGACATGAGCCCT
Brac_A_3'end_for	CCCTTCCTGCTCTTCATCATGG
Brac_A_3'end_rev	GGACCCCAGGACGAACCAC

Table 5: Degenerate primers designed to get *atp1a2a* sequence from South American gymnotiforms.

Primer name	Primer sequence (5'-3')
U_NaK FOR	TAGCGAGTCGTTATGGGGTGGA
U_NaK REV	GAGGAGGGCCGTTTGATCTTTG
U_NaK FOR 2	TTCACCCACTCTGGGGTGG
U_NaK REV 2	GCCCACTGCACCACCAC
NaK Deg For 1	WAGRGAYGGDCCWAACGCYCTGAC
NaK Deg Rev 1	CCCAGYACTCTCTCYCCCAG
NaK Deg For 2	YGTRCCTGARGGWCTGCTGG
NaK Deg Rev 2	GGSAWAGCRCARAACCACCA
NaK Deg For 3	KSMRGGAGACCTGGTGGAGA
NaK Deg Rev 3	SAGGATGGTVACRGTKCCCA
NaK Deg For 4	TGGGTSAAGTTCTGCAARCAGC
NaK Deg Rev 4	RTGGCARAAACCCAGHACTC
NaK Deg For 5	MACCCTSACYCAGAACCGMA
NaK Deg Rev 5	KCCCAGGTCRATGCASAGRA
fx NaK deg for 1	ATATATGCTCTTCTAGTWAGRGAYGGDCCWAACGCYCTGAC
fx NaK deg rev 1	TATATAGCTCTTCATGCCCCAGYACTCTCTCYCCCAG
Fx NaK deg for 2	ATATATGCTCTTCTAGTYGTRCCTGARGGWCTGCTGG
Fx NaK deg rev 2	TATATAGCTCTTCATGCGGSAWAGCRCARAACCACCA
Fx NaK deg for 4	ATATATGCTCTTCTAGTTGGGTSAAGTTCTGCAARCAGC
Fx NaK deg rev 4	TATATAGCTCTTCATGCRTGGCARAAACCCAGHACTC
Fx NaK deg for 5	ATATATGCTCTTCTAGTMACCCTSACYCAGAACCGMA
Fx NaK deg rev 5	TATATAGCTCTTCATGCKCCCAGGTCRATGCASAGRA
NaK Forward 121	TCGTTATGGGGTGGACCTG
NaK Reverse 533	TCTCCACCTTTAATCTCCACCA
NaK Forward 447	AAGAACATGGTGCCTCAGCA
NaK Reverse 958	GCCAGCAGTCCTTCAGGTAC
NaK Forward 940	GGAATCATCGTCGCCAA
NaK Reverse 1414	ACTTGTTGGTGGAGTTGAA
NaK Forward 1322	TCTGAATCTGCTCTGCTGAAGTG
NaK Reverse 1877	TCTTCCACTGTCTCGTTGCC
NaK Forward 1709	GAGCAGATGTGCTTCCTG
NaK Reverse 2266	CTTCTTCAGGTTATCAAAGATCAAA
NaK Forward 2255	GAGGAGGGCCGTTTGATCTT
NaK Reverse 2724	GCCCACTGCACCACCAC
NaK Forward 2580	TTGTCCTGGCGGAGAATGG
NaK Reverse 3003	TCCACCCAACCTCCAGGAT

Table 6: Final length and region covered of the Na, K-ATPase *atp1a2a* from gymnotiform electric organ obtained by PCR amplification.

Species	# Nucleotides (atp1a2a)	# Amino acids	Region covered (amino acids)
B. gauderio	3030	1010	Full coding region
E. trilineata	2649	883	46-932
E. virescens	3027	1008	Full coding region
G. carapo	2655	885	45-932
R. rostratus	2213	737	70-807
S. elegans	2728	909	94-1015

Table 7: Results of site models run in PAML (Yang, 2007). For each model, the log likelihood (lnL) is listed, as well as the null model used for the likelihood ratio tests (LRTs). The LRT equals the difference of log likelihood (model-null) times two. The result is compared to the Chi-squared distribution (*indicates $p<0.01$). Site class ω values and proportions are listed for models M0-M3. Parameters for the beta distribution of models M7 and M8 are listed (p and q).

Model	lnL	Parameters			Null	LRTs
		ω0/p	ω1/q	ω2/ωp		
M0	-21341.819777	0.06939				
M1	-20816.258395	0.03271 (87.9%)	1.0 (12.1%)			
M2	-20814.692947	0.03278 (87.8%)	1.0 (12.1%)	3.93104 (0.1%)	M1	3.130896
M3	-20589.047562	0.00532 (71%)	0.18537 (23.1%)	0.74715 (5.8%)	M0	1505.54443 *
M7	-20592.579633	0.14492	1.30068			
M8	-20582.233086	0.16463	1.94652	1.25000	M7	20.693094*

Table 8: 18 sites identified by site models and BEB analysis with a probability (>0.5) for being under positive selection. Amino acid designation determined by the residue at that site for *A. anguilla*.

Site	Probability ω>1
13A	0.853
16S	0.913
17E	0.925
46T	0.755
52R	0.633
59T	0.792
68A	0.792
304S	0.611
406S	0.756
408T	0.542
466S	0.810
469D	0.658
475V	0.532
559F	0.752
668G	0.917
881S	0.998**
882T	0.982*
1012N	0.726

Table 9: Results of running branch models of Codeml in PAML (Yang, 2007). The foreground branch numbers correspond to the labeling of nodes in tree of Figure 2. * indicates foreground branches with significant different ω ratio than background.

Branch	Background dN/dS	Foreground dN/dS	lnL	LRT
Null	0.06939		-21341.819777	
1	0.07102	0.00242	-21337.754625	8.130304*
2	0.07241	0.03206	-21334.034713	15.570128*
3	0.06927	0.07190	-21341.805562	0.02843
4	0.06933	0.07200	-21341.813101	0.013352
5	0.06946	0.00010	-21341.422671	0.794212
6	0.0695	0.05414	-21341.726731	0.186092
7	0.07149	0.02047	-21336.127338	11.384878
8	0.07141	0.02759	-21337.505231	8.629092*
9	0.0668	0.14975	-21335.149975	13.339604*
10	0.06737	4.06698	-21329.002609	25.634336*
11	0.6796	3.56018	-21334.941562	13.75643*
12	0.06863	0.29156	-21339.878912	3.88173
13	0.06865	0.13093	-21340.323667	2.99222
14	0.06959	0.05712	-21341.722178	0.195198
15	0.06882	0.08253	-21341.397353	0.844848

Figures

Figure 1. The electric organ discharge (EOD) in *Eigenmannia virescens*. (A) The medullary pacemaker nucleus innervates electrocytes of the electric organ through spinal motor neurons. The simultaneous action potentials produce the EOD. (B) A simplified electrocyte showing innervation of the spinal motor neuron at the posterior face via a cholinergic synapse. Synaptic activation opens voltage-gated channels which allow Na^+ to enter the cell. The Na^+ current flows towards the head. (C) A section of EO tissue. Once skin is removed, the densely-packed electrocytes are easy to visualize. One electrocyte is outlined for clarity. (D) All electrocytes produce action potentials simultaneously, with the current summing together in the direction of the head. The return path of the current is through the water towards the tail. Positive current is designated as current moving towards the head. (E) A trace of 1 EOD, the result of summing a single action potential from all electrocytes. (F) The waveform of a wave-type fish producing EODs at ~500 Hz.

Figure 2: Phylogenetic tree based on single-gene data from the alignment of full or partial *atp1a2a* amino acid sequences from 18 species (full alignment in appendix figure). Branches and species are color coded: black are non-electrogenic, orange are African mormyrids, and purple are South American gymnotiforms. Numbers at the branch nodes indicate the sequential 'foreground' branches used for branch models, with asterisks indicating those branches where the foreground dN/dS ratio was statistically different from the background. Blue numbers indicate foreground branch dN/dS ratios (blue). The background dN/dS ratio was 0.0694.

Figure 3: Amino acid alignment of the first 70 residues, one region composing part of the A domain of the Na, K-ATPase. Species names are color coded: black (non-electrogenic), orange (African mormyrid), and purple (S. American gymnotiform). Sequences for *G. carapo, R. rostratus, S. elegans,* and E. *trilineata* are not complete in this region. Several sites in this region were identified by site models in having a >0.5 probability of being positively selected (red). Changes to this region can affect pump function, one example being site 66 (green), where a mutation was found to destabilize interactions between this N-terminal region and the other cytoplasmic domains, to the point of causing FHM in humans (Tonelli et al., 2007).

Figure 4: Amino acid alignment of residues 1009 to 1023 in the C-terminal region of Na, K-ATPase α2. Species names are color coded: black (non-electrogenic), orange (African mormyrid), and purple (South American gymnotiform). Sequences for *G. carapo, R. rostratus, S. elegans,* and *E. trilineata* are incomplete in this region. Site 1012 (red) was identified by site models with a probability of 0.726 of being under positive selection. This site has also been implicated in cases of human disorder (Gallanti et al., 2011). Gray shading are amino acids acting as a cytoplasmic plug and are involved in sodium affinity (Morth et al., 2011)

Figure 5: Amino acid alignment for residues 870-892. Species names are color coded: black (non-electrogenic), orange (African mormyrid), and purple (S. American gymnotiform). Sequence data are incomplete for *R. rostratus* in this region. Sites 881

and 882 (red) were identified by site models with statistically significant chance of being under positive selection. Site 872 (blue) was not identified as under positive selection, but shows an isoleucine to valine substitution in all Gymnotiform representatives, a substitution previously identified in squid increasing pump turnover rate by ~40% (Colina et al., 2010). Residue 890 (green) has previously been identified as a location where mutation can cause complete loss of function, resulting in human FHM (Koenderink et al., 2005).

Figure 6: There are several sites that were not identified by site models as under positive selection, but that still may be of interest in future research due to interesting patterns of substitution (blue). Specifically, at these sites, amino acid substitutions are found that are exclusive to either the gymnotiform lineage, or the mormyrid lineage, but not both. These patterns are found at several locations in functionally important regions, with the following examples from the A and N domains. Species names are color coded: black (non-electrogenic), orange (African mormyrid), and purple (S. American gymnotiform). Amino acids 202-210 of the A domain are in the intracellular loop between transmembrane segments 2 and 3. The N domain example includes amino acids close to conserved motifs involved in ATP binding (gray shading).

Figure 1

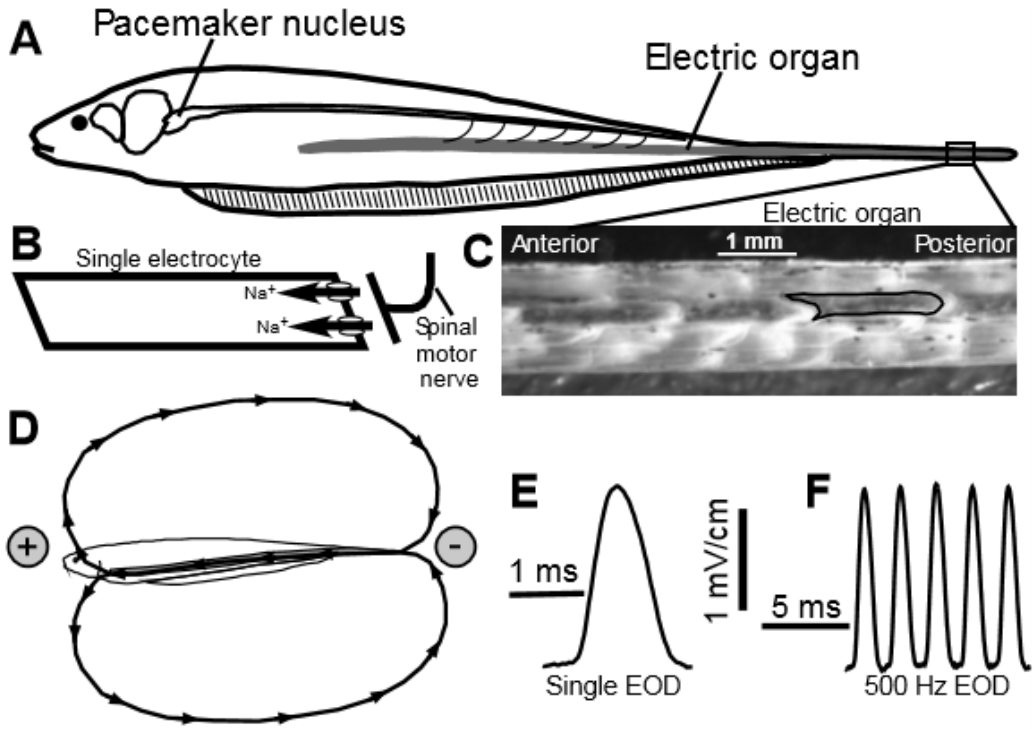
A
Pacemaker nucleus
Electric organ
B
Single electrocyte
Na+
Na+
Spinal
motor
nerve
C
Electric organ
Anterior
1 mm
Posterior
D
E
1 ms
1 mV/cm
Single EOD
F
5 ms
500 Hz EOD

Figure 2

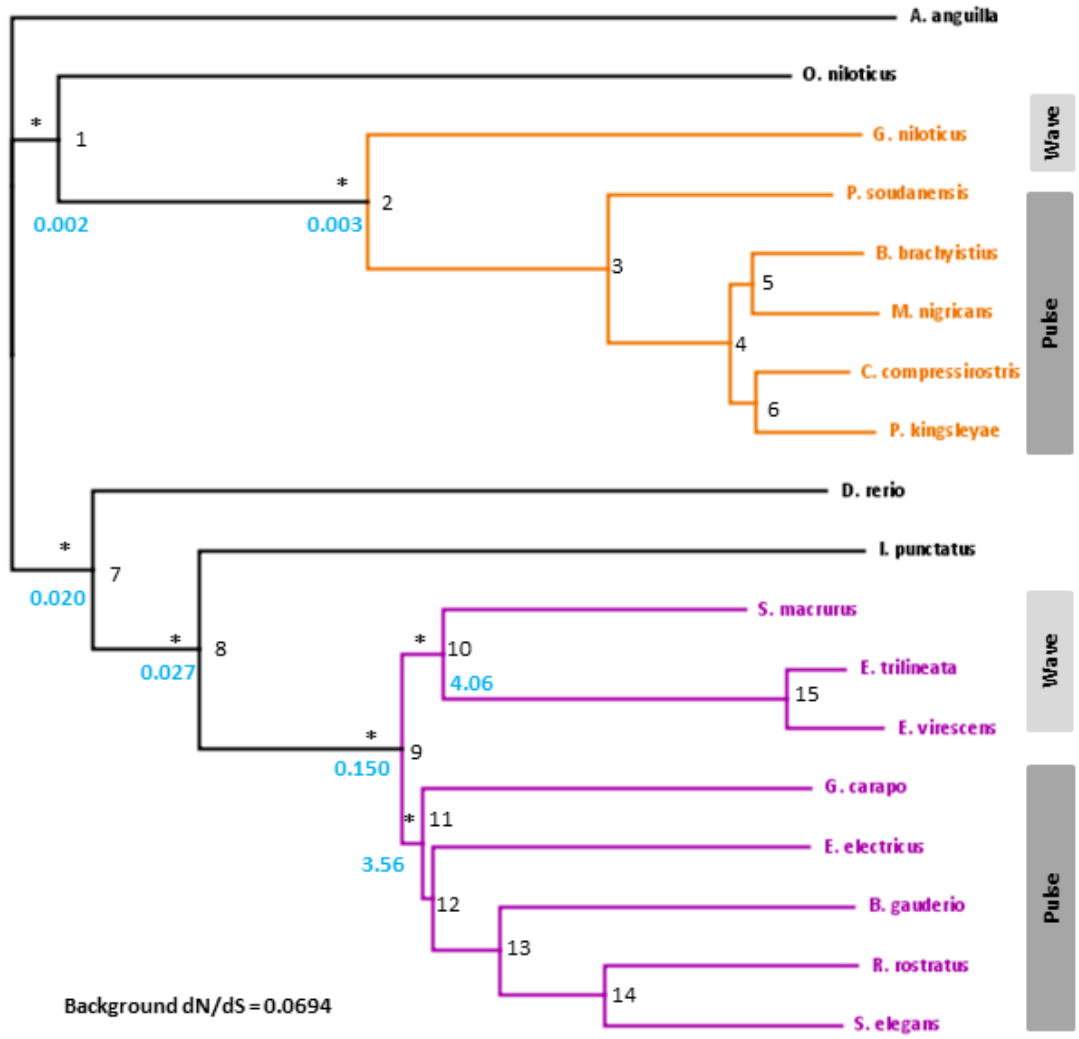
A. anguilla
O. niloticus
G. niloticus
P. soudanensis
B. brachyistius
M. nigricans
C. compressirostris
P. kingsleyae
D. rerio
I. punctatus
S. macrurus
E. trilineata
E. virescens
G. carapo
E. electricus
B. gauderio
R. rostratus
S. elegans
Wave
Pulse
Wave
Pulse
1
2
3
4
5
6
7
8
9
10
11
12
13
14
15
*
0.002
0.003
0.020
0.027
0.150
4.06
3.56
Background dN/dS = 0.0694

Figure 3

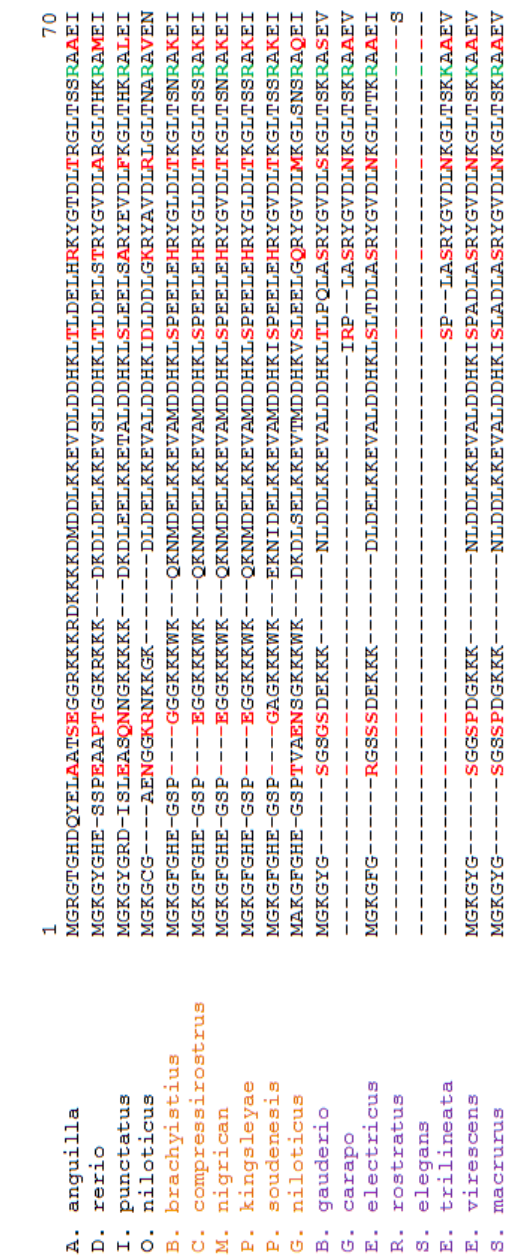
1
70
A. anguilla
D. rerio
I. punctatus
O. niloticus
B. brachyistius
C. compressirostrus
M. nigrican
P. kingsleyae
P. soudenesis
G. nilloticus
B. gauderio
G. carapo
E. electricus
R. rostratus
S. elegans
E. trilineata
E. virescens
S. macrurus

Figure 4

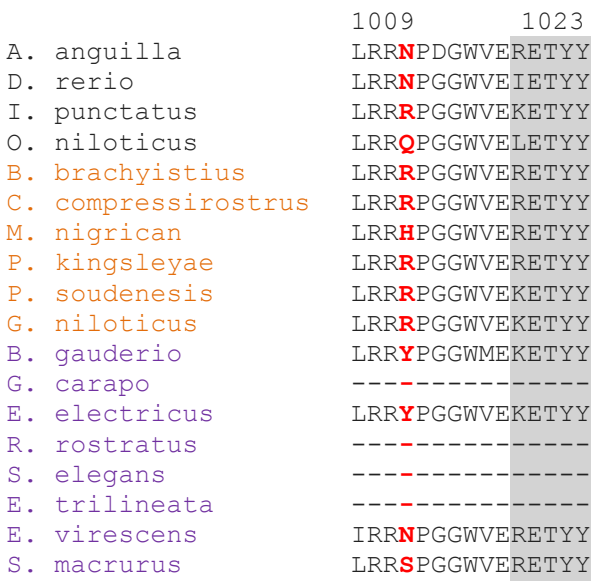
1009 1023
A. anguilla LRRNPDGWVERETYY
D. rerio LRRNPGGWVEIETYY
I. punctatus LRRRPGGWVEKETYY
O. niloticus LRRQPGGWVELETYY
B. brachyistius LRRRPGGWVERETYY
C. compressirostrus LRRRPGGWVERETYY
M. nigrican LRRHPGGWVERETYY
P. kingsleyae LRRRPGGWVERETYY
P. soudenesis LRRRPGGWVEKETYY
G. niloticus LRRRPGGWVEKETYY
B. gauderio LRRYPGGWMEKETYY
G. carapo ---------- ----------
E. electricus LRRYPGGWVEKETYY
R. rostratus ---------- ----------
S. elegans ---------- ----------
E. trilineata ---------- ----------
E. virescens IRRNPGGWVERETYY
S. macrurus LRRSPGGWVERETYY

Figure 5

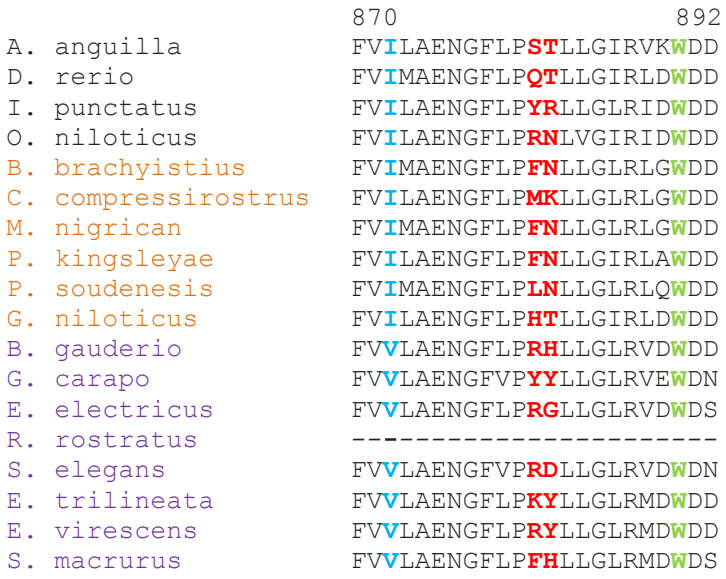
870 892
A. anguilla FVILAENGFLPSTLLGIRVKWDD
D. rerio FVIMAENGFLPQTLLGIRLDWDD
I. punctatus FVILAENGFLPYRLLGLRIDWDD
O. niloticus FVILAENGFLPRNLVGIRIDWDD
B. brachyistius FVIMAENGFLPFNLLGLRLGWDD
C. compressirostrus FVILAENGFLPMKLLGLRLGWDD
M. nigrican FVIMAENGFLPFNLLGLRLGWDD
P. kingsleyae FVILAENGFLPFNLLGIRLAWDD
P. soudenesis FVIMAENGFLPLNLLGLRLQWDD
G. niloticus FVILAENGFLPHTLLGIRLDWDD
B. gauderio FVVLAENGFLPRHLLGLRVDWDD
G. carapo FVVLAENGFVPYYLLGLRVEWDN
E. electricus FVVLAENGFLPRGLLGLRVDWDS
R. rostratus ----------
S. elegans FVVLAENGFVPRDLLGLRVDWDN
E. trilineata FVVLAENGFLPKYLLGLRMDWDD
E. virescens FVVLAENGFLPRYLLGLRMDWDD
S. macrurus FVVLAENGFLPFHLLGLRMDWDS

Figure 6

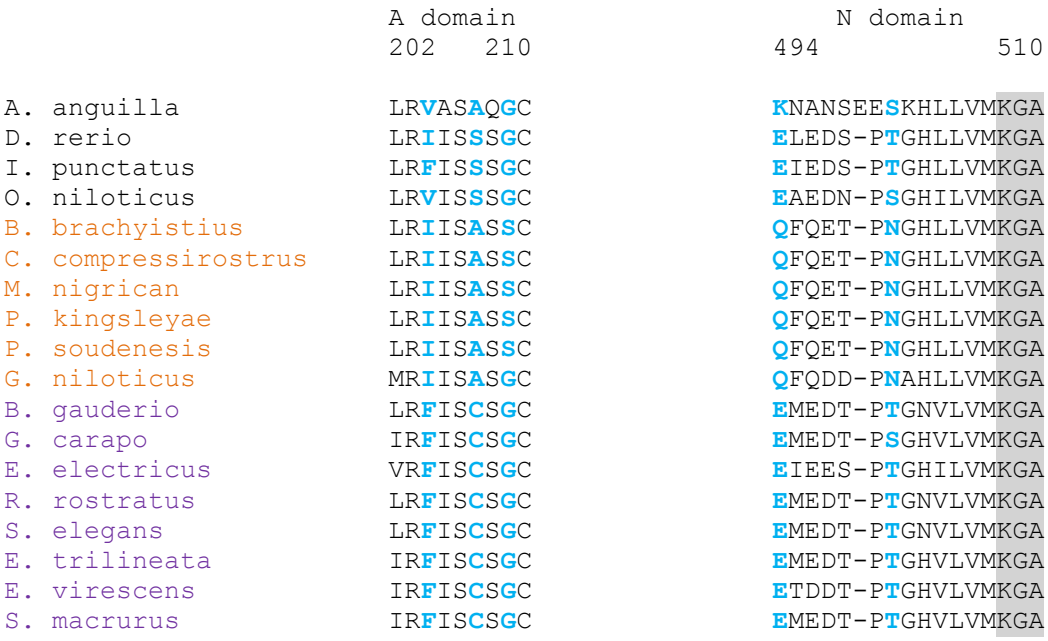
A domain
202 210
N domain
494 510
A. anguilla LRVASAQGC KNANSEESKHLLVMKGA
D. rerio LRIISSSGC ELEDS-PTGHLLVMKGA
I. punctatus LRFISSSGC EIEDS-PTGHLLVMKGA
O. niloticus LRVISSSGC EAEDN-PSGHILVMKGA
B. brachyistius LRIISASSC QFQET-PNGHLLVMKGA
C. compressirostrus LRIISASSC QFQET-PNGHLLVMKGA
M. nigrican LRIISASSC QFQET-PNGHLLVMKGA
P. kingsleyae LRIISASSC QFQET-PNGHLLVMKGA
P. soudenesis LRIISASSC QFQET-PNGHLLVMKGA
G. niloticus MRIISASGC QFQDD-PNAHLLVMKGA
B. gauderio LRFISCSGC EMEDT-PTGNVLVMKGA
G. carapo IRFISCSGC EMEDT-PSGHVLVMKGA
E. electricus VRFISCSGC EIEES-PTGHILVMKGA
R. rostratus LRFISCSGC EMEDT-PTGNVLVMKGA
S. elegans LRFISCSGC EMEDT-PTGNVLVMKGA
E. trilineata IRFISCSGC EMEDT-PTGHVLVMKGA
E. virescens IRFISCSGC ETDDT-PTGHVLVMKGA
S. macrurus IRFISCSGC EMEDT-PTGHVLVMKGA

Chapter 4: Summary and Future Directions

Weakly electric fish have a unique ability to generate electric organ discharges (EODs) as both a sensory and communication system. Like all other communication modalities, this system had to develop while balancing the benefits and associated costs of signaling. Two lineages of weakly electric fish (African mormyrids and South American gymnotiforms) use this system to obtain an incredibly clear image of their environment and communicate with conspecifics, but it also exposes them to electroreceptive predators and incurs a large energetic cost. This research focused on this associated energetic cost of signaling and, more specifically, the Na, K-ATPases that uses this energy.

While initial estimates of energy required for EOD production varied widely and suggested that signaling only used a small amount of the daily energy budget, recent theoretical estimates put this cost up to ~30% depending on fish-type, an estimate later confirmed experimentally (Lewis et al., 2014; Salazar et al., 2013). This energy is used by the Na, K-ATPases that hydrolyze ATP to restore the ionic gradients after action potentials. Measurement of the Na+ current for an action potential from a single *Eigenmannia virescens* electrocyte provides a number of Na+ ions, and therefore ATP molecules required: 6.3×10^{10} Na^{+} and 2.1×10^{10} per EOD per electrocyte, respectively (Lewis et al., 2014). *E. virescens*, which produce EODs at up to 500 Hz, have less than a millisecond for this large Na^{+} current to be removed from the cell between action potentials by the Na, K-ATPases.

The Na, K-ATPase requires two subunits, an α and β. The main catalytic subunit is the ~1000 amino acid α subunit, which has three vital cytoplasmic domains, 10

transmembrane segments, and several extracellular loops. Within these regions are ion binding, nucleotide binding, and phosphorylation sites important during the pump catalytic cycle (reviewed in Kaplan, 2002). Mutations or substitutions within these regions affect pump function, subjecting the pump to both purifying and positive selection. Because the molecule responsible for generating EODs (voltage-gated Na+ channels) is under positive selection in two lineages of weakly electric fish (Arnegard et al., 2010; Zakon et al., 2006), this research was performed to see if the Na, K-ATPases were under similar patterns of selection.

Full or partial sequences of the α2 isoform were obtained for gymnotiform and mormyrid representatives with myogenic electric organs. The alignment of these sequences was used to create a single-gene phylogenetic tree, and then PAML (Phylogenetic Analysis of Maximum Likelihood) software was used to detect branches and sites that may be under selection (Yang, 2007). Branch models determined that the mormyrids are under intense purifying selection, while the branches for both the pulse-type and higher frequency wave-type gymnotiforms were under positive selection. This is not consistent with the pattern of positive selection on the voltage-gated Na+ channels of both studied weakly electric fish lineages. The mormyrids show less diversity in EOD frequency, with only a single example of a higher-frequency wave-type fish. However, the gymnotiforms have many examples of both pulse-type and wave-type fish. In these lower frequency mormyrids, the α2 subunit of the EO Na, K-ATPase may already function sufficiently signaling. The positive selection acting on both types of gymnotiforms may have provided for more efficient pumps for those with higher EOD frequencies. However, changes of the α2 isoform are not the only way that

Na, K-ATPase action could be optimized in these cells, as they are also highly expressed. The ubiquitous α1 isoform also helps manage these demands on the pump, especially in the mormyrid lineage, and could also be under positive selection.

Eighteen sites were identified as possibly under positive selection. These 18 sites are found throughout the protein, including in the functionally significant cytoplasmic domains or extracellular loops. Mutations and substitutions in these regions have previously been identified in both impairing and improving pump function. In humans, several mutations of atp1a2a in these regions have been identified as causing disease, like familial hemiplegic migraine (FHM), by altering domain interactions, binding of ligands, or other steps of the catalytic cycle (Morth et al., 2009). These 18 identified sites provide a starting point for future research for the understanding molecular mechanisms involved in EOD production and management of the associated cost.

A substitution originally identified in squid that increased pump turnover rate by 40% was found previously found in the electric eel (Colina et al., 2010). In this study, this substitution was found in all gymnotiform representatives, but not in any non-electric or mormyrid representatives. While this substitution has already been found to significantly change how the pump functions (specifically its release of sodium ions to the extracellular space), it was not identified as a positively selected site in this study. After visual examination of the alignment, we identified other amino acids that may be of interest with similar substitution patterns, which were also not identified by the site models as under positive selection. Because the isoleucine to valine substitution is a functionally important substitution, these other interesting residues found by visual

review of the alignment may also be worth including in future electrophysiology and mutagenesis studies, in the aim to understand how these changes to the pump may be affecting pump efficiency.

While this research provides a good starting point these future studies, there are several other questions regarding the Na, K-ATPases of weakly electric fish. In the previous studies identifying patterns of positive selection on the voltage-gated Na+ channels of weakly electric fish, there were unique patterns of expression of the different copies of the channel between skeletal muscle and the EO (a skeletal muscle derivative). While the channels of the EO were under intense positive selection, those of muscle were not (Arnegard et al., 2010; Zakon et al., 2009; Zakon et al., 2006). For this reason, a comparison of the Na, K-ATPase between the skeletal muscle and EO of electric fish may provide more information about how electrocytes function, although preliminary data suggests the pump of *Brachyhypopomus gauderio* muscle and EO appear the same. Another interesting addition to this research would be the inclusion of the *atp1a2a* of the gymnotiform family *Apteronotus*. This family is unique in that adults have neurogenic EOs compared the myogenic EO of all other species, which could mean expression of a different primary α isoform. For this reason, they produce the highest known EOD frequencies, with some species and individuals up to 2000 Hz. Completion of the partial *atp1a2a* sequences obtained for this family so far in our lab would provide more data from representatives of high frequency, wave-type fish gymnotiforms.

This research provides sites of interest that may aid in understanding the molecule that incurs the metabolic cost of this signaling system. Further research on

these sites and how they may affect pump function will help elucidate the molecular mechanisms of electrocyte action potentials and also aid in understanding how animals are balancing the metabolic demand of costly signaling systems. While used as a novel communication and sensory system in weakly electric fish, electrical signaling is also vital for humans (e.g., muscle movement or beating hearts) and further understanding of this electric signaling system may aid in understanding in other bioelectric systems.

References

Ackermann, U., Geering, K., 1992. β1- and β3-subunits can associate with presynthesized α-subunits of *Xenopus* oocyte Na,K-ATPase. The Journal of Biological Chemistry 267, 12911-12915.

Aguilera, P.A., Caputi, A.A., 2003. Electroreception in *G. carapo*: detection of changes in waveform of the electrosensory signals. Journal of Experimental Biology 206, 989.

Aguilera, P.A., Castello, M.E., Caputi, A.A., 2001. Electroreception in *Gymnotus carapo*: differences between self-generated and conspecific-generated signal carriers. Journal of Experimental Biology 204, 185.

Akopyanz, N.S., Broude, N.E., Bekman, E.P., Marzen, E.O., Sverdlov, E.D., 1991. Tissue-specific expression of Na,K-ATPase β-subunit. Does β2 expression correlate with tumorigenesis? FEBS Letters 289, 8-10.

Albers, R.W., 1967. Biochemical Aspects of Active Transport. Annual Review of Biochemistry 36, 727-756.

Albert, J.S., Crampton, W.G.R., 2005. Diversity and Phylogeny of Neotropical Electric Fishes (Gymnotiformes), in: Bullock, T.H., Hopkins, C.D., Popper, A.N., Fay, R.R. (Eds.), Electroreception. Springer New York, New York, NY, pp. 360-409.

Albert, J.S., Crampton, W.G.R., 2006. Electroreception and electrogenesis, in: Evans, D.H., Claiborne, J.B. (Eds.), The Physiology of Fishes, 3rd Edition ed.

Alevizopoulos, K., Calogeropoulou, T., Lang, F., Stournaras, C., 2014. Na^+/K^+ ATPase Inhibitors in Cancer. Current Drug Targets 15, 988-1000.

Arnegard, M.E., Zwickl, D.J., Lu, Y., Zakon, H.H., 2010. Old gene duplication facilitates origin and diversification of an innovative communication system--twice. Proceedings of the National Academy of Sciences of the United States of America 107, 22172-22177.

Ashcroft, F.M., 2006. From molecule to malady. Nature 440, 440-447.

Attwell, D., Laughlin, S.B., 2001. An energy budget for signaling in the grey matter of the brain. Journal of Cerebral Blood Flow and Metabolism. 21, 1133-1145.

Babula, P., Masarik, M., Adam, V., Provaznik, I., Kizek, R., 2013. From Na^+/K^+-ATPase and cardiac glycosides to cytotoxicity and cancer treatment. Anti-cancer Agents in Medicinal Chemistry 13, 1069-1087.

Ban, Y., Smith, B.E., Markham, M.R., 2015. A highly polarized excitable cell separates sodium channels from sodium-activated potassium channels by more than a millimeter. Journal of Neurophysiolology 114, 520-530.

Barwe, S.P., Anilkumar, G., Moon, S.Y., Zheng, Y., Whitelegge, J.P., Rajasekaran, S.A., Rajasekaran, A.K., 2005. Novel Role for Na,K-ATPase in Phosphatidylinositol 3-Kinase Signaling and Suppression of Cell Motility. Molecular Biology of the Cell 16, 1082-1094.

Bass, A.H., Hopkins, C.D., 1983. Hormonal-Control of Sexual Differentiation- Changes in Electric Organ Discharge Waveform. Science 220, 971-974.

Bean, B.P., 2007. The action potential in mammalian central neurons. Nature Reviews. Neuroscience 8, 451-465.

Beggah, A., Mathews, P., Beguin, P., Geering, K., 1996. Degradation and Endoplasmic Reticulum Retention of Unassembled α- and β-Subunits of Na,K-ATPase Correlate with Interaction of BiP. Journal of Biological Chemistry. 271, 20895-20902.

Benjamini, Y., 2010. Discovering the false discovery rate. Journal of the Royal Statistical Society: Series B (Statistical Methodology) 72, 405-416.

Bennett, M.V., 1961. Modes of Operation of Electric Organs. Annals of the New York Academy of Sciences. 94, 458-509.

Bennett, M.V.L., 1971. Electric Organs, in: Hoar, W.S., Randall, D.J. (Eds.), Fish Physiology. Academic Press, New York, pp. 347-491.

Bennett, M.V.L., Grundfest, H., 1961. The Electrophysiology of Electric Organs of Marine Electric Fishes : III. The electroplaques of the stargazer, *Astroscopus y-graecum*. The Journal of General Physiology 44, 819-843.

Betancur, R.R., Broughton, R.E., Wiley, E.O., Carpenter, K., Lopez, J.A., Li, C., Holcroft, N.I., Arcila, D., Sanciangco, M., Cureton Ii, J.C., Zhang, F., Buser, T., Campbell, M.A., Ballesteros, J.A., Roa-Varon, A., Willis, S., Borden, W.C., Rowley, T., Reneau, P.C., Hough, D.J., Lu, G., Grande, T., Arratia, G., Orti, G., 2013. The tree of life and a new classification of bony fishes. PLoS Currents 5.

Blanco, G., Mercer, R.W., 1998. Isozymes of the Na-K-ATPase: Heterogeneity in structure, diversity in function. American Journal of Physiology 275, F633-F650.

Bradbury, J.W., Vehrencamp, S.L., 2011. Principles of Animal Communication, Second ed. Sinauer Associates, Inc. Publishers, Sunderland, MA.

Bublitz, M., Morth, J.P., Nissen, P., 2011. P-type ATPases at a glance. Journal of Cell Science 124, 2515.

Bullock, T.H., Hopkins, C.D., Popper, A.N., Fay, R.R., 2005. Electroreception. Springer New York.

Capendeguy, O., Iwaszkiewicz, J., Michielin, O., Horisberger, J.D., 2008. The fourth extracellular loop of the alpha subunit of Na,K-ATPase. Functional evidence for close

proximity with the second extracellular loop. The Journal of Biological Chemistry 283, 27850-27858.

Caputi, A.A., 1999. The electric organ discharge of pulse gymnotiforms: the transformation of a simple impulse into a complex spatio-temporal electromotor pattern. The Journal of Experimental Biology 202, 1229-1241.

Carter, B.C., Bean, B.P., 2009. Sodium entry during action potentials of mammalian central neurons: incomplete inactivation and reduced metabolic efficiency in fast-spiking neurons. Neuron 64, 898-909.

Catania, K., 2014. The shocking predatory strike of the electric eel. Science 346, 1231-1234.

Chen, D., Song, M., Mohamad, O., Yu, S.P., 2014. Inhibition of Na^+/K^+-ATPase induces hybrid cell death and enhanced sensitivity to chemotherapy in human glioblastoma cells. BMC Cancer 14, 1-15.

Cheung, J.Y., Zhang, X.Q., Song, J., Gao, E., Chan, T.O., Rabinowitz, J.E., Koch, W.J., Feldman, A.M., Wang, J., 2013. Coordinated regulation of cardiac $Na(^+)$/Ca (2^+) exchanger and Na $(^+)$-K $(^+)$-ATPase by phospholemman (FXYD1). Advances in Experimental Medicine and Biology 961, 175-190.

Ching, B., Woo, J.M., Hiong, K.C., Boo, M.V., Choo, C.Y.L., Wong, W.P., Chew, S.F., Ip, Y.K., 2015. Na plus /K plus -ATPase α-subunit (nka α) Isoforms and Their mRNA Expression Levels, Overall Nka α Protein Abundance, and Kinetic Properties of Nka in the Skeletal Muscle and Three Electric Organs of the Electric Eel, *Electrophorus electricus*. PLoS One 10, 24.

Colina, C., Palavicini, J.P., Srikumar, D., Holmgren, M., Rosenthal, J.J., 2010. Regulation of Na^+/K^+ ATPase transport velocity by RNA editing. PLoS biology 8, e1000540.

Crambert, G., Geering, K., 2003. FXYD proteins: new tissue-specific regulators of the ubiquitous Na,K-ATPase. Science's STKE : Signal Transduction Knowledge Environment 2003, Re1.

Dai, H., Song, D., Xu, J., Li, B., Hertz, L., Peng, L., 2013. Ammonia-induced Na,K-ATPase/ouabain-mediated EGF receptor transactivation, MAPK/ERK and PI3K/AKT signaling and ROS formation cause astrocyte swelling. Neurochemistry International 63, 610-625.

Daiho, T., Yamasaki, K., Danko, S., Suzuki, H., 2007. Critical role of Glu40-Ser48 loop linking actuator domain and first transmembrane helix of $Ca2^+$-ATPase in $Ca2^+$ deocclusion and release from ADP-insensitive phosphoenzyme. The Journal of Biological Chemistry 282, 34429-34447.

Daly, S.E., Lane, L.K., Blostein, R., 1994. Functional consequences of amino-terminal diversity of the catalytic subunit of the Na,K-ATPase. The Journal of Biological Chemistry 269, 23944-23948.

de Souza, W.F., Barbosa, L.A., Liu, L., de Araujo, W.M., de-Freitas-Junior, J.C., Fortunato-Miranda, N., Fontes, C.F., Morgado-Diaz, J.A., 2014. Ouabain-induced alterations of the apical junctional complex involve alpha1 and beta1 Na,K-ATPase downregulation and ERK1/2 activation independent of caveolae in colorectal cancer cells. Journal of Membrane Biology 247, 23-33.

Dimas, K., Papadopoulou, N., Baskakis, C., Prousis, K.C., Tsakos, M., Alkahtani, S., Honisch, S., Lang, F., Calogeropoulou, T., Alevizopoulos, K., Stournaras, C., 2014. Steroidal cardiac Na^+/K^+ ATPase inhibitors exhibit strong anti-cancer potential in vitro and in prostate and lung cancer xenografts in vivo. Anti-Cancer Agents in Medicinal Chemistry 14, 762-770.

Dunlap, K.D., McAnelly, M.L., Zakon, H.H., 1997. Estrogen modifies an electrocommunication signal by altering the electrocyte sodium current in an electric fish, *Sternopygus*. Journal of Neuroscience 17, 2869-2875.

Durlacher, C.T., Chow, K., Chen, X.W., He, Z.X., Zhang, X.J., Yang, T.X., Zhou, S.F., 2015. Targeting Na^+/K^+-translocating adenosine triphosphatase in cancer treatment. Clinical and Experimental Pharmacology and Physiology. 42, 427-443.

Espineda, C.E., Chang, J.H., Twiss, J., Rajasekaran, S.A., Rajasekaran, A.K., 2004. Repression of Na,K-ATPase β1-subunit by the transcription factor snail in carcinoma. Molecular Biology of the Cell 15, 1364-1373.

Ferrari, M.B., McAnelly, M.L., Zakon, H.H., 1995. Individual variation in and androgen-modulation of the sodium current in electric organ. The Journal of neuroscience : the official journal of the Society for Neuroscience 15, 4023-4032.

Ferrari, M.B., Zakon, H.H., 1993. Conductances contributing to the action potential of *Sternopygus* electrocytes. Journal of Comparative Physiology A: Neuroethology, Sensory, Neural, and Behavioral Physiology 173, 281-292.

Gallant, J.R., Hopkins, C.D., Deitcher, D.L., 2012. Differential expression of genes and proteins between electric organ and skeletal muscle in the mormyrid electric fish Brienomyrus brachyistius. Journal of Experimental Biology 215, 2479-2494.

Gallant, J.R., Traeger, L.L., Volkening, J.D., Moffett, H., Chen, P.-H., Novina, C.D., Phillips, G.N., Jr., Anand, R., Wells, G.B., Pinch, M., Gueth, R., Unguez, G.A., Albert, J.S., Zakon, H.H., Samanta, M.P., Sussman, M.R., 2014. Genomic basis for the convergent evolution of electric organs. Science 344, 1529-1532.

Gallanti, A., Cardin, V., Tonelli, A., Bussone, G., Bresolin, N., Mariani, C., Bassi, M.T., 2011. The genetic features of 24 patients affected by familial and sporadic hemiplegic migraine. Neurological Sciences 32 Suppl 1, S141-142.

Gallanti, A., Tonelli, A., Cardin, V., Bussone, G., Bresolin, N., Bassi, M.T., 2008. A novel de novo nonsense mutation in ATP1A2 associated with sporadic hemiplegic migraine and epileptic seizures. Journal of the Neurological Sciences 273, 123-126.

Gavassa, S., Silva, A.C., Stoddard, P.K., 2011. Tight hormonal phenotypic integration ensures honesty of the electric signal of male and female *Brachyhypopomus gauderio*. Hormones and Behavior 60, 420-426.

Geering, K., 2001. The functional role of β subunits in oligomeric P-type ATPases. Journal of Bioenergetics and Biomembranes 33, 425-438.

Geertsma, E.R., Dutzler, R., 2011. A versatile and efficient high-throughput cloning tool for structural biology. Biochemistry 50, 3272-3278.

Gheorghiade, M., Adams, K.F., Colucci, W.S., 2004. Digoxin in the Management of Cardiovascular Disorders. Circulation 109, 2959.

Gritz, S.M., Radcliffe, R.A., 2013. Genetic effects of ATP1A2 in familial hemiplegic migraine type II and animal models. Human Genomics 7.

Håkansson, K.O., 2003. The Crystallographic Structure of Na,K-ATPase N-domain at 2.6 Å Resolution. Journal of Molecular Biology 332, 1175-1182.

Hanika, S., Kramer, B., 2000. Electrosensory prey detection in the African sharptooth catfish, *Clarias gariepinus* (Clariidae), of a weakly electric mormyrid fish, the bulldog (*Marcusenius macrolepidotus*). Behavioral Ecology and Sociobiology 48, 218-228.

Heinzen, E.L., Arzimanoglou, A., Brashear, A., Clapcote, S.J., Gurrieri, F., Goldstein, D.B., Johannesson, S.H., Mikati, M.A., Neville, B., Nicole, S., Ozelius, L.J., Poulsen, H., Schyns, T., Sweadner, K.J., van den Maagdenberg, A., Vilsen, B., Grp, A.A.W., 2014. Distinct neurological disorders with ATP1A3 mutations. Lancet Neurology 13, 503-514.

Holdensen, A.N., Andersen, J.P., 2009. The Length of the A-M3 Linker Is a Crucial Determinant of the Rate of the $Ca2^{+}$ Transport Cycle of Sarcoplasmic Reticulum $Ca2^{+}$-ATPase. Journal of Biological Chemistry 284, 12258-12265.

Holmgren, M., Wagg, J., Bezanilla, F., Rakowski, R.F., De Weer, P., Gadsby, D.C., 2000. Three distinct and sequential steps in the release of sodium ions by the Na^{+}/K^{+}-ATPase. Nature 403, 898-901.

Hopkins, C.D., 1986. Behavior of Mormyridae, in: Bullock, T.H., Heiligenberg, W.F. (Eds.), Electroreception. John Wiley & Sons, New York, pp. 527-576.

Hopkins, C.D., 1999. Design features for electric communication. Journal of Experimental Biology 202, 1217-1228.

Howarth, C., Gleeson, P., Attwell, D., 2012. Updated energy budgets for neural computation in the neocortex and cerebellum. Journal of Cerebral Blood Flow and Metabolism 32, 1222-1232.

Hurley, I.A., Mueller, R.L., Dunn, K.A., Schmidt, E.J., Friedman, M., Ho, R.K., Prince, V.E., Yang, Z., Thomas, M.G., Coates, M.I., 2007. A new time-scale for ray-finned fish evolution. Proceedings of the Royal Society B: Biological Sciences 274, 489-498.

Jewell, E.A., Lingrel, J.B., 1991. Comparison of the substrate dependence properties of the rat Na,K-ATPase α1, α2, and α3 isoforms expressed in HeLa cells. Journal of Biological Chemistry 266, 16925-16930.

Jiang, Y., Zhang, Y., Luan, J., Duan, H., Zhang, F., Yagasaki, K., Zhang, G., 2010. Effects of bufalin on the proliferation of human lung cancer cells and its molecular mechanisms of action. Cytotechnology 62, 573-583.

Jimenez, T., McDermott, J.P., Sanchez, G., Blanco, G., 2011. Na,K-ATPase α4 isoform is essential for sperm fertility. Proceedings of the National Academy of Sciences of the United States of America 108, 644-649.

Jorgensen, P.L., Hakansson, K.O., Karlish, S.J., 2003. Structure and mechanism of Na,K-ATPase: functional sites and their interactions. Annual Review of Physiology 65, 817-849.

Jost, M.C., Hillis, D.M., Lu, Y., Kyle, J.W., Fozzard, H.A., Zakon, H.H., 2008. Toxin-Resistant Sodium Channels: Parallel Adaptive Evolution across a Complete Gene Family. Molecular Biology and Evolution 25, 1016-1024.

Jukes, T.H., Cantor, C.R., 1969. Evolution of Protein Molecules. Academy Press.

Julian, D., Crampton, W.G., Wohlgemuth, S.E., Albert, J.S., 2003. Oxygen consumption in weakly electric Neotropical fishes. Oecologia 137, 502-511.

Kanai, R., Ogawa, H., Vilsen, B., Cornelius, F., Toyoshima, C., 2013. Crystal structure of a Na^+-bound Na^+,K^+-ATPase preceding the E1P state. Nature 502, 201-206.

Kaplan, J.H., 2002. Biochemistry of Na,K-ATPase. Annual Review of Biochemistry 71, 511-535.

Karpova, L., Eva, A., Kirch, U., Boldyrev, A., Scheiner-Bobis, G., 2010. Sodium pump α1 and α3 subunit isoforms mediate distinct responses to ouabain and are both essential for survival of human neuroblastoma. The FEBS Journal 277, 1853-1860.

Kearse, M., Moir, R., Wilson, A., Stones-Havas, S., Cheung, M., Sturrock, S., Buxton, S., Cooper, A., Markowitz, S., Duran, C., Thierer, T., Ashton, B., Meintjes, P., Drummond, A., 2012. Geneious Basic: an integrated and extendable desktop software platform for the organization and analysis of sequence data. Bioinformatics 28, 1647-1649.

Koenderink, J.B., Zifarelli, G., Qiu, L.Y., Schwarz, W., De Pont, J.J.H.H.M., Bamberg, E., Friedrich, T., 2005. Na,K-ATPase mutations in familial hemiplegic migraine lead to functional inactivation. Biochimica et Biophysica Acta (BBA) - Biomembranes 1669, 61-68.

Koster, J.C., Blanco, G., Mercer, R.W., 1995. A cytoplasmic region of the Na,K-ATPase α-subunit is necessary for specific α/α association. The Journal of Biological Chemistry 270, 14332-14339.

Kubala, M., Grycova, L., Lansky, Z., Sklenovsky, P., Janovska, M., Otyepka, M., Teisinger, J., 2009. Changes in Electrostatic Surface Potential of Na^+/K^+-ATPase Cytoplasmic Headpiece Induced by Cytoplasmic Ligand(s) Binding. Biophysical Journal 97, 1756-1764.

Larkin, M.A., Blackshields, G., Brown, N.P., Chenna, R., McGettigan, P.A., McWilliam, H., Valentin, F., Wallace, I.M., Wilm, A., Lopez, R., Thompson, J.D., Gibson, T.J., Higgins, D.G., 2007. Clustal W and Clustal X version 2.0. Bioinformatics 23, 2947-2948.

Laursen, M., Yatime, L., Nissen, P., Fedosova, N.U., 2013. Crystal structure of the high-affinity Na^+K^+-ATPase-ouabain complex with $Mg2^+$ bound in the cation binding site. Proceedings of the National Academy of Sciences of the United States of America 110, 10958-10963.

Lavoué, S., Miya, M., Arnegard, M.E., Sullivan, J.P., Hopkins, C.D., Nishida, M., 2012. Comparable Ages for the Independent Origins of Electrogenesis in African and South American Weakly Electric Fishes. PLoS One 7, e36287.

Lefranc, F., Kiss, R., 2008. The sodium pump α1 subunit as a potential target to combat apoptosis-resistant glioblastomas. Neoplasia 10, 198-206.

Lenoir, G., Picard, M., Gauron, C., Montigny, C., Le Maréchal, P., Falson, P., le Maire, M., Møller, J.V., Champeil, P., 2004. Functional Properties of Sarcoplasmic Reticulum $Ca2^+$-ATPase after Proteolytic Cleavage at Leu119-Lys120, Close to the A-domain. Journal of Biological Chemistry 279, 9156-9166.

Lewis, J.E., Gilmour, K.M., Moorhead, M.J., Perry, S.F., Markham, M.R., 2014. Action Potential Energetics at the Organismal Level Reveal a Trade-Off in Efficiency at High Firing Rates. The Journal of Neuroscience 34, 197-201.

Liu, L., Zhao, X., Pierre, S.V., Askari, A., 2007. Association of PI3K-Akt signaling pathway with digitalis-induced hypertrophy of cardiac myocytes. American Journal of Physiology. Cell physiology 293, C1489-1497.

Lopina, O.D., 2000. Na+,K+-ATPase: structure, mechanism, and regulation. Membrane and Cell Biology 13, 721-744.

Lowe, J., Araujo, G.M.N., Pedrenho, A.R., Nunes-Tavares, N., Ribeiro, M.G.L., Hassón-Voloch, A., 2004. Polarized distribution of Na^+, K^+-ATPase α-subunit isoforms in electrocyte membranes. Biochimica et Biophysica Acta (BBA) - Biomembranes 1661, 40-46.

Macadar, O., Lorenzo, D., Velluti, J.C., 1989. Waveform generation of the electric organ discharge in *Gymnotus carapo*. Journal of Comparative Physiology A 165, 353-360.

Markham, M.R., 2013. Electrocyte physiology: 50 years later. Journal of Experimental Biology 216, 2451-2458.

Markham, M.R., Ban, Y., McCauley, A.G., Maltby, R., 2016. Energetics of Sensing and Communication in Electric Fish: A Blessing and a Curse in the Anthropocene? Integrative and Comparative Biology 56, 889-900.

Markham, M.R., Kaczmarek, L.K., Zakon, H.H., 2013. A sodium-activated potassium channel supports high-frequency firing and reduces energetic costs during rapid modulations of action potential amplitude. Journal of Neurophysiology 109, 1713-1723.

Markham, M.R., McAnelly, M.L., Stoddard, P.K., Zakon, H.H., 2009. Circadian and social cues regulate ion channel trafficking. PLoS Biol. 7, e1000203.

Markham, M.R., Stoddard, P.K., 2005. Adrenocorticotropic hormone enhances the masculinity of an electric communication signal by modulating the waveform and timing of action potentials within individual cells. Journal of Neuroscience 25, 8746-8754.

McAnelly, L., Zakon, H.H., 1996. Protein Kinase A Activation Increases Sodium Current Magnitude in the Electric Organ of *Sternopygus*. The Journal of Neuroscience 16, 4383-4388.

Mijatovic, T., Kiss, R., 2013. Cardiotonic Steroids-Mediated Na^+/K^+-ATPase Targeting Could Circumvent Various Chemoresistance Pathways. Planta Medica 79, 189-198.

Mills, A., Zakon, H.H., Marchaterre, M.A., Bass, A.H., 1992. Electric organ morphology of *Sternopygus macrurus*, a wave-type, weakly electric fish with a sexually dimorphic EOD. Journal of Neurobiology 23, 920-932.

Moller, P., 1995. Electric fishes : history and behavior, 1st ed. Chapman & Hall, London ; New York.

Moller, P., Serrier, J., Belbenoit, P., 1976. Electric organ discharges of the weakly electric fish *Gymnarchus niloticus* (Mormyriformes) in its natural habitat. Experientia 32, 1007-1008.

Morais-Cabral, J.H., Zhou, Y., MacKinnon, R., 2001. Energetic optimization of ion conduction rate by the K^+ selectivity filter. Nature 414, 37-42.

Morth, J.P., Pedersen, B.P., Buch-Pedersen, M.J., Andersen, J.P., Vilsen, B., Palmgren, M.G., Nissen, P., 2011. A structural overview of the plasma membrane Na^+,K^+-ATPase and H^+-ATPase ion pumps. Nature Reviews. Molecular Cell Biology 12, 60-70.

Morth, J.P., Pedersen, B.P., Toustrup-Jensen, M.S., Sorensen, T.L., Petersen, J., Andersen, J.P., Vilsen, B., Nissen, P., 2007. Crystal structure of the sodium-potassium pump. Nature 450, 1043-1049.

Morth, J.P., Poulsen, H., Toustrup-Jensen, M.S., Schack, V.R., Egebjerg, J., Andersen, J.P., Vilsen, B., Nissen, P., 2009. The structure of the Na^+,K^+-ATPase and mapping of isoform differences and disease-related mutations. Philosophical Transactions of the Royal Society B: Biological Sciences 364, 217-227.

Nelson, M.E., MacIver, M.A., 2006. Sensory acquisition in active sensing systems. Journal of Comparative Physiology A 192, 573.

Niven, J.E., Laughlin, S.B., 2008. Energy limitation as a selective pressure on the evolution of sensory systems. The Journal of Experimental Biology 211, 1792-1804.

Nyblom, M., Poulsen, H., Gourdon, P., Reinhard, L., Andersson, M., Lindahl, E., Fedosova, N., Nissen, P., 2013. Crystal Structure of Na^+, K^+-ATPase in the Na+-Bound State. Science 342, 123-127.

Ogawa, H., Shinoda, T., Cornelius, F., Toyoshima, C., 2009. Crystal structure of the sodium-potassium pump (Na+,K+-ATPase) with bound potassium and ouabain. Proceedings of the National Academy of Sciences of the United States of America 106, 13742-13747.

Ohnishi, T., Yanazawa, M., Sasahara, T., Kitamura, Y., Hiroaki, H., Fukazawa, Y., Kii, I., Nishiyama, T., Kakita, A., Takeda, H., Takeuchi, A., Arai, Y., Ito, A., Komura, H., Hirao, H., Satomura, K., Inoue, M., Muramatsu, S., Matsui, K., Tada, M., Sato, M., Saijo, E., Shigemitsu, Y., Sakai, S., Umetsu, Y., Goda, N., Takino, N., Takahashi, H., Hagiwara, M., Sawasaki, T., Iwasaki, G., Nakamura, Y., Nabeshima, Y., Teplow, D.B., Hoshi, M., 2015. Na, K-ATPase α3 is a death target of Alzheimer patient amyloid-β assembly. Proceedings of the National Academy of Sciences of the United States of America 112, E4465-E4474.

Olesen, C., Picard, M., Winther, A.-M.L., Gyrup, C., Morth, J.P., Oxvig, C., Moller, J.V., Nissen, P., 2007. The structural basis of calcium transport by the calcium pump. Nature 450, 1036-1042.

Post, R.L., Hegyvary, C., Kume, S., 1972. Activation by Adenosine Triphosphate in the Phosphorylation Kinetics of Sodium and Potassium Ion Transport Adenosine Triphosphatase. J. Biol. Chem. 247, 6530-6540.

Prassas, I., Diamandis, E.P., 2008. Novel therapeutic applications of cardiac glycosides. Nature reviews. Drug discovery 7, 926-935.

Reardon, E.E., Parisi, A., Krahe, R., Chapman, L.J., 2011. Energetic constraints on electric signalling in wave-type weakly electric fishes. The Journal of Experimental Biology 214, 4141-4150.

Rose, A.M., Valdes, R., Jr., 1994. Understanding the sodium pump and its relevance to disease. Clinical Chemistry 40, 1674-1685.

Ruxton, G.D., 2009. Non-visual crypsis: a review of the empirical evidence for camouflage to senses other than vision. Philosophical Transactions of the Royal Society of London. Series B, Biological sciences 364, 549-557.

Salazar, V.L., Krahe, R., Lewis, J.E., 2013. The energetics of electric organ discharge generation in gymnotiform weakly electric fish. The Journal of Experimental Biology 216, 2459-2468.

Salazar, V.L., Stoddard, P.K., 2008. Sex differences in energetic costs explain sexual dimorphism in the circadian rhythm modulation of the electrocommunication signal of the gymnotiform fish *Brachyhypopomus pinnicaudatus*. The Journal of Experimental Biology 211, 1012-1020.

Salazar, V.L., Stoddard, P.K., 2009. Social competition affects electric signal plasticity and steroid levels in the gymnotiform fish *Brachyhypopomus gauderio*. Hormones and Behavior 56, 399-409.

Sawtell, N.B., Williams, A., Bell, C.C., 2005. From sparks to spikes: information processing in the electrosensory systems of fish. Current Opinion in Neurobiology 15, 437-443.

Schwartz, I.R., Pappas, G.D., Bennett, M.V.L., 1975. The fine structure of electrocytes in weakly electric teleosts. Journal of Neurocytology 4, 87-114.

Segall, L., Daly, S.E., Blostein, R., 2001. Mechanistic Basis for Kinetic Differences between the Rat α1, α2, and α3 Isoforms of the Na,K-ATPase. Journal of Biological Chemistry 276, 31535-31541.

Segall, L., Javaid, Z.Z., Carl, S.L., Lane, L.K., Blostein, R., 2003. Structural basis for α1 versus α2 isoform-distinct behavior of the Na,K-ATPase. The Journal of Biological Chemistry 278, 9027-9034.

Selvakumar, P., Owens, T.A., David, J.M., Petrelli, N.J., Christensen, B.C., Lakshmikuttyamma, A., Rajasekaran, A.K., 2014. Epigenetic silencing of Na,K-ATPase β1 subunit gene ATP1B1 by methylation in clear cell renal cell carcinoma. Epigenetics 9, 579-586.

Shinoda, T., Ogawa, H., Cornelius, F., Toyoshima, C., 2009. Crystal structure of the sodium-potassium pump at 2.4 A resolution. Nature 459, 446-450.

Silverman, M.E., 1989. William Withering and an account of the foxglove. Clinical Cardiology 12, 415-418.

Sinnett, P.M., Markham, M.R., 2015. Food deprivation reduces and leptin increases the amplitude of an active sensory and communication signal in a weakly electric fish. Hormones and Behavior 71, 31-40.

Skou, J.C., 1957. The influence of some cations on an adenosine triphosphatase from peripheral nerves. Biochimica et Biophysica Acta 23, 394-401.

Smith, M.J., Harper, D.G.C., 1995. Animal Signals: Models and Terminology. Journal of Theoretical Biology 177, 305-311.

Sorensen, T.L., Moller, J.V., Nissen, P., 2004. Phosphoryl transfer and calcium ion occlusion in the calcium pump. Science 304, 1672-1675.

Stoddard, P.K., 1999. Predation enhances complexity in the evolution of electric fish signals. Nature 400, 254-256.

Stoddard, P.K., Markham, M.R., 2008. Signal Cloaking by Electric Fish. BioScience 58, 415-425.

Stoddard, P.K., Markham, M.R., Salazar, V.L., 2003. Serotonin modulates the electric waveform of the gymnotiform electric fish *Brachyhypopomus pinnicaudatus*. Journal of Experimental Biology 206, 1353-1362.

Stoddard, P.K., Markham, M.R., Salazar, V.L., Allee, S., 2007. Circadian rhythms in electric waveform structure and rate in the electric fish *Brachyhypopomus pinnicaudatus*. Physiology and Behavior. 90, 11-20.

Stoddard, P.K., Salazar, V.L., 2011. Energetic cost of communication. Journal of Experimental Biology 214, 200-205.

Tagliacollo, V.A., Bernt, M.J., Craig, J.M., Oliveira, C., Albert, J.S., 2016. Model-based total evidence phylogeny of Neotropical electric knifefishes (Teleostei, Gymnotiformes). Molecular Phylogenetics and Evolution 95, 20-33.

Tonelli, A., Gallanti, A., Bersano, A., Cardin, V., Ballabio, E., Airoldi, G., Redaelli, F., Candelise, L., Bresolin, N., Bassi, M.T., 2007. Amino acid changes in the amino terminus of the Na,K-adenosine triphosphatase α2 subunit associated to familial and sporadic hemiplegic migraine. Clinical Genetics 72, 517-523.

Toyoshima, C., Kanai, R., Cornelius, F., 2011. First Crystal Structures of Na^+,K^+-ATPase: New Light on the Oldest Ion Pump. Structure 19, 1732-1738.

Toyoshima, C., Mizutani, T., 2004. Crystal structure of the calcium pump with a bound ATP analogue. Nature 430, 529-535.

Vedovato, N., Gadsby, D.C., 2014. Route, mechanism, and implications of proton import during Na^+/K^+ exchange by native Na^+/K^+-ATPase pumps. Journal of General Physiology 143, 449-464.

von der Emde, G., 2006. Non-visual environmental imaging and object detection through active electrolocation in weakly electric fish. Journal of Comparative Physiology A 192, 601.

Wang, Z., Zheng, M., Li, Z., Li, R., Jia, L., Xiong, X., Southall, N., Wang, S., Xia, M., Austin, C.P., Zheng, W., Xie, Z., Sun, Y., 2009. Cardiac glycosides inhibit p53 synthesis by a mechanism relieved by Src or MAPK inhibition. Cancer Research 69, 6556-6564.

Weigand, K.M., Swarts, H.G., Fedosova, N.U., Russel, F.G., Koenderink, J.B., 2012. Na,K-ATPase activity modulates Src activation: a role for ATP/ADP ratio. Biochimica et Biophysica Acta 1818, 1269-1273.

Wu, J., Akkuratov, E.E., Bai, Y., Gaskill, C.M., Askari, A., Liu, L., 2013. Cell signaling associated with $Na(^+)/K(^+)$-ATPase: activation of phosphatidylinositide 3-kinase IA/Akt by ouabain is independent of Src. Biochemistry 52, 9059-9067.

Yan, Y., Shapiro, J.I., 2016. The physiological and clinical importance of sodium potassium ATPase in cardiovascular diseases. Current Opinion in Pharmacology 27, 43-49.

Yang, Z., 2007. PAML 4: Phylogenetic Analysis by Maximum Likelihood. Molecular Biology and Evolution 24, 1586-1591.

Ye, Q., Lai, F., Banerjee, M., Duan, Q., Li, Z., Si, S., Xie, Z., 2013. Expression of mutant alpha1 Na/K-ATPase defective in conformational transition attenuates Src-mediated signal transduction. The Journal of Biological Chemistry 288, 5803-5814.

Zahavi, A., 1975. Mate selection—A selection for a handicap. Journal of Theoretical Biology 53, 205-214.

Zakon, H.H., 2012. Adaptive evolution of voltage-gated sodium channels: The first 800 million years. Proceedings of the National Academy of Sciences 109, 10619-10625.

Zakon, H.H., Jost, M.C., Zwickl, D.J., Lu, Y., Hillis, D.M., 2009. Molecular evolution of Na^+ channels in teleost fishes. Integrative Zoology 4, 64-74.

Zakon, H.H., Lu, Y., Zwickl, D.J., Hillis, D.M., 2006. Sodium channel genes and the evolution of diversity in communication signals of electric fishes: convergent molecular evolution. Proceedings of the National Academy of Sciences of the United States of America 103, 3675-3680.

Zhu, Z., Sun, H., Ma, G., Wang, Z., Li, E., Liu, Y., Liu, Y., 2012. Bufalin induces lung cancer cell apoptosis via the inhibition of PI3K/Akt pathway. International Journal of Molecular Sciences 13, 2025-2035.

Appendix: Full Translation Alignment of atp1a2a

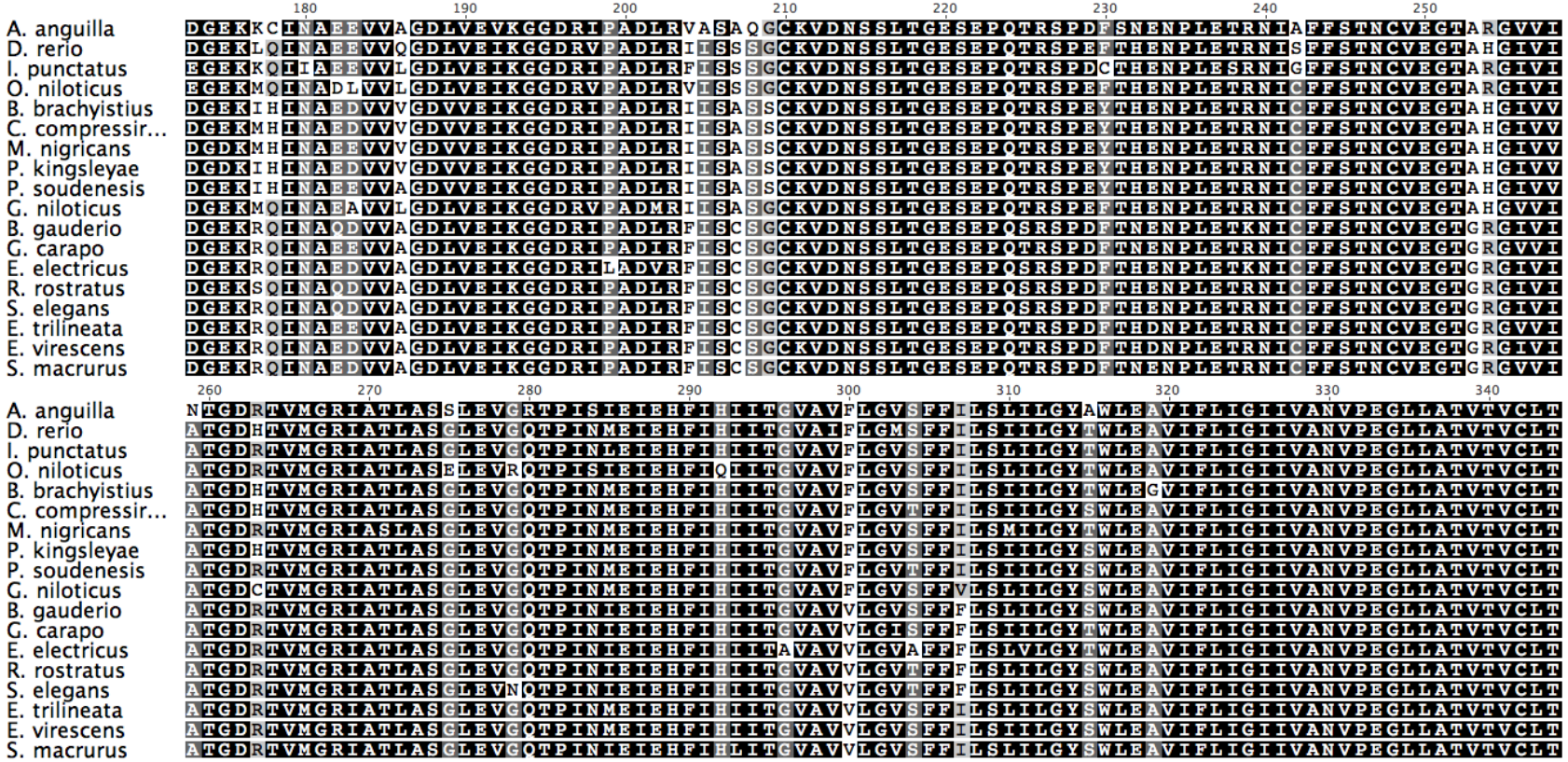
180 190 200 210 220 230 240 250
A. anguilla DGEKKCINAEEVVAGDLVEVKGGDRIPADLRVASAQGCKVDNSSLTGESEPQTRSPDFSNENPLETRNIAFFSTNCVEGTARGVVI
D. rerio DGEKLQINAEEVVQGDLVEIKGGDRVPADLRIISSSGCKVDNSSLTGESEPQTRSPEFTHENPLETRNISFFSTNCVEGTAHGIVI
I. punctatus EGEKKQIIAEEVVLGDLVEIKGGDRIPADLRFISSSGCKVDNSSLTGESEPQTRSPDCTHENPLESRNIGFFSTNCVEGTARGIVI
O. niloticus EGEKMQINADLVVLGDLVEIKGGDRVPADLRVISSSGCKVDNSSLTGESEPQTRSPEFTHENPLETRNICFFSTNCVEGTARGIVI
B. brachyistius DGEKIHINAEDVVVGDVVEIKGGDRIPADLRIISASSCKVDNSSLTGESEPQTRSPEYTHENPLETRNICFFSTNCVEGTAHGIVV
C. compressir... DGEKMHINAEDVVVGDVVEIKGGDRIPADLRIISASSCKVDNSSLTGESEPQTRSPEYTHENPLETRNICFFSTNCVEGTAHGIVV
M. nigricans DGDKMHINAEEVVVGDVVEIKGGDRIPADLRIISASSCKVDNSSLTGESEPQTRSPEYTHENPLETRNICFFSTNCVEGTAHGIVV
P. kingsleyae DGDKIHINAEDVVVGDVVEIKGGDRIPADLRIISASSCKVDNSSLTGESEPQTRSPEYTHENPLETRNICFFSTNCVEGTAHGIVV
P. soudenesis DGEKIHINAEEVVAGDVVEIKGGDRIPADLRIISASSCKVDNSSLTGESEPQTRSPEYTHENPLETRNICFFSTNCVEGTAHGIVV
G. niloticus DGEKMQINAEAVVLGDLVEIKGGDRVPADMRIISASGCKVDNSSLTGESEPQTRSPEFTHENPLETRNICFFSTNCVEGTAHGVVI
B. gauderio DGEKRQINAQDVVAGDLVEIKGGDRIPADLRFISCSGCKVDNSSLTGESEPQSRSPDFTNENPLETKNICFFSTNCVEGTGRGIVI
G. carapo DGEKRQINAEEVVAGDLVEIKGGDRIPADIRFISCSGCKVDNSSLTGESEPQTRSPDFTNENPLETRNICFFSTNCVEGTGRGVVI
E. electricus DGEKRQINAEDVVAGDLVEIKGGDRILADVRFISCSGCKVDNSSLTGESEPQSRSPDFTHENPLETKNICFFSTNCVEGTGRGIVI
R. rostratus DGEKSQINAQDVVAGDLVEIKGGDRIPADLRFISCSGCKVDNSSLTGESEPQSRSPDFTHENPLETRNICFFSTNCVEGTGRGIVI
S. elegans DGEKRQINAQDVVAGDLVEIKGGDRIPADLRFISCSGCKVDNSSLTGESEPQSRSPDFTHENPLETRNICFFSTNCVEGTGRGIVI
E. trilineata DGEKRQINAEEVVAGDLVEIKGGDRIPADIRFISCSGCKVDNSSLTGESEPQTRSPDFTHDNPLETRNICFFSTNCVEGTGRGVVI
E. virescens DGEKRQINAEDVVAGDLVEIKGGDRIPADIRFISCSGCKVDNSSLTGESEPQTRSPDFTHDNPLETRNICFFSTNCVEGTGRGIVI
S. macrurus DGEKRQINAEDVVAGDLVEIKGGDRIPADIRFISCSGCKVDNSSLTGESEPQTRSPDFTNENPLETRNICFFSTNCVEGTGRGVVI
260 270 280 290 300 310 320 330 340
A. anguilla NTGDRTVMGRIATLASSLEVGRTPISIEIEHFIHIITGVAVFLGVSFFILSLILGYAWLEAVIFLIGIIVANVPEGLLATVTVCLT
D. rerio ATGDHTVMGRIATLASGLEVGQTPINMEIEHFIHIITGVAIFLGMSFFILSIILGYTWLEAVIFLIGIIVANVPEGLLATVTVCLT
I. punctatus ATGDRTVMGRIATLASGLEVGQTPINLEIEHFIHIITGVAVFLGVSFFILSLILGYTWLEAVIFLIGIIVANVPEGLLATVTVCLT
O. niloticus ATGDRTVMGRIATLASELEVRQTPISIEIEHFIQIITGVAVFLGVSFFILSLILGYTWLEAVIFLIGIIVANVPEGLLATVTVCLT
B. brachyistius ATGDHTVMGRIATLASGLEVGQTPINMEIEHFIHIITGVAVFLGVSFFILSIILGYTWLEGVIFLIGIIVANVPEGLLATVTVCLT
C. compressir... ATGDHTVMGRIATLASGLEVGQTPINMEIEHFIHIITGVAVFLGVTFFILSIILGYSWLEAVIFLIGIIVANVPEGLLATVTVCLT
M. nigricans ATGDRTVMGRIASLASGLEVGQTPINMEIEHFIHIITGVAVFLGVSFFILSMILGYTWLEAVIFLIGIIVANVPEGLLATVTVCLT
P. kingsleyae ATGDHTVMGRIATLASGLEVGQTPINMEIEHFIHIITGVAVFLGVSFFILSIILGYSWLEAVIFLIGIIVANVPEGLLATVTVCLT
P. soudenesis ATGDRTVMGRIATLASGLEVGQTPINMEIEHFIHIITGVAVFLGVTFFILSIILGYSWLEAVIFLIGIIVANVPEGLLATVTVCLT
G. niloticus ATGDCTVMGRIATLASGLEVGQTPINMEIEHFIHIITGVAVFLGVSFFVLSLILGYSWLEAVIFLIGIIVANVPEGLLATVTVCLT
B. gauderio ATGDRTVMGRIATLASGLEVGQTPINIEIEHFIHIITGVAVVLGVSFFFLSLILGYSWLEAVIFLIGIIVANVPEGLLATVTVCLT
G. carapo ATGDRTVMGRIATLASGLEVGQTPINIEIEHFIHIITGVAVVLGISFFFLSIILGYTWLEAVIFLIGIIVANVPEGLLATVTVCLT
E. electricus ATGDRTVMGRIATLASGLEVGQTPINIEIEHFIHIITAVAVVLGVAFFFLSLVLGYTWLEAVIFLIGIIVANVPEGLLATVTVCLT
R. rostratus ATGDRTVMGRIATLASGLEVGQTPINIEIEHFIHIITGVAVVLGVTFFFLSLILGYSWLEAVIFLIGIIVANVPEGLLATVTVCLT
S. elegans ATGDRTVMGRIATLASGLEVNQTPINIEIEHFIHIITGVAVVLGVTFFFLSLILGYSWLEAVIFLIGIIVANVPEGLLATVTVCLT
E. trilineata ATGDRTVMGRIATLASGLEVGQTPINMEIEHFIHIITGVAVVLGVSFFILSLILGYSWLEAVIFLIGIIVANVPEGLLATVTVCLT
E. virescens ATGDRTVMGRIATLASGLEVGQTPINMEIEHFIHIITGVAVVLGVSFFILSIILGYSWLEAVIFLIGIIVANVPEGLLATVTVCLT
S. macrurus ATGDRTVMGRIATLASGLEVGQTPINIEIEHFIHLITGVAVVLGVSFFILSLILGYSWLEAVIFLIGIIVANVPEGLLATVTVCLT

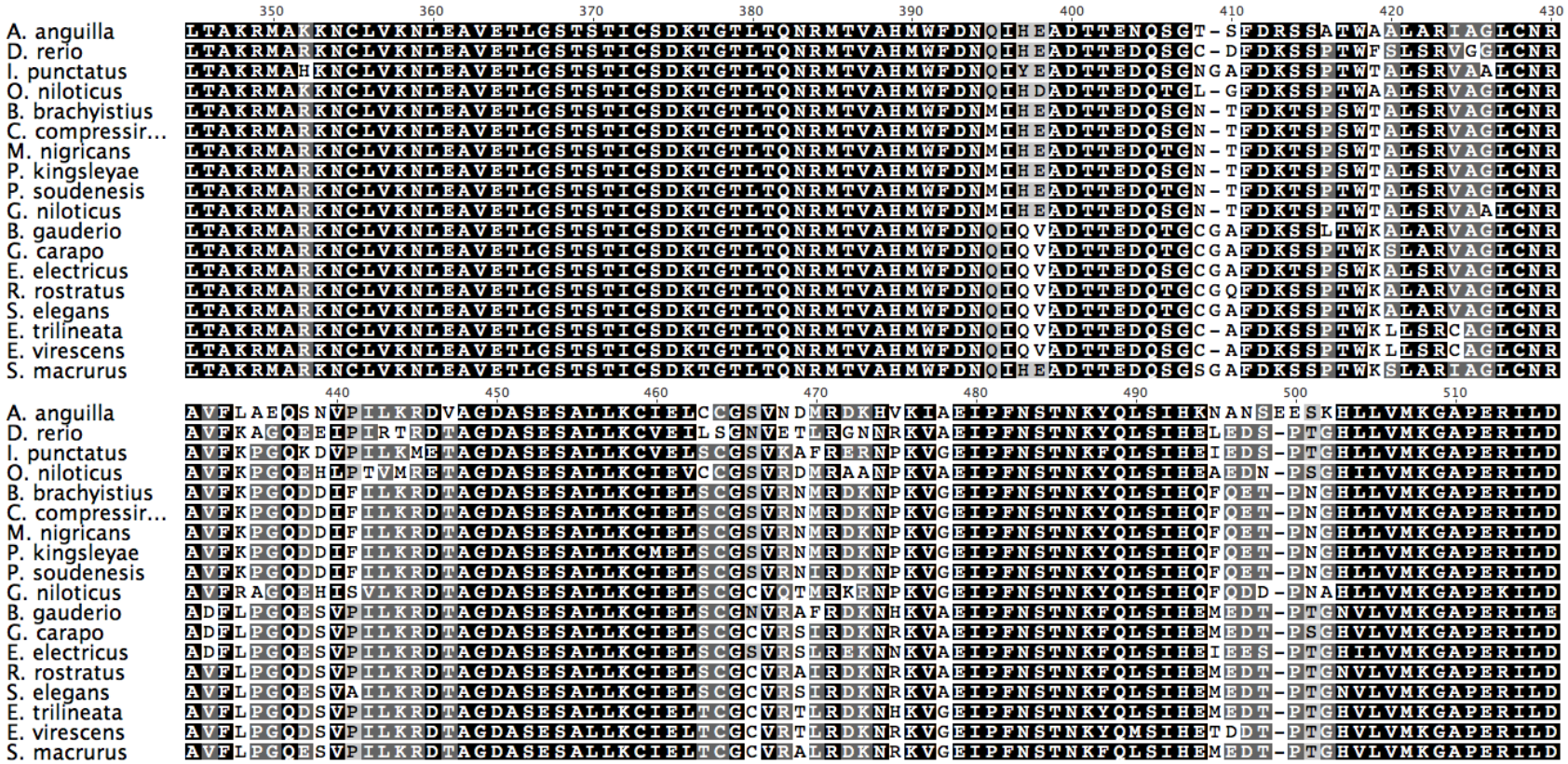
350 360 370 380 390 400 410 420 430
A. anguilla LTAKRMAKKNCLVKNLEAVETLGSTSTICSDKTGTLTQNRMTVAHMWFDNQIHEADTTENQSGT-SFDRSSATWAALARIAGLCNR
D. rerio LTAKRMARKNCLVKNLEAVETLGSTSTICSDKTGTLTQNRMTVAHMWFDNQIHEADTTEDQSGC-DFDKSSPTWFSLSRVGGLCNR
I. punctatus LTAKRMAHKNCLVKNLEAVETLGSTSTICSDKTGTLTQNRMTVAHMWFDNQIYEADTTEDQSGNGAFDKSSPTWTALSRVAALCNR
O. niloticus LTAKRMAKKNCLVKNLEAVETLGSTSTICSDKTGTLTQNRMTVAHMWFDNQIHDADTTEDQTGL-GFDKSSPTWAALSRVAGLCNR
B. brachyistius LTAKRMARKNCLVKNLEAVETLGSTSTICSDKTGTLTQNRMTVAHMWFDNMIHEADTTEDQSGN-TFDKTSPSWTALSRVAGLCNR
C. compressir... LTAKRMARKNCLVKNLEAVETLGSTSTICSDKTGTLTQNRMTVAHMWFDNMIHEADTTEDQSGN-TFDKTSPSWTALSRVAGLCNR
M. nigricans LTAKRMARKNCLVKNLEAVETLGSTSTICSDKTGTLTQNRMTVAHMWFDNMIHEADTTEDQTGN-TFDKTSPSWTALSRVAGLCNR
P. kingsleyae LTAKRMARKNCLVKNLEAVETLGSTSTICSDKTGTLTQNRMTVAHMWFDNMIHEADTTEDQSGN-TFDKTSPSWTALSRVAGLCNR
P. soudenesis LTAKRMARKNCLVKNLEAVETLGSTSTICSDKTGTLTQNRMTVAHMWFDNMIHEADTTEDQTGN-TFDKTSPTWTALSRVAGLCNR
G. niloticus LTAKRMARKNCLVKNLEAVETLGSTSTICSDKTGTLTQNRMTVAHMWFDNMIHEADTTEDQSGN-TFDKTSPTWTALSRVAALCNR
B. gauderio LTAKRMARKNCLVKNLEAVETLGSTSTICSDKTGTLTQNRMTVAHMWFDNQIQVADTTEDQTGCGAFDKSSLTWKALARVAGLCNR
G. carapo LTAKRMARKNCLVKNLEAVETLGSTSTICSDKTGTLTQNRMTVAHMWFDNQIQVADTTEDQTGCGAFDKSSPTWKSLARVAGLCNR
E. electricus LTAKRMARKNCLVKNLEAVETLGSTSTICSDKTGTLTQNRMTVAHMWFDNQIQVADTTEDQSGCGAFDKTSPSWKALSRVAGLCNR
R. rostratus LTAKRMARKNCLVKNLEAVETLGSTSTICSDKTGTLTQNRMTVAHMWFDNQIQVADTTEDQTGCGQFDKSSPTWKALARVAGLCNR
S. elegans LTAKRMARKNCLVKNLEAVETLGSTSTICSDKTGTLTQNRMTVAHMWFDNQIQVADTTEDQTGCGAFDKSSPTWKALARVAGLCNR
E. trilineata LTAKRMARKNCLVKNLEAVETLGSTSTICSDKTGTLTQNRMTVAHMWFDNQIQVADTTEDQSGC-AFDKSSPTWKLLSRCAGLCNR
E. virescens LTAKRMARKNCLVKNLEAVETLGSTSTICSDKTGTLTQNRMTVAHMWFDNQIQVADTTEDQSGC-AFDKSSPTWKLLSRCAGLCNR
S. macrurus LTAKRMARKNCLVKNLEAVETLGSTSTICSDKTGTLTQNRMTVAHMWFDNQIHEADTTEDQSGSGAFDKSSPTWKSLARIAGLCNR
440 450 460 470 480 490 500 510
A. anguilla AVFLAEQSNVPILKRDVAGDASESALLKCIELCCGSVNDMRDKHVKIAEIPFNSTNKYQLSIHKNANSEESKHLLVMKGAPERILD
D. rerio AVFKAGQEETPIRTRDTAGDASESALLKCVETLSGNVETLRGNNRKVAEIPFNSTNKYQLSIHELEDS-PTGHLLVMKGAPERILD
I. punctatus AVFKPGQKDVPILKMETAGDASESALLKCVELSCGSVKAFRERNPKVGEIPFNSTNKFQLSIHEIEDS-PTGHLLVMKGAPERILD
O. niloticus AVFKPGQEHLPTVMRETAGDASESALLKCIEVCCGSVRDMRAANPKVAEIPFNSTNKYQLSIHEAEDN-PSGHILVMKGAPERILD
B. brachyistius AVFKPGQDDIFILKRDTAGDASESALLKCIELSCGSVRNMRDKNPKVGEIPFNSTNKYQLSIHQFQET-PNGHLLVMKGAPERILD
C. compressir... AVFKPGQDDIFILKRDTAGDASESALLKCIELSCGSVRNMRDKNPKVGEIPFNSTNKYQLSIHQFQET-PNGHLLVMKGAPERILD
M. nigricans AVFKPGQDDIFILKRDTAGDASESALLKCIELSCGSVRNMRDKNPKVGEIPFNSTNKYQLSIHQFQET-PNGHLLVMKGAPERILD
P. kingsleyae AVFKPGQDDIFILKRDTAGDASESALLKCMELSCGSVRNMRDKNPKVGEIPFNSTNKYQLSIHQFQET-PNGHLLVMKGAPERILD
P. soudenesis AVFKPGQDDIFILKRDTAGDASESALLKCIELSCGSVRNIRDKNPKVGEIPFNSTNKYQLSIHQFQET-PNGHLLVMKGAPERILD
G. niloticus AVFRAGQEHISVLKRDTAGDASESALLKCIELSCGCVQTMRKRNPKVGEIPFNSTNKYQLSIHQFQDD-PNAHLLVMKGAPEKILD
B. gauderio ADFLPGQESVPILKRDTAGDASESALLKCIELSCGNVRAFRDKNHKVAEIPFNSTNKFQLSIHEMEDT-PTGNVLVMKGAPERILE
G. carapo ADFLPGQDSVPILKRDTAGDASESALLKCIELSCGCVRSIRDKNRKVAEIPFNSTNKFQLSIHEMEDT-PSGHVLVMKGAPERILD
E. electricus ADFLPGQESVPILKRDTAGDASESALLKCIELSCGSVRSLREKNNKVAEIPFNSTNKFQLSIHEIEES-PTGHILVMKGAPERILD
R. rostratus AVFLPGQDSVPILKRDTAGDASESALLKCIELSCGCVRAIRDKNRKVAEIPFNSTNKFQLSIHEMEDT-PTGNVLVMKGAPERILD
S. elegans AVFLPGQESVAILKRDTAGDASESALLKCIELSCGCVRSIRDKNRKVAEIPFNSTNKFQLSIHEMEDT-PTGNVLVMKGAPERILD
E. trilineata AVFLPGQDSVPILKRDTAGDASESALLKCIELTCGCVRTLRDKNRKVGEIPFNSTNKYQMSIHETDDT-PTGHVLVMKGAPERILD
E. virescens AVFLPGQDSVPILKRDTAGDASESALLKCIELTCGCVRTLRDKNRKVGEIPFNSTNKYQMSIHETDDT-PTGHVLVMKGAPERILD
S. macrurus AVFLPGQESVPILKRDTAGDASESALLKCIELTCGCVRALRDKNRKVGEIPFNSTNKFQLSIHEMEDT-PTGHVLVMKGAPERILD

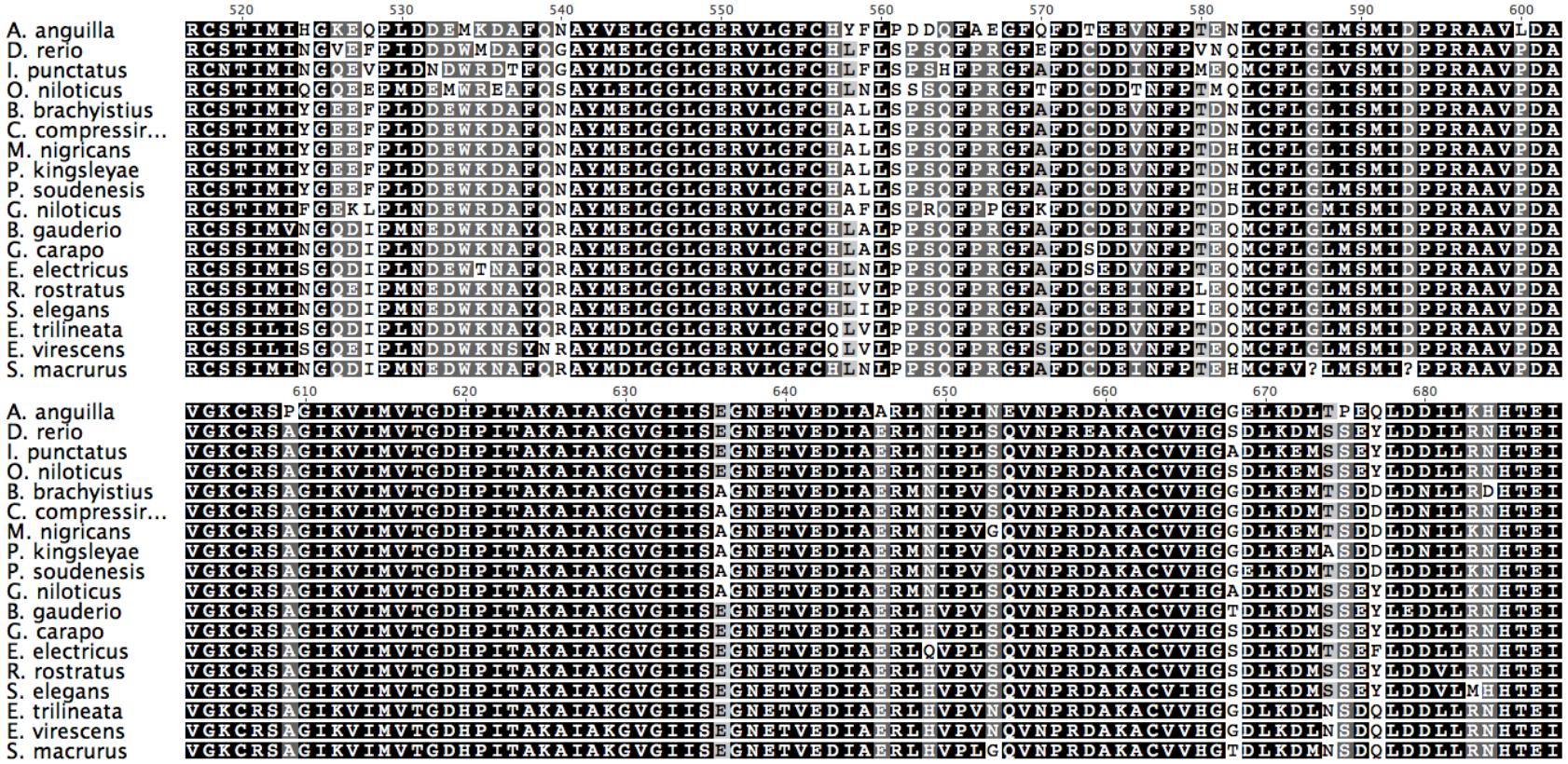
520 530 540 550 560 570 580 590 600
A. anguilla RCSTIMIHGKEQPLDDEMKDAFQNAYVELGGLGERVLGFCHYFLPDDQFAEGFQFDTEEVNFPTENLCFIGLMSMIDPPRAAVLDA
D. rerio RCSTIMINGVEFPIDDDWMDAFQGAYMELGGLGERVLGFCHLFLSPSQFPRGFEFDCDDVNFPVNQLCFLGLISMVDPPRAAVPDA
I. punctatus RCNTIMINGQEVPLDNDWRDTFQGAYMDLGGLGERVLGFCHLFLSPSHFPRGFAFDCDDINFPMEQMCFLGLVSMIDPPRAAVPDA
O. niloticus RCSTIMIQGQEEPMDEMWREAFQSAYLELGGLGERVLGFCHLNLSSSQFPRGFTFDCDDTNFPTMQLCFLGLISMIDPPRAAVPDA
B. brachyistius RCSTIMIYGEEFPLDDEWKDAFQNAYMELGGLGERVLGFCHALLSPSQFPRGFAFDCDEVNFPTDNLCFLGLISMIDPPRAAVPDA
C. compressir... RCSTIMIYGEEFPLDDEWKDAFQNAYMELGGLGERVLGFCHALLSPSQFPRGFAFDCDDVNFPTDNLCFLGLISMIDPPRAAVPDA
M. nigricans RCSTIMIYGEEFPLDDEWKDAFQNAYMELGGLGERVLGFCHALLSPSQFPRGFAFDCDEVNFPTDHLCFLGLISMIDPPRAAVPDA
P. kingsleyae RCSTIMIYGEEFPLDDEWKDAFQNAYMELGGLGERVLGFCHALLSPSQFPRGFAFDCDEVNFPTDNLCFLGLISMIDPPRAAVPDA
P. soudenesis RCSTIMIYGEEFPLDDEWKDAFQNAYMELGGLGERVLGFCHALLSPSQFPRGFAFDCDEVNFPTDHLCFLGLMSMIDPPRAAVPDA
G. niloticus RCSTIMIFGEKLPLNDEWRDAFQNAYMELGGLGERVLGFCHAFLSPRQFPPGFKFDCDDVNFPTDDLCFLGMISMIDPPRAAVPDA
B. gauderio RCSSIMVNGQDIPMNEDWKNAYQRAYMELGGLGERVLGFCHLALPPSQFPRGFAFDCDEINFPTEQMCFLGLMSMIDPPRAAVPDA
G. carapo RCSSIMINGQDIPLNDDWKNAFQRAYMELGGLGERVLGFCHLALSPSQFPRGFAFDSDDVNFPTEQMCFLGLMSMIDPPRAAVPDA
E. electricus RCSSIMISGQDIPLNDEWTNAFQRAYMELGGLGERVLGFCHLNLPPSQFPRGFAFDSEDVNFPTEQMCFLGLMSMIDPPRAAVPDA
R. rostratus RCSSIMINGQEIPMNEDWKNAYQRAYMELGGLGERVLGFCHLVLPPSQFPRGFAFDCEEINFPLEQMCFLGLMSMIDPPRAAVPDA
S. elegans RCSSIMINGQDIPMNEDWKNAYQRAYMELGGLGERVLGFCHLILPPSQFPRGFAFDCEEINFPIEQMCFLGLMSMIDPPRAAVPDA
E. trilineata RCSSILISGQDIPLNDDWKNAYQRAYMDLGGLGERVLGFCQLVLPPSQFPRGFSFDCDDVNFPTDQMCFLGLMSMIDPPRAAVPDA
E. virescens RCSSILISGQEIPLNDDWKNSYNRAYMDLGGLGERVLGFCQLVLPPSQFPRGFSFDCDEVNFPTEQMCFLGLMSMIDPPRAAVPDA
S. macrurus RCSSIMINGQDIPMNEDWKNAFQRAYMDLGGLGERVLGFCHLNLPPSQFPRGFAFDCDEINFPTEHMCFV?LMSMI?PPRAAVPDA
610 620 630 640 650 660 670 680
A. anguilla VGKCRSPGIKVIMVTGDHPITAKAIAKGVGIISEGNETVEDIAARLNIPINEVNPRDAKACVVHGGELKDLTPEQLDDILKHHTEI
D. rerio VGKCRSAGIKVIMVTGDHPITAKAIAKGVGIISEGNETVEDIAERLNIPLSQVNPREAKACVVHGSDLKDMSSEYLDDILRNHTEI
I. punctatus VGKCRSAGIKVIMVTGDHPITAKAIAKGVGIISEGNETVEDIAERLNIPLSQVNPRDAKACVVHGADLKEMSSEYLDDLLRNHTEI
O. niloticus VGKCRSAGIKVIMVTGDHPITAKAIAKGVGIISEGNETVEDIAERLNIPLSQVNPRDAKACVVHGSDLKEMSSEYLDDLLRNHTEI
B. brachyistius VGKCRSAGIKVIMVTGDHPITAKAIAKGVGIISAGNETVEDIAERMNIPVSQVNPRDAKACVVHGGDLKEMTSDDLDNLLRDHTEI
C. compressir... VGKCRSAGIKVIMVTGDHPITAKAIAKGVGIISAGNETVEDIAERMNIPVSQVNPRDAKACVVHGGDLKDMTSDDLDNILRNHTEI
M. nigricans VGKCRSAGIKVIMVTGDHPITAKAIAKGVGIISAGNETVEDIAERMNIPVGQVNPRDAKACVVHGGDLKEMTSDDLDNILKNHTEI
P. kingsleyae VGKCRSAGIKVIMVTGDHPITAKAIAKGVGIISAGNETVEDIAERMNIPVSQVNPRDAKACVVHGGDLKEMASDDLDNILRNHTEI
P. soudenesis VGKCRSAGIKVIMVTGDHPITAKAIAKGVGIISAGNETVEDIAERMNIPVSQVNPRDAKACVVHGGELKDMTSDDLDDILKNHTEI
G. niloticus VGKCRSAGIKVIMVTGDHPITAKAIAKGVGIISAGNETVEDIAERMNIPLSQVNPRDAKACVIHGADLKDMSSEYLDDLLKNHTEI
B. gauderio VGKCRSAGIKVIMVTGDHPITAKAIAKGVGIISEGNETVEDIAERLHVPVSQVNPRDAKACVVHGTDLKDMSSEYLEDLLRNHTEI
G. carapo VGKCRSAGIKVIMVTGDHPITAKAIAKGVGIISEGNETVEDIAERLHVPLSQINPRDAKACVVHGSDLKDMSSEYLDDLLRNHTEI
E. electricus VGKCRSAGIKVIMVTGDHPITAKAIAKGVGIISEGNETVEDIAERLQVPLSQVNPRDAKACVVHGSDLKDMTSEFLDDLLRNHTEI
R. rostratus VGKCRSAGIKVIMVTGDHPITAKAIAKGVGIISEGNETVEDIAERLHVPVSQVNPRDAKACVVHGSDLKDMSSEYLDDVLRNHTEI
S. elegans VGKCRSAGIKVIMVTGDHPITAKAIAKGVGIISEGNETVEDIAERLHVPVSQVNPRDAKACVIHGSDLKDMSSEYLDDVLMHHTEI
E. trilineata VGKCRSAGIKVIMVTGDHPITAKAIAKGVGIISEGNETVEDIAERLHVPVNQVNPRDAKACVVHGGDLKDLNSDQLDDLLRNHTEI
E. virescens VGKCRSAGIKVIMVTGDHPITAKAIAKGVGIISEGNETVEDIAERLHVPVNQVNPRDAKACVVHGGDLKDLNSDQLDDLLRNHTEI
S. macrurus VGKCRSAGIKVIMVTGDHPITAKAIAKGVGIISEGNETVEDIAERLHVPLGQVNPRDAKACVVHGTDLKDMNSDQLDDLLRNHTEI

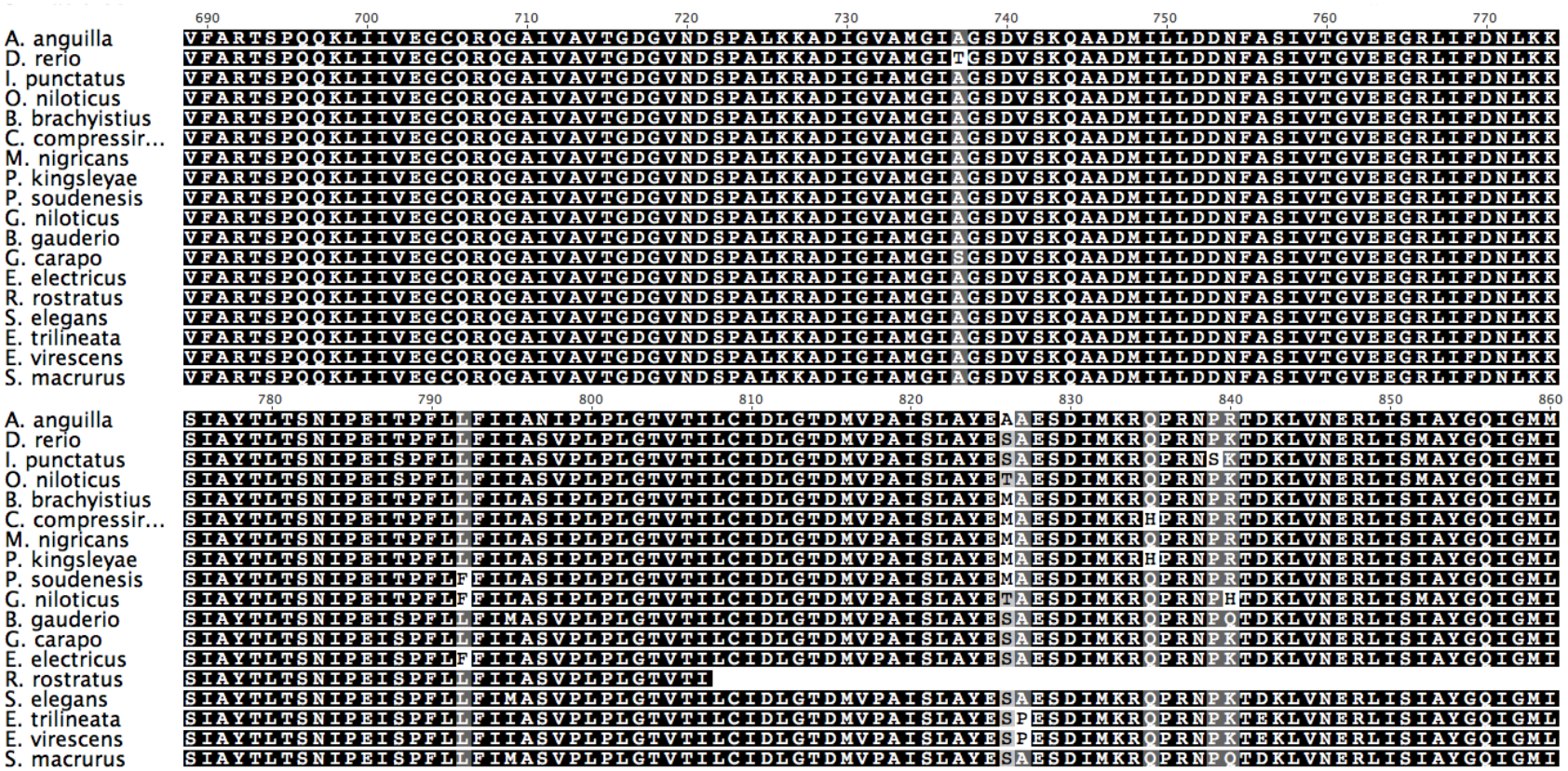
690 700 710 720 730 740 750 760 770
A. anguilla VFARTSPQQKLIIVEGCQRQGAIVAVTGDGVNDSPALKKADIGVAMGIAGSDVSKQAADMILLDDNFASIVTGVEEGRLIFDNLKK
D. rerio VFARTSPQQKLIIVEGCQRQGAIVAVTGDGVNDSPALKKADIGVAMGITGSDVSKQAADMILLDDNFASIVTGVEEGRLIFDNLKK
I. punctatus VFARTSPQQKLIIVEGCQRQGAIVAVTGDGVNDSPALKRADIGIAMGIAGSDVSKQAADMILLDDNFASIVTGVEEGRLIFDNLKK
O. niloticus VFARTSPQQKLIIVEGCQRQGAIVAVTGDGVNDSPALKKADIGVAMGIAGSDVSKQAADMILLDDNFASIVTGVEEGRLIFDNLKK
B. brachyistius VFARTSPQQKLIIVEGCQRQGAIVAVTGDGVNDSPALKKADIGVAMGIAGSDVSKQAADMILLDDNFASIVTGVEEGRLIFDNLKK
C. compressir... VFARTSPQQKLIIVEGCQRQGAIVAVTGDGVNDSPALKKADIGVAMGIAGSDVSKQAADMILLDDNFASIVTGVEEGRLIFDNLKK
M. nigricans VFARTSPQQKLIIVEGCQRQGAIVAVTGDGVNDSPALKKADIGVAMGIAGSDVSKQAADMILLDDNFASIVTGVEEGRLIFDNLKK
P. kingsleyae VFARTSPQQKLIIVEGCQRQGAIVAVTGDGVNDSPALKKADIGVAMGIAGSDVSKQAADMILLDDNFASIVTGVEEGRLIFDNLKK
P. soudenesis VFARTSPQQKLIIVEGCQRQGAIVAVTGDGVNDSPALKKADIGVAMGIAGSDVSKQAADMILLDDNFASIVTGVEEGRLIFDNLKK
G. niloticus VFARTSPQQKLIIVEGCQRQGAIVAVTGDGVNDSPALKKADIGVAMGIAGSDVSKQAADMILLDDNFASIVTGVEEGRLIFDNLKK
B. gauderio VFARTSPQQKLIIVEGCQRQGAIVAVTGDGVNDSPALKRADIGIAMGIAGSDVSKQAADMILLDDNFASIVTGVEEGRLIFDNLKK
G. carapo VFARTSPQQKLIIVEGCQRQGAIVAVTGDGVNDSPALKRADIGIAMGISGSDVSKQAADMILLDDNFASIVTGVEEGRLIFDNLKK
E. electricus VFARTSPQQKLIIVEGCQRQGAIVAVTGDGVNDSPALKRADIGIAMGIAGSDVSKQAADMILLDDNFASIVTGVEEGRLIFDNLKK
R. rostratus VFARTSPQQKLIIVEGCQRQGAIVAVTGDGVNDSPALKRADIGIAMGIAGSDVSKQAADMILLDDNFASIVTGVEEGRLIFDNLKK
S. elegans VFARTSPQQKLIIVEGCQRQGAIVAVTGDGVNDSPALKRADIGIAMGIAGSDVSKQAADMILLDDNFASIVTGVEEGRLIFDNLKK
E. trilineata VFARTSPQQKLIIVEGCQRQGAIVAVTGDGVNDSPALKKADIGIAMGIAGSDVSKQAADMILLDDNFASIVTGVEEGRLIFDNLKK
E. virescens VFARTSPQQKLIIVEGCQRQGAIVAVTGDGVNDSPALKKADIGIAMGIAGSDVSKQAADMILLDDNFASIVTGVEEGRLIFDNLKK
S. macrurus VFARTSPQQKLIIVEGCQRQGAIVAVTGDGVNDSPALKKADIGIAMGIAGSDVSKQAADMILLDDNFASIVTGVEEGRLIFDNLKK
780 790 800 810 820 830 840 850 860
A. anguilla SIAYTLTSNIPEITPFLLFIIANIPLPLGTVTILCIDLGTDMVPAISLAYEAAESDIMKRQPRNPRTDKLVNERLISIAYGQIGMM
D. rerio SIAYTLTSNIPEITPFLLFIIASVPLPLGTVTILCIDLGTDMVPAISLAYESAESDIMKRQPRNPKTDKLVNERLISMAYGQIGMI
I. punctatus SIAYTLTSNIPEISPFLLFIIASVPLPLGTVTILCIDLGTDMVPAISLAYESAESDIMKRQPRNSKTDKLVNERLISMAYGQIGMI
O. niloticus SIAYTLTSNIPEISPFLLFIIASVPLPLGTVTILCIDLGTDMVPAISLAYETAESDIMKRQPRNPKTDKLVNERLISMAYGQIGMI
B. brachyistius SIAYTLTSNIPEITPFLLFIILASIPLPLGTVTILCIDLGTDMVPAISLAYEMAESDIMKRQPRNPRTDKLVNERLISIAYGQIGML
C. compressir... SIAYTLTSNIPEITPFLLFIILASIPLPLGTVTILCIDLGTDMVPAISLAYEMAESDIMKRHPRNPRTDKLVNERLISIAYGQIGML
M. nigricans SIAYTLTSNIPEITPFLLFIILASIPLPLGTVTILCIDLGTDMVPAISLAYEMAESDIMKRQPRNPRTDKLVNERLISIAYGQIGML
P. kingsleyae SIAYTLTSNIPEITPFLLFIILASIPLPLGTVTILCIDLGTDMVPAISLAYEMAESDIMKRHPRNPRTDKLVNERLISIAYGQIGML
P. soudenesis SIAYTLTSNIPEITPFLFFIILASIPLPLGTVTILCIDLGTDMVPAISLAYEMAESDIMKRQPRNPRTDKLVNERLISIAYGQIGML
G. niloticus SIAYTLTSNIPEITPFLFFIILASIPLPLGTVTILCIDLGTDMVPAISLAYETAESDIMKRQPRNPHTDKLVNERLISMAYGQIGMI
B. gauderio SIAYTLTSNIPEISPFLLFIMASVPLPLGTVTILCIDLGTDMVPAISLAYESAESDIMKRQPRNPQTDKLVNERLISIAYGQIGMI
G. carapo SIAYTLTSNIPEISPFLLFIIASVPLPLGTVTILCIDLGTDMVPAISLAYESAESDIMKRQPRNPKTDKLVNERLISIAYGQIGMI
E. electricus SIAYTLTSNIPEISPFLFFIIASVPLPLGTVTILCIDLGTDMVPAISLAYESAESDIMKRQPRNPKTDKLVNERLISIAYGQIGMI
R. rostratus SIAYTLTSNIPEISPFLLFIIASVPLPLGTVTI
S. elegans SIAYTLTSNIPEISPFLLFIMASVPLPLGTVTILCIDLGTDMVPAISLAYESAESDIMKRQPRNPKTDKLVNERLISIAYGQIGMI
E. trilineata SIAYTLTSNIPEISPFLLFIIASVPLPLGTVTILCIDLGTDMVPAISLAYESPESDIMKRQPRNPKTEKLVNERLISIAYGQIGML
E. virescens SIAYTLTSNIPEISPFLLFIIASVPLPLGTVTILCIDLGTDMVPAISLAYESPESDIMKRQPRNPKTEKLVNERLISIAYGQIGML
S. macrurus SIAYTLTSNIPEISPFLLFIMASVPLPLGTVTILCIDLGTDMVPAISLAYESAESDIMKRQPRNPQTDKLVNERLISIAYGQIGMI

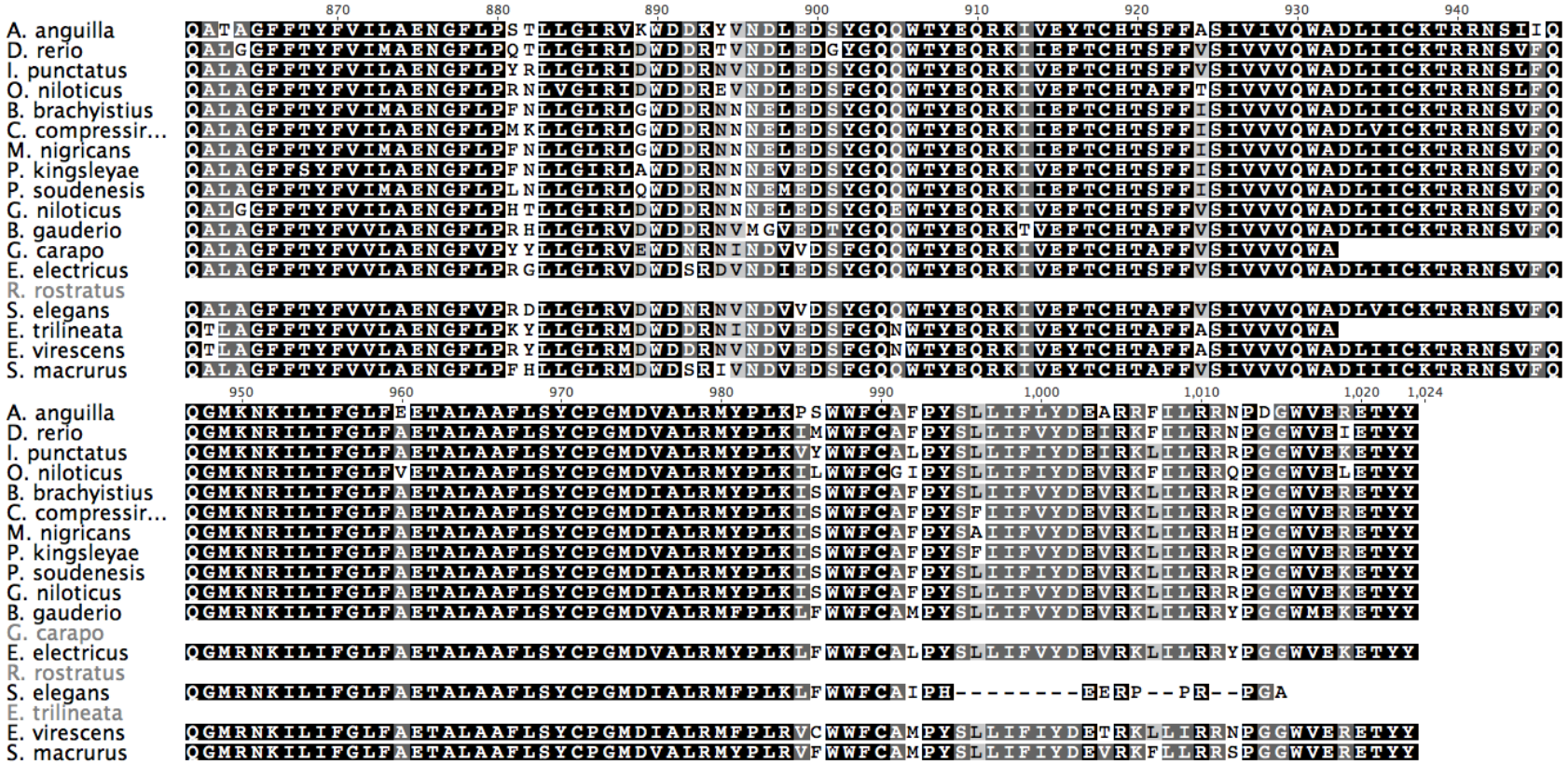
870
880
890
900
910
920
930
940
A. anguilla
D. rerio
I. punctatus
O. niloticus
B. brachyistius
C. compressir...
M. nigricans
P. kingsleyae
P. soudenesis
G. niloticus
B. gauderio
G. carapo
E. electricus
R. rostratus
S. elegans
E. trilineata
E. virescens
S. macrurus
950
960
970
980
990
1,000
1,010
1,020
1,024
A. anguilla
D. rerio
I. punctatus
O. niloticus
B. brachyistius
C. compressir...
M. nigricans
P. kingsleyae
P. soudenesis
G. niloticus
B. gauderio
G. carapo
E. electricus
R. rostratus
S. elegans
E. trilineata
E. virescens
S. macrurus